The interplay of perception and physiology: unraveling the neural mechanisms of Binocular Rivalry with Interocular Grouping

Eric Mokri

Integrated Program in Neuroscience

McGill University

Montreal, Quebec, Canada

June 2024

A thesis submitted to McGill University in partial fulfillment

of the requirements of the degree of Doctor of Philosophy

Table of Contents

Abstract ..... **III**
Résumé ..... **V**
Acknowledgements ..... **VII**
Contribution to Original Knowledge ..... **IX**
Author Contributions ..... **X**
List of Figures ..... **XI**
List of Tables ..... **XIII**
List of Abbreviations ..... **XIV**

Chapter 1 - *Introduction* **1**
1.1 Perceptual Illusions 2
1.2 Binocular Rivalry 3
1.2.A Models of Binocular Rivalry 4
1.2.B Neuroimaging Studies of Binocular Rivalry 5
1.3 Interocular Grouping 7
1.3.A Models of Interocular Grouping 9
1.3.B Neuroimaging Studies of Interocular Grouping 9
1.4 Interocular Grouping Demands 10
1.4.A Complimentary Bistable Patches 10
1.4.B Vertical versus Horizontal Image Meridian Division 11
1.5 Individual Differences 13
1.5.A Fast versus Slow Switchers 13
1.5.B Excitation and Inhibition Ratio 14
1.6 Magnetoencephalography 15
1.6.A Flicker Frequency-Tagging 16
1.7 Alpha Oscillations 18
1.7.A Alpha as an Inhibitor in the Visual System 18
1.7.B Alpha and Bistable Perception 19
Chapter 2 - *Effects of Interocular Grouping Demands on Binocular Rivalry* **20**
2.1 Preface 21
2.2 Abstract 22

2.3 Introduction 23
2.4 Methods 28
2.5 Results 30
2.6 Discussion 42
2.7 Acknowledgements 51
2.8 References 52
Chapter 3 - *Neural Markers of Interocular Grouping during Binocular Rivalry with MEG* 56
3.1 Preface 57
3.2 Abstract 58
3.3 Introduction 59
3.4 Methods 63
3.5 Results 74
3.6 Discussion 88
3.7 References 95
Chapter 4 - *Changes in Visual Perception Predicted by Alpha Band Power during Binocular Rivalry* 100
4.1 Preface 101
4.2 Abstract 102
4.3 Introduction 103
4.4 Methods 106
4.5 Results 114
4.6 Discussion 128
4.7 References 135
Chapter 5 - *General Discussion* 140
5.1 Binocular Rivalry and Increasing Interocular Grouping Demands 141
5.2 Individual Differences 146
5.3 Models of Binocular Rivalry 148
5.4 Neural Mechanisms of Perception 151
Conclusion & Summary 153

Master References 155
Appendix 160

Abstract

Visual illusions have long been studied as a device to provide insight into perception. A well-known illusion, binocular rivalry, is experienced when two incompatible, non-fusible images are shown independently to each eye. Perception alternates between periods of near complete dominance of one image, with the alternate image suppressed from perception. Remarkably, the experience of rivalry persists even when images are subdivided and presented in complementary bistable patches across the eyes, a phenomenon termed interocular grouping. The first chapter of this thesis provides a comprehensive literature review of these perceptual illusions, highlighting key insights within the field and emphasizing the potential advantages of using neuroimaging to study both forms of perceptual rivalry. In the second chapter, I characterize the behavioural measures of binocular rivalry with increasing interocular grouping demands. This is performed in a two-fold manner, through both increasing the number of divisions, and changing the orientation of the central meridian division. It was found that interocular grouping demonstrated robust stability in mean dominant percept durations and viewing proportions as the number of complementary bistable patches increased from two, to four, to six. In contrast, mixed percepts were disproportionately affected in higher order grouping conditions. Mixed percepts are argued to have a significant contribution to the experience of rivalry, and the notion of tristability is reinforced through their stability and overwhelming presence during transition phases. A preference for grouping across the vertical meridian was present and supported by previous findings. The third chapter presents cutting-edge brain imaging methods on a subset of the participant pool to investigate physiological markers of alternation in the visual system. Magnetoencephalography was combined with frequency-tagging while participants experienced both binocular rivalry and interocular grouping with two and four complementary bistable patches. In line with behavioural observations, I demonstrate that the neural markers of rivalry during interocular grouping resemble that of binocular rivalry, however, they are weaker. Physiological markers of rivalry were observed in, and beyond the primary visual cortex, with differences observed between dominant and suppressed perceptual states. Machine learning methods were used to disentangle neural mechanisms both between and within conditions. In the fourth chapter, I dive further into the neural mechanisms of rivalry during untagged binocular rivalry images with

magnetoencephalography. The specific focus is on alpha oscillations, a range of brain oscillations that have previously been associated with inhibition in the visual system. A decrease in alpha power over the occipital and parietal cortex was consistently observed prior to the report of dominant percepts during binocular rivalry. This is contrasted both to the increase in alpha power reported prior to mixed percepts, and the earlier markers of alpha power change that occur for a replay control condition. Measures of connectivity highlighted inhibitory feedback from higher to lower visual areas prior to alternations. The findings of the presented projects bridge the gap between the behavioral experience during binocular rivalry and interocular grouping, offering novel insights into their neural correlates.

Résumé

Les illusions visuelles ont longtemps été étudiées comme moyen de donner un aperçu de la perception. Une illusion bien connue, la rivalité binoculaire, est ressentie lorsque deux images incompatibles et non fusibles sont présentées indépendamment à chaque œil. La perception alterne entre des périodes de domination presque complète d'une image, l'image alternative étant supprimée de la perception. Remarquablement, l'expérience de rivalité persiste même lorsque les images sont subdivisées et présentées en zones bistables complémentaires sur les yeux, un phénomène appelé regroupement interoculaire. Le premier chapitre propose une revue complète de la littérature sur ces illusions perceptuelles, mettant en évidence les informations clés dans le domaine et soulignant les avantages potentiels de l'utilisation de la neuroimagerie pour étudier les deux formes de rivalité perceptuelle. Dans le deuxième chapitre, je caractérise les mesures comportementales de la rivalité binoculaire avec des demandes de regroupement interoculaire. Ceci s'effectue de deux manières, à la fois en augmentant le nombre de divisions et en modifiant l'orientation de la division du méridien central. Il a été constaté que le regroupement interoculaire démontrait une stabilité robuste dans les durées moyennes de perception dominante et les proportions de visualisation à mesure que le nombre de patchs bistables complémentaires augmentait de deux, à quatre, à six. En revanche, les perceptions mixtes étaient affectées de manière disproportionnée dans les conditions de regroupement d'ordre supérieur. Il est avancé que les perceptions mixtes contribuent de manière significative à l'expérience de rivalité, et la notion de tristabilité est renforcée par leur stabilité et leur présence écrasante pendant les phases de transition. Une préférence pour le regroupement sur le méridien vertical était présente et étayée par des découvertes précédentes. Le troisième chapitre présente des méthodes d'imagerie cérébrale sur un sous-ensemble des participants pour étudier les marqueurs physiologiques de l'alternance dans le système visuel. La magnétoencéphalographie a été combinée à un marquage de fréquence tandis que les participants ont expérimenté la rivalité binoculaire et le regroupement interoculaire avec deux et quatre patchs bistables complémentaires. Conformément aux observations comportementales, je démontre que les marqueurs neuronaux de la rivalité lors du regroupement interoculaire ressemblent à ceux de la rivalité binoculaire, mais ils sont plus faibles. Des marqueurs physiologiques de rivalité ont été observés dans et au-delà du cortex visuel primaire, avec des

différences observées entre les états perceptuels dominants et supprimés. Des méthodes d'apprentissage automatique ont été utilisées pour démêler les mécanismes neuronaux entre et au sein des conditions. Dans le quatrième chapitre, j'approfondis les mécanismes neuronaux de la rivalité lors d'images de rivalité binoculaires non marquées avec magnétoencéphalographie. L'accent est spécifiquement mis sur les oscillations alpha, une gamme d'oscillations cérébrales précédemment associées à l'inhibition du système visuel. Une diminution du pouvoir alpha sur le cortex occipital et pariétal a été systématiquement observée avant le rapport des percepts dominants lors de la rivalité binoculaire. Ceci contraste avec l'augmentation de la puissance alpha signalée avant les perceptions mixtes et avec les marqueurs antérieurs de changement de puissance alpha qui se produisent pour une condition de contrôle. Les mesures de connectivité ont mis en évidence un retour inhibiteur des zones visuelles supérieures vers inférieures avant les alternances. Les résultats des projets présentés comblent le fossé entre l'expérience comportementale lors de la rivalité binoculaire et le regroupement interoculaire, offrant ainsi de nouvelles perspectives sur leurs corrélats neuronaux.

Acknowledgements

I would like to start by thanking my supervisor, Dr. Janine Mendola, for granting me the opportunity to pursue my doctoral studies under her guidance. I discovered that your exceptional ingenuity in project planning is equaled, if not surpassed by your kindness. I consider myself fortunate to have been profoundly influenced by your mentorship, leaving an indelible mark on my education and personal growth.

Thank you to my collaborators and co-authors, Dr. Mathieu Landry and Dr. Jason da Silva Castanheira, your help was invaluable to the completion of our projects. New to the field of neuroimaging, your experience and willingness to teach was greatly appreciated. I relied on both of your feedback when dealing with uncharacteristic statistical questions and methodology inherit with the vast amount of data we obtained. The help Jason provided during the piloting and data collection phases of the MEG projects allowed us to be ambitious in our recruitment and participant testing. Your willingness to contribute while completing your own doctoral studies is admirable. Mathieu's creativity and broad expertise spanned from creating a novel stimulus that allowed us to study multiple perceptual illusions, to leveraging unique machine learning approaches. To this end, I also benefited from the collaboration formed with Elizabeth Bock that occurred before my doctoral studies. Much of the data collection methods and MEG analysis built on your frequency-tagged rivalry projects published with Dr. Mendola.

To my advisory committee, thank you for your insightful feedback throughout our many discussions. I am fortunate for the diverse knowledge and experiences you brought to our interactions. Dr. Fred Kingdom provided both a friendly interaction within our department and the reminder to dive deeper into the broader conceptual impact of my research. Dr. Sylvain Baillet provided expertise to the specificities of brain imaging and MEG research. The discussions and feedback I received from members of Dr. Baillet's lab furthered my understanding of recent trends in the field. I would also like to thank the constructive feedback received from the thesis examiners.

Much of this work came to fruition due in large part to the MEG lab at the McConnell Brain Imaging Centre at McGill University, Montreal. This facility allows cutting-edge neuroimaging research to be conducted. Marc Lanlacette provided hands on training and the

education to operate the MEG system independently. His ability to problem-solve is remarkable and saved several data collection sessions.

To my fellow lab members, Sujeevini and Austin, thank you for your support and comradery as we navigated our journey through graduate school together in a new and unfamiliar environment. The memories we shared both inside and outside of the lab shaped my experience throughout our studies. I would also like to acknowledge help I received from three fellow McGill University students, that expressed interest in vision research. Sidrah, already holding a graduate degree in vision science, was crucial in starting the recruitment and data collection phases. My understanding of mixed percepts was enhanced by research projects undertaking by Abigail. Finally, I reinforced my understanding of our methods the research project on monocular pattern rivalry with Sophie. I gained valuable project management experience from these interactions.

I received funding to complete my doctoral work and research projects through two streams provided by the Natural Sciences and Engineering Research Council of Canada (NSERC). Dr. Mendola obtained an NSERC discovery grant that allowed me to pursue my doctoral degree at McGill University under her supervision, and I further obtained funding through the Canada Graduate Scholarship-Master's Alexander Graham Bell award.

Lastly, I owe tremendous gratitude to my family, parents and partner. Their unwavering encouragement and belief in my abilities kept me focused and determined through the highs and lows of doctoral studies, even during the most challenging times. They showed great patience, understanding, and support. Serving as a constant source of strength and perseverance, I owe my deepest thanks.

Contribution to Original Knowledge

The three manuscripts presented in this thesis are all originally authored by Eric Mokri, under the supervision of Dr. Janine Mendola. The aim of my doctoral studies was to bridge behavioural and physiological results for binocular rivalry and interocular grouping.

The thesis builds on previous work in the field of binocular rivalry through several means. The second chapter; *Effects of interocular grouping demands on binocular rivalry*, systematically manipulated the stimuli to observe the effects of increasing interocular grouping demands on rivalry. A thorough examination of the behavioural results is provided through both systematically increasing the grouping demands from two, four, and six bistable complementary patches, and changing the central meridian image division between horizontal and vertical orientations. The third chapter; *Neural Markers of Interocular Grouping during Binocular Rivalry with MEG*, chapter introduces neuroimaging techniques of MEG and frequency-tagging to the study of interocular grouping to uncover the similarities and differences of the neural correlates between grouping demands and traditional binocular rivalry. Machine learning methods are leveraged to uncover distinct patterns not only between rivalrous conditions, but also between dominance and suppression. The fourth chapter; *Changes in Visual Perception Predicted by Alpha Band Power during Binocular Rivalry*, directly addresses limitations of frequency-tagging by observing naturally occurring brain dynamics during the experience of rivalry with MEG. The results provide a concrete example supporting the recent trends in literature that link alpha oscillations to inhibition and perception within the visual system.

The research projects presented in this thesis were originally showcased at international conferences: Vision Sciences Society (VSS), Organization for Human Brain Mapping (OHBM), and European Conference on Visual Perception (ECVP). We received insightful feedback from these conferences that pushed the projects forward.

Author Contributions

Chapter 2: Mokri, E., da Silva Castanheira, J., Laldin, S., Landry, M., & Mendola, J. D. Effects of interocular grouping demands on binocular rivalry.

E.M.: Conceptualization and study design, data collection, analysis, writing first draft and revisions. J.d.S.C.: Creating stimuli, analysis, revisions. S.L.: Data collection. M.L.: Creating stimuli, revisions. J.D.M.: conceptualization and study design, writing and revisions, funding acquisition, project supervision.

Chapter 3: Mokri, E., da Silva Castanheira, J., Landry, M., & Mendola, J. D. Neural Markers of Interocular Grouping during Binocular Rivalry with MEG

E.M.: Conceptualization and study design, data collection, analysis, writing first draft and revisions. J.d.S.C.: Creating stimuli, data collection. M.L.: Creating stimuli, machine learning analysis, writing and revisions. J.D.M.: conceptualization and study design, writing and revisions, funding acquisition, project supervision.

Chapter 4: Mokri, E., da Silva Castanheira, J., & Mendola, J. D. Changes in Visual Perception Predicted by Alpha Band Power during Binocular Rivalry

E.M.: Conceptualization and study design, data collection, analysis, writing first draft and revisions. J.d.S.C.: Creating stimuli, data collection. J.D.M.: Conceptualization and study design, writing and revisions, funding acquisition, project supervision.

List of Figures

Chapter 1

1.1 Necker cube visual illusion 2
1.2 Binocular rivalry stimulus 3
1.3 Binocular rivalry percepts 4
1.4 Interocular grouping stimulus 7
1.5 Visual percepts experienced during four-patch interocular grouping 8
1.6 Increasing interocular grouping demands 11
1.7 Two-patch interocular grouping stimulus 12
1.8 MEG power spectrum density analysis during BR in the primary visual cortex 16
1.9 SSVEF response during MEG frequency-tagged binocular rivalry in the primary visual cortex 17

Chapter 2

2.1 Example of interocular grouping stimuli adapted from literature review 24
2.2 Experimental design and BR stimuli with increasing interocular grouping demands 27
2.3 Comparison of flicker frequencies 31
2.4 Mean duration and proportion of viewing time for BR and interocular grouping 32
2.5 Correlation matrix with *R* values plotted of mean values for participants depicting relationship between BR and interocular grouping 38
2.6 Scatterplot depicting correlations between the alternation rate and mean duration of mixed percepts, with linear lines of best fit 39
2.7 Transition probabilities between perceptual states during rivalry 40
2.8 Visual model that accounts for tristable paradigm observed during BR. 50

Chapter 3

3.1 Experiment design and stimulus for BR and IOG conditions 66
3.2 MEG frequency-tagging in the primary visual cortex during BR and IOG 69
3.3 Psychophysics results for BR and IOG conditions 76
3.4 SSVEF signal for dominance and suppression during BR and IOG conditions at the time of alternation 79
3.5 SSVEF analysis between BR and IOG conditions from 0 to 500ms after perceptual alternations 81

3.6 Hilbert Transform time-frequency analysis for BR and IOG conditions across regions of interest 83
3.7 Multivariate logistic regression between BR and IOG conditions 85
3.8 Decoding neural markers of dominance versus suppression during BR and IOG conditions 87

Chapter 4

4.1 Visual stimulus and two-button press-and-hold design. 109
4.2 Psychophysics results for BR and BR replay conditions 114
4.3 MEG alpha band topography during binocular rivalry 117
4.4 Full cortex posterior view depicting the baseline normalized (z-score) changes in alpha band power during BR dominant percepts 119
4.5 Hilbert transform analysis for BR and BR replay conditions in the primary visual cortex 121
4.6 Hilbert transform analysis on alpha band power across regions of interest during BR 122
4.7 Individual differences in alpha power prior to BR mixed percepts predict their mean duration 124
4.8 Directed phase transfer entropy (dPTE) analysis for alpha band activity during BR dominant percepts 126

Chapter 5

5.1 Proposed neural model of binocular rivalry and interocular grouping 148

Appendix

A.1 Scatter plots depicting the correlation results between binocular rivalry and two-patch interocular grouping conditions 160
A.2 Alpha band power in V1 during BR and BR control conditions without baseline normalization 161
A.3 Phase transfer entropy (PTE) connectivity analysis for alpha band activity during binocular rivalry 162

List of Tables

Chapter 2

2.1 Multiple linear regression analysis between binocular rivalry and interocular grouping for mean dominant percept durations 32

2.2 Multiple linear regression analysis for increasing interocular grouping demands across the number and orientation of image division 34

2.3 Multiple linear regression analysis between binocular rivalry and interocular grouping for mean mixed percept durations and alternation rate 35

2.4 Multiple linear regression analysis between binocular rivalry and interocular grouping for alternation rate.....37

Chapter 3

3.1 Regions of interest generated for each participant for scout-based MEG analysis.....70

Chapter 4

4.1 Regions of interest generated for each participant for scout-based MEG analysis..... 112

List of Abbreviations

BOLD blood-oxygen-level-dependent

BR binocular rivalry

CI confidence interval

dB decibel

df degrees of freedom

DOI digital object identifier

dPTE directed phase transfer entropy

ECG electrocardiogram

EEG electroencephalography

E:I excitation and inhibition ratio

ERP event-related potential

EOG electrooculogram

f_1 first fundamental frequency

f_2 second fundamental frequency

FDR false discovery rate

fMRI functional magnetic resonance imaging

FWER family-wise error rate

HCP human connectome project

HM horizontal image meridian

Hz hertz

IOG interocular grouping

IOG2H two-patch interocular grouping with horizontal image meridian

IOG2V two-patch interocular grouping with vertical image meridian

IOG4 four-patch interocular grouping

IOG6H six-patch interocular grouping with horizontal image meridian

IOG6V six-patch interocular grouping with vertical image meridian

IP intraparietal brain region

LO lateral occipital brain region

M mean

MEG magnetoencephalography

MRI magnetic resonance imaging

N number of participants

p probability value

PAC phase-amplitude coupling

PSD power spectrum density

POS parieto-occipital sulcus

PTE phase transfer entropy

R correlation coefficient

RGBA red, blue, green, alpha values

ROI region of interest

SD standard deviation

SE standard error

SNR signal-to-noise ratio

SSVEF steady-state visually evoked field

SSVEP steady-state visually evoked potential

SSVER steady-state visually evoked response

SVM support vector machine

TMS transcranial magnetic stimulation

V1 primary visual cortex

VM vertical image meridian

1

Introduction

1.1 Perceptual Illusions

Perceptual illusions have long been studied to gain further insight into mechanisms of sensory processing. One class of illusions are famously called bi-stable perceptions. Rooted in their ambiguity, they elicit multiple interpretations, much to the desired intent of scientists. These interpretations can even alternate dynamically in perception, whereas the physical properties of the illusion remain unchanged. A common example of such a reversible figure is the Necker cube (Necker, 1832) illustrated in Figure 1.1A. When viewed for a prolonged period, observers can experience changes in perception between bottom-left (Figure 1.1B) and top-right (Figure 1.1C) orientation interpretations. This is remarkable, as the physical properties of the cube remain unchanged, highlighting the dynamic nature of human vision. The illusions functions in part, due to the lack of visual cues guiding perception. The value properties of visual illusions in scientific research provides tools to further uncover the neural mechanisms underlying visual perception.

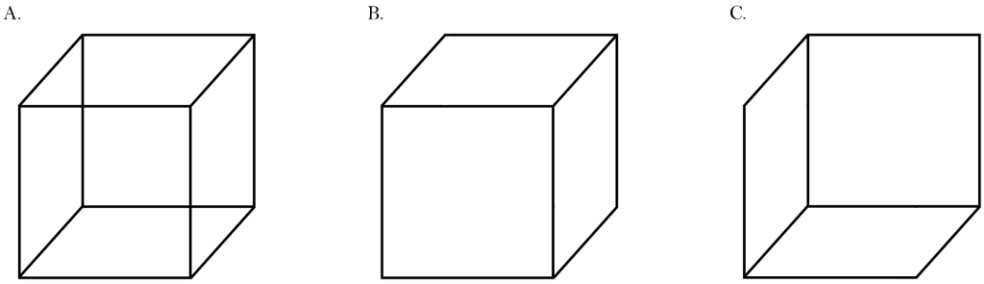

Figure 1.1 Necker cube visual illusion. The Necker cube is a bistable visual illusion, where observers can experience alternations in the interpretation of the orientation of the cube when viewed for a prolonged period. **A.** Necker cube illustration. **B.** Bottom-left perceptual interpretation. **C.** Top-right perceptual interpretation.

The study of visual illusions provides multifaceted benefits, as they encompass perceptual dominance, suppression, and ambiguity. These properties are conducive for neuroimaging experiments, where the stimuli remain unchanged while the brain dynamically shifts between perceptual states. Furthermore, disentangling the neural mechanisms of perceptual dominance from perceptual ambiguity provides a more encompassing view of the human visual system.

1.2 Binocular Rivalry

The human visual system is equipped with two frontal placed eyes that take in sensory information from our rich and dynamic environment. Although we often perceive a unified image of our world, our eyes independently project a slightly different image to the brain, due to their positioning on either side of the nose. Conflict resolution is handled by our visual system to ensure a unified perception, and often runs smoothly and unnoticed in normal human vision.

However, when each eye is presented with a dissimilar, non-fusible image (example shown in Figure 1.2), viewers experience alternations of conscious perceptual representations. Binocular rivalry (BR) is a vision perception phenomenon that is experienced when competing images are presented independently to each eye (Blake, 1989; Blake & Logothetis, 2002; Tong et al., 2006). Although the stimulus remains unchanged during the experience of BR, perception alternates between periods of dominance of the attended image and near complete suppression of the unattended image. This bistable perception phenomenon provides valuable insight into the functioning of the visual system, highlighting its dynamic nature and the intricate mechanisms involved in reconciling conflicting sensory inputs and perceptual ambiguity.

In this thesis, I use binocular rivalry to reveal the neural correlates of bistable perception and present experiments designed to provide deeper insights into the mechanisms underlying the visual system's function during this phenomenon.

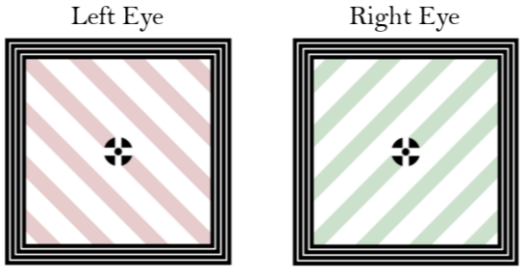

Figure 1.2 Binocular rivalry stimulus. In this example, each eye is shown either red or green orthogonal gratings. The competing gratings have an interocular orientation difference of 90°.

During binocular rivalry induced by the images depicted in Figure 1.2, participants experience perceptual shifts between near complete and exclusive visibility of either red or green stimuli. Amid these transitions, a third perceptual state emerges, wherein partial visibility of both right and left eye images is perceived simultaneously, termed mixed percepts. These experiences signify perceptual ambiguity, as illustrated in Figure 1.3C, where neither red nor green is dominantly perceived. These mixed periods are typically characterized by the perception of piecemeal percepts rather than superimposed, plaid-like, patterns (Alais & Melcher, 2007).

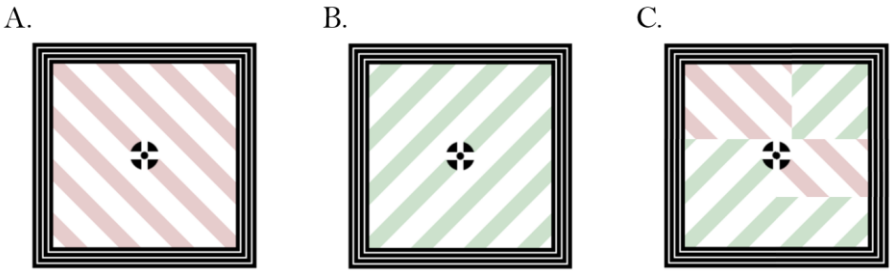

Figure 1.3 Binocular rivalry percepts. During binocular rivalry with red and green orthogonal gratings shown independently to each eye (i.e., Figure 1.1), three percepts are generally reported. **A.** Dominant red percept. **B.** Dominant green percept. **C.** Example of mixed percepts, where portions of each dominant percept are perceived. The experiments in chapters two, three and four, include reporting procedures during rivalry that include all three perceptual states; dominant red, dominant green, and mixed.

1.2.A Models of Binocular Rivalry

Early theoretical models of binocular rivalry focused on reciprocal inhibition between monocular neurons (i.e., neurons that receive input solely from one eye) (Blake, 1989) mainly found in the primary visual cortex (Hubel & Wiesel, 1968; Blasdel & Fitzpatrick, 1984). These models focused on eye-versus-eye mechanism of perceptual competition of rivalry, and reciprocal inhibition, where the retinal input from each independently viewed image competed for perceptual dominance. However, other models, such as multistage models proposed by Wilson (2003) and Freeman (2005), suggested that the rivalry process involves multiple stages of neural processing, each with the potential for competitive interactions between competing percepts. Hybrid models,

like those by Tong et al. (2006), have attempted to reconcile these different perspectives. Moreover, subsequent models of binocular rivalry have underscored the importance of binocular neurons, which receive sensory information from both eyes (Logothetis et al., 1996; Kovacs et al., 1996; Wilson, 2003; Said & Heeger, 2013). These models have provided a more nuanced understanding of the neural mechanisms underlying binocular rivalry. In recent years, tristable models of rivalry have emerged, offering support for mixed perceptual states (Riesen et al., 2019; Qiu et al., 2020). These models have expanded our understanding of the complexity of bistable and multistable perception, highlighting the dynamic nature of perceptual competition in the visual system.

Throughout this thesis, I explore these theoretical interpretations and propose a neural model of binocular rivalry that highlights the significance of binocular neurons and feedback mechanisms. This model aims to integrate the findings of the experiments I present on binocular rivalry, particularly as they relate to increasing demands for interocular grouping.

1.2.B Neuroimaging Studies of Binocular Rivalry

Neuroimaging studies of binocular rivalry have covered a depth of techniques (i.e., EEG, MEG, fMRI) each providing insights into the neural correlates of bistable perception.

Magnetoencephalography (MEG) studies have identified various brain regions involved in bistable perception, though the extent of these regions is debated. Some studies have found activity across several cortical regions beyond the occipital cortex, including temporal, parietal, and frontal areas (Tononi et al., 1998; Srinivasan et al., 1999; Cosmelli et al., 2004). However, MEG studies using frequency-tagging methods with phase-locking techniques between the brain responseand the signals from the fundamental frequencies have reported more restricted topography of activity, mainly in the occipital cortex and early visual areas (Kamphuisen et al., 2008; Bock et al., 2019).

Functional magnetic resonance imaging (fMRI) studies of BR have shown increased blood-oxygen-level-dependent (BOLD) signals in multiple cortical regions beyond the occipital pole, particularly in the right frontal, parietal, and occipital areas during rivalry viewing (Wilcke et al., 2009; Rees, 2007). Specifically, Buckthought et al. (2011) identified BOLD signals in early visual areas (V1, V2, V3) and high-level extrastriate areas (lateral occipital and medial temporal). Further studies highlighted the role of the right hemisphere's inferior and superior parietal areas

(Buckthought et al., 2015). Additionally, Wunderlich et al. (2005) found neural correlates of BR as early as the lateral geniculate nucleus.

Using more causal methods to uncover brain regions important during binocular rivalry (BR), transcranial magnetic stimulation (TMS) studies have shown that disrupting activity in the parietal cortex affects BR dynamics (Carmel et al., 2010; Zaretskaya et al., 2010). Although both studies highlighted regions in the parietal cortex, their effects were conflicting: Zaretskaya et al. (2010) reported that stimulating the right intraparietal sulcus prolonged periods of stable percepts, while Carmel et al. (2010) found that stimulating the right superior parietal cortex significantly shortened dominance durations. Nevertheless, these findings emphasize the importance of parietal brain regions.

In this thesis and presented in the MEG experiments in the third and fourth chapters, I will explore the diverse brain regions implicated in previous studies of binocular rivalry, with a particular focus on event-related changes in steady-state visual evoked field (SSVEF) that are time-locked to the experience of bistable perception. Specifically, I will investigate how SSVEFs correlate with perceptual transitions during binocular rivalry, hypothesizing that distinct cortical areas, including both early visual (i.e., V1 and V2) and higher-order regions (i.e., extrastriate regions such as the lateral occipital and parietal cortex), exhibit unique SSVEF patterns that correspond to shifts in perceptual dominance. This approach aims to elucidate the temporal dynamics and neural mechanisms underlying bistable perception.

1.3 Interocular Grouping

Within the context of 'eye-based' versus 'stimulus-based' rivalry, it has been observed that alternations in perception can occur even in the absence of traditional binocular rivalry images. This phenomenon, known as interocular grouping (IOG), is characterized by the subdivision and presentation of portions of each dominant representation across both eyes (Diaz-Caneja, 1928; translated by Alais, O'Shea, Mesana-Alais, & Wilson, 2000; Kovacs et al., 1996). IOG presents a remarkable instance of bistable perception that underscores the pivotal role of binocular neurons, facilitating perceptual integration in brain regions receiving input from both eyes.

Interocular grouping occurs when complementary bistable patches of a whole image are subdivided and presented across both eyes (see Figure 1.4). The brain integrates these coherent percepts through binocular combination processes, resulting in perceptual alternations akin to those observed in traditional binocular rivalry.

While mixed percepts during IOG share similarities in perceptual ambiguity with those experienced during BR, they exhibit fundamental differences. In BR, mixed percepts depict a state where portions of images presented independently to each eye compete for dominance. Similarly, this competition can arise during IOG; however, the monocular input presented to each eye may also constitute a mixed percept, as shown in Figure 1.5D-E.

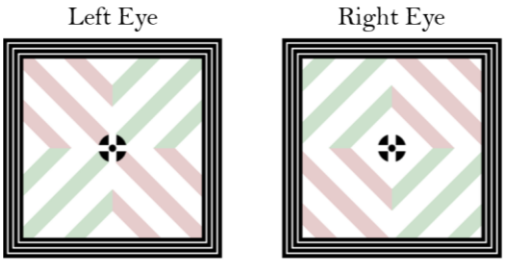

Figure 1.4 Interocular grouping stimulus. Each eye is shown complementary bistable patches of red and green orthogonal gratings. The traditional binocular rivalry images (i.e., Figure 1.1) were subdivided into four patches for interocular grouping. The red and green gratings have an interocular orientation difference of 90º.

As depicted in Figure 1.4, participants experiencing four-patch interocular grouping will report different visual percepts. The phenomenon of IOG will be experienced with periods of binocular integration, where participants perceived the majority of the image as being either red (Figure 1.5A) or green (Figure 1.5B). These perceptual instances where red or green orthogonal gratings are perceived in the majority of the image are termed dominant percepts. In addition, as presented in Figure 1.3 during BR, participants experiencing interocular grouping will also report periods where portions of both red and green orthogonal gratings are perceived. These instances (Figure 1.5C-E) are termed mixed percepts. It is important to note that a key distinction is made between mixed percepts experienced during BR and IOG conditions. In this thesis, mixed percepts during IOG include both binocularly viewed (Figure 1.5C) and monocularly viewed (Figure 1.5D-E) percepts, whereas mixed percepts experienced during BR are restricted to piecemeal percepts that include portions of both red and green gratings that were independently shown to individual eyes (Figure 1.2).

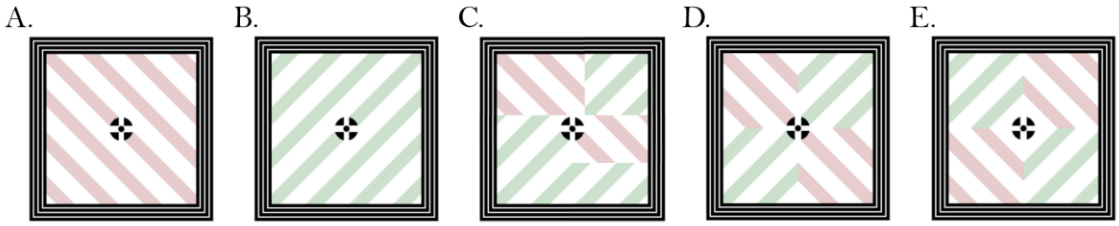

Figure 1.5 Visual percepts experienced during four-patch interocular grouping. When participants experience interocular grouping with four bistable complementary patches in the experiments presented in chapters two and three (Figure 1.4), five types of percepts were reported. **A.** Dominant red percept. **B.** Dominant green percept. **C.** Mixed percepts from patches of images shown to each eye. **D.** Monocularly viewed image (i.e., left eye) characterized as a mixed percept. **E.** Monocularly viewed image (i.e., right eye) characterized as a mixed percept.

1.3.A Models of Interocular Grouping

Early investigations in visual psychophysics demonstrated that dichoptic presentation of complementary concentric circles and parallel lines triggered alternating periods of "eye-based" monocular images and remarkably, unified percepts necessitating integration of inputs from both eyes (Diaz-Caneja, 1928; translated by Alais, O'Shea, Mesana-Alais, & Wilson, 2000). These insights from IOG experiments strongly suggest compelling evidence underscoring the significant involvement of binocular neurons in governing perceptual dominance and suppression during bistable perception. The fundamental principles of interocular grouping stand in direct contrast to the 'eye versus eye' models of rivalry. Thus, interocular grouping serves as a remarkable instance of perceptual rivalry, emphasizing the role of binocular neurons within the visual system and higher-order processes such as Gestalt principles of grouping based on similarity and continuity.

1.3.B Neuroimaging Studies of Interocular Grouping

Neuroimaging investigations into interocular grouping have historically been less extensive compared to studies on binocular rivalry and have often been explored in conjunction with the latter.

An fMRI study examining interocular grouping alongside binocular rivalry revealed intriguing findings. Buckthought et al. (2021) reported increased blood-oxygen-level-dependent (BOLD) signal in the lateral occipital (LO) and intraparietal (IP) regions during interocular grouping compared to binocular rivalry. Moreover, EEG research conducted by Sutoyo & Srinivasan (2009) contributed valuable insights. They observed reduced activity during interocular grouping relative to binocular rivalry conditions, with the most pronounced markers localized in the occipital electrodes. These findings underscore the importance of exploring interocular grouping in its own right, shedding light on the distinct neural mechanisms underlying this phenomenon and its interplay with binocular rivalry.

In the third chapter, I present novel findings on a neuroimaging study of interocular grouping using magnetoencephalography that uncover neural correlates of bistable perception during this phenomenon.

1.4 Interocular Grouping Demands

Interocular grouping serves as a valuable tool for investigating perception alongside binocular rivalry. This involves utilizing specific stimuli in conjunction with interocular grouping to compare rivalry conditions (Kovacs et al., 1996; Sutoyo & Srinivasan, 2009; Buckthought et al., 2021; Yoon & Hong, 2024). To deepen our understanding of perceptual grouping, I conducted experiments using various types of IOG images. Initially, an image can be divided into two equal parts and presented in patches across the eyes. This basic approach offers insights into the mechanisms of perceptual grouping when contrasted with traditional binocular rivalry. However, it remains unclear whether the outcomes of grouping would be affected if the original image were subdivided into a larger number of complimentary bistable patches, such as transitioning from two-patch to four-patch IOG configurations.

1.4.A Complimentary Bistable Patches

Interocular grouping further emphasizes the role of binocular integration by presenting complementary bistable patches taken from subdividing a traditional BR image across the two eyes (Kovacs et al., 1996). In the experiments presented in Chapters Two and Three, the interocular grouping stimulus contains images with an increasing number of complementary bistable patches to explore the effects of escalating grouping demands during bistable perception. Images with two-, four-, and six-patch interocular grouping are tested to investigate these effects.

The increase in the number of complementary bistable patches for a matched stimulus is demonstrated for binocular rivalry (Figure 1.6A) and interocular grouping with two- (Figure 1.6B) and four-patches (Figure 1.6C). Within this context, I hypothesize that higher-order grouping conditions will result in fewer dominant percepts (i.e., reduced alternation rates) due to the increased requirements for unscrambling monocularly presented images into coherent perceptions of red and green whole-images. Additionally, I present psychophysics and neuroimaging experiments aimed at uncovering these mechanisms.

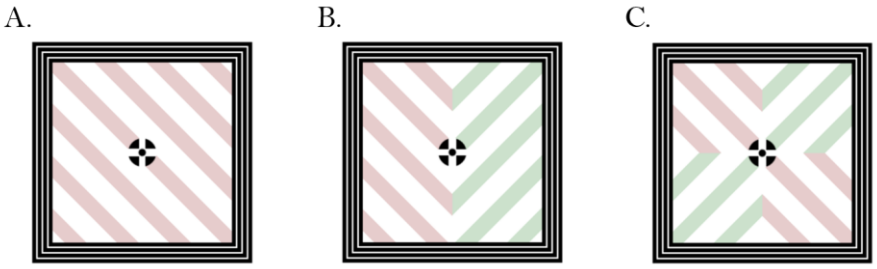

Figure 1.6 Increasing interocular grouping demands. The interocular grouping demands are increased from binocular rivalry, to two- and four-patch interocular grouping for a perceptually matched stimulus. **A.** One eye's stimulus for traditional binocular rivalry. **B.** One eye's stimulus for two-patch vertical meridian division interocular grouping. **C.** One eye's stimulus for four-patch interocular grouping.

1.4.B Vertical versus Horizontal Image Meridian Division

Drawing from physiological evidence indicating distinct visual processing across vertical and horizontal meridians (Tootell et al., 1998; Larsson & Heeger, 2006; Large et al., 2008), I conducted experiments to investigate interocular grouping conditions involving both vertical and horizontal image meridian divisions (see Figure 1.7). Vertical image meridian division during interocular grouping (IOG) (Figure 1.7A) entails grouping right and left visual hemifields together in the brain for a unified percept, while horizontal division (Figure 1.7B) necessitates grouping the top and bottom visual hemifields. These variations in meridian orientation impose distinct physiological demands on the visual system during bistable perception.

Tootell et al. (1998) proposed a multi-stage processing model where visual information progresses from the contralateral to ipsilateral visual fields via the lateral occipital (LO) region. Larsson & Heeger (2006) identified finer regions within the lateral occipital, LO1 and LO2, as key in integrating shape information across the entire contralateral visual hemifield. Additionally, Large et al. (2008) suggested a two-stage model in which LO processes visual representations for upper and lower visual fields before integrating them across both visual hemifields. Collectivity, these studies highlight the pivotal role of the lateral occipital region in integrating visual information. I hypothesize that grouping mechanisms may show broad similarities between vertical and horizontal two-patch IOG. However, differences in finer scales of sensory processing may emerge between the two orientations, particularly in specific brain regions such as LO.

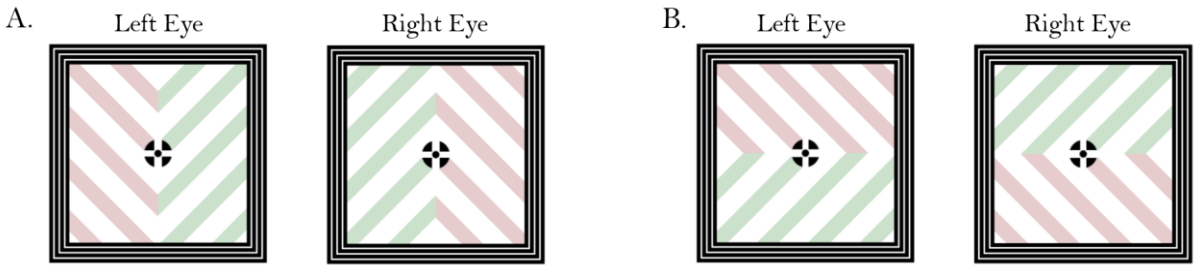

Figure 1.7 Two-patch interocular grouping stimulus. Each eye is shown complementary interocular grouping subdivided into two complementary bistable patches. **A.** Two-patch interocular grouping with the central division along the vertical image meridian. **B.** Two-patch interocular grouping with the central division along the horizontal image meridian.

1.5 Individual Differences

Although bistable perception phenomena, such as binocular rivalry, are universally acknowledged, the perceptual dynamics and the factors influencing perceptual switches can vary greatly among individuals. This variability underscores the intricate nature of human perception, where individual differences play a significant role in shaping perceptual experiences. Individual variances in bistable perception encompass the interpretation of ambiguous stimuli encountered in tasks like binocular rivalry. For instance, the alternation rate between dominant percepts during binocular rivalry differs significantly between observers (Brascamp et al., 2015). Furthermore, twin studies have unveiled that this trait-like binocular rivalry alternation rate is partially heritable, highlighting the interplay between genetic factors and perceptual processes (Miller et al., 2010; Shannon et al., 2011). In this thesis, I explore the subject of individual differences in bistable perception investigate whether the behavioral measures of binocular rivalry (i.e., alternation rate) align with those observed during interocular grouping. This is significant, as similarities would provide support towards a shared foundation in the underlying mechanisms of perception between these two phenomena.

1.5.A Fast versus Slow Switchers

Expanding on individual differences in switch rates between dominant percepts during bistable perception, observers have previously been characterized as ‘fast’ and ‘slow’ switchers in neural correlates of rivalry (Fesi & Mendola, 2015; Bock et al., 2019). Notably, fast switchers demonstrate more frequent alternations between dominant perceptions of rivaling images, while slow switchers experience fewer alternations. However, this categorization provides a broad overview, as within-participant variability persists, and the distribution of dominant durations is best described by a gamma-shaped distribution (Levelt, 1956; Fox & Herrmann, 1967). Within this framework, I propose that predictive neural markers may be identified between alternation rates during bistable perception, such as naturally occurring alpha oscillations, which have been frequently associated with inhibition (see section 1.7).

1.5.B Excitation and Inhibition Ratio

The balance between excitation and inhibition (E:I) in the visual system is crucial for the neural mechanism of bistable perception. This significance is highlighted by binocular rivalry studies involving individuals with autism, a neurodevelopmental condition believed to be influenced by an imbalance in the E:I ratio (Rubenstein & Merzenich, 2003). These studies have reported altered rivalry dynamics and slowed alternation rates during binocular rivalry in autism populations (Robertson et al., 2013; Spiegel et al., 2019; Skerswetat et al., 2022). Understanding the role of excitation and inhibition in bistable perception provides valuable insights into the underlying mechanisms of perceptual switching, contributing to our broader understanding of sensory processing and cognitive function. Within participants, I hypothesize that the dynamic interaction and real-time modulation between excitation and inhibition in the visual system contribute significantly to the mechanism underlying bistable perception.

1.6 Magnetoencephalography

Magnetoencephalography (MEG) is a non-invasive neuroimaging technique that records neural activity by measuring magnetic fields generated by electrical activity in neuronal populations (Cohen, 1968; Baillet, 2017; Gross, 2019). It represents a pivotal advancement in brain imaging technology, offering distinct advantages over conventional methods such as functional magnetic resonance imaging (fMRI) and electroencephalography (EEG). MEG's superior temporal resolution compared to fMRI, capturing neural activity with millisecond precision, allows researchers to investigate the dynamics of brain function, including oscillatory or event-related processes, providing valuable insights into the temporal sequence of cognitive events. Additionally, MEG boasts superior spatial resolution compared to EEG, providing researchers with a more precise understanding of brain dynamics.

Furthermore, MEG allows for the study of brain activity in real-time, enabling researchers to investigate the temporal dynamics of cognitive processes as they unfold. This capability offers unique opportunities for studying the dynamic interplay between different brain regions and cognitive functions.

Moreover, integrating MEG with T1-weighted anatomical MRI allows for individual anatomical co-registration, enhancing spatial resolution and enabling precise source localization. This combination empowers researchers to pinpoint the neural generators of MEG signals with unprecedented accuracy, elucidating the underlying neural mechanisms of cognitive processes. Furthermore, MEG's non-invasive nature and minimal interference from external noise sources make it an appealing choice for studying brain function across various experimental settings.

In chapters three and four, I leverage MEG methods to uncover novel neural mechanisms underlying bistable perception during binocular rivalry and interocular grouping. By utilizing MEG's superior temporal and spatial resolution, I aim to elucidate the dynamics of neural activity associated with bistable perceptual phenomena, contributing to our understanding of the neural basis of perception.

1.6.A Flicker Frequency-Tagging

When flickering visual stimuli are presented, neural entrainment in the visual cortex is observed and recorded at the frequencies matching the stimulus (Adrian & Matthews, 1934; Walter et al., 1946; Regan, 1966). This phenomenon underscores the brain's remarkable and adaptive ability to synchronize its activity with external sensory inputs. Such activity highlights neural correlates of perception and populations of neurons that respond to the visual information. This entrainment is an essential tool for understanding how the brain processes and integrates sensory information.

Frequency-tagging methods during bistable perception (i.e., binocular rivalry) entail presenting dichoptic flicker frequencies independently to each eye (Brown & Norcia, 1997). This approach allows researchers to selectively entrain neural responses corresponding to each eye's input, providing insights into the dynamics of perceptual alternations during binocular rivalry. An example of this phenomenon is shown in Figure 1.8, illustrating the differential neural responses in the primary visual cortex during binocular rivalry with untagged and frequency-tagged stimuli, highlighting the efficacy of this method in dissecting the underlying neural mechanisms.

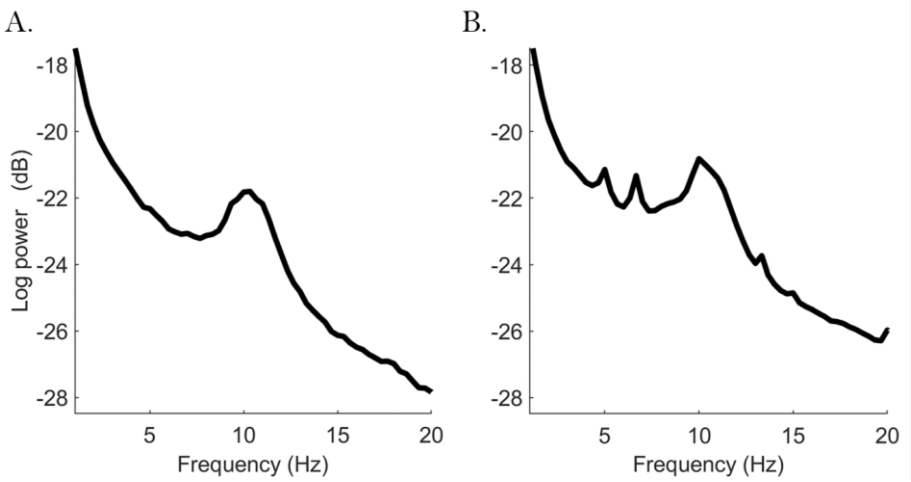

Figure 1.8 MEG power spectrum density analysis during BR in the primary visual cortex. **A.** Power spectrum analysis during untagged binocular rivalry recorded with MEG (N = 25) in the primary visual cortex. **B.** Power spectrum analysis during frequency-tagged (f_1 = 5 Hz and f_2 = 6.67 Hz) binocular rivalry recorded with MEG (N = 25) in the primary visual cortex. The data used for the power spectrum density analysis is presented in chapters three and four.

Further, steady-state visual evoked responses (SSVER), which are robust and steady responses of neural activity to visual stimuli presented at fixed frequencies, can be recorded with EEG/MEG to investigate neural entrainment and perceptual responses during frequency-tagging paradigms (Norcia et al., 2015). Specifically, SSVERs can be subdivided into steady-state visually evoked potentials (SSVEP) that are recorded with EEG, and steady-state visually evoked fields (SSVEF) that are recorded with MEG. This integrated approach allows for the simultaneous measurement of neural oscillations and perceptual dynamics, providing valuable insights into the underlying mechanisms of visual processing. A well-documented phenomenon is the observation of waxing and waning of the SSVER to perceptually dominant and suppressed percepts during binocular rivalry (Brown & Norcia, 1997; Zhang et al., 2011; Jamison et al., 2015; Spiegel et al., 2019; Bock et al., 2019), as exemplified in Figure 1.9.

In the third chapter, I utilized methods of frequency-tagging and record SSVEF responses with MEG during binocular rivalry with interocular grouping to disentangle neural correlates of dominance and suppression during bistable perception.

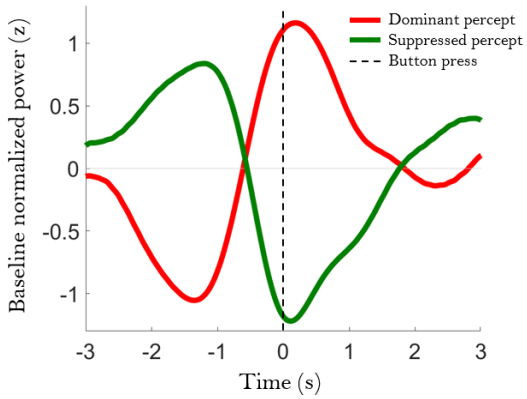

Figure 1.9 SSVEF response during MEG frequency-tagged binocular rivalry in the primary visual cortex. In this experimental design, unique flicker frequencies were presented dichoptically to each eye during binocular rivalry (i.e., 5 Hz and 6.67 Hz) during continuous MEG recording. The brain's response to these frequencies were filtered to isolate the fundamental frequencies. This figure shows the waxing and waning of SSVEF response for dominant and suppressed percepts in the primary visual cortex, centered around a button press reported by participants as a dominant percept alternation. These results, presented in the third chapter, serve as an illustration of dichoptic frequency-tagged methods.

1.7 Alpha Oscillations

Oscillatory brain dynamics are often grouped into frequency bands. Alpha oscillations are a type of neural oscillation that occur between the frequencies of approximately 8 to 13 Hz. They are predominantly observed (i.e., with EEG or MEG) over the occipital and parietal cortex (Chapman et al., 1984; Ciulla et al., 1999; Katyal et al., 2019). Alpha oscillations have been associated with several functions in the visual system, such as inhibition, attention, and perception (Clayton et al., 2018). Neural oscillations, in general, are rhythmic brain activities that are thought to play critical roles in a variety of functions including perception and attention. Alpha oscillations, specifically, are believed to modulate the excitability of cortical networks, thereby influencing cognitive processes and sensory information processing.

1.7.A Alpha as an Inhibitor in the Visual System

Alpha oscillations have been hypothesized to exert inhibitory effects on neural activity (Klimesch et al., 2007; Jensen & Mazaheri, 2010; Klimesch et al., 2012) and to contribute to pulsed-inhibition of ongoing visual processing (Mathewson et al., 2011). Within the visual system, alpha oscillations are thought to play an inhibitory role, modulating visual perception by selectively suppressing irrelevant or distracting information (Clayton et al., 2018).

In the context of binocular rivalry, inhibition mediated by alpha oscillations may influence which of the competing images dominates perception at any given time. This is relevant, as several theories of bistable perception have posited the role of reciprocal monocular inhibition (Matsuoka 1984; Lehky 1988; Blake, 1989). The inhibitory effects of alpha oscillations may be involved in the suppression of the unattended image, thereby facilitating the dominance of the attended, consciously perceived image. This dynamic interplay of excitation and inhibition, modulated by alpha oscillations, is crucial for understanding how the brain resolves conflicting sensory information to produce a coherent perceptual experience.

In the fourth chapter, I hypothesize that alpha band power changes facilitate perceptual transitions during binocular rivalry. Increased alpha power is expected to stabilize the dominant percept, while disruptions may enhance the suppressed image's salience, leading to a switch.

1.7.B Alpha and Bistable Perception

Within the context of bistable perception, a handful of studies have investigated alpha oscillations within the context of bistable perception. Piantoni et al. (2017) examined changes in alpha band power during bistable perception using EEG and a Necker cube-type image. They found that alpha power around the parieto-occipital sulcus predicted the duration of bistable percepts, with a decrease in alpha power preceding perceptual alternations.

Katyal et al. (2019) explored characteristics of peak alpha oscillations during binocular rivalry (BR) using EEG electrodes over the occipital cortex. They reported significant correlations between peak alpha frequency during BR and alternation rate. Additionally, they found that peak alpha frequency measured during a fixation period prior to image presentation was correlated with percept durations during BR, with faster alpha oscillations predicting shorter percept durations, particularly over bilateral occipital channels. Cuello et al. (2022) investigated the relationship between peak alpha frequency during BR and perceptual alternations. They found significant correlations between peak alpha frequency and alternation rate, suggesting a potential role of alpha oscillations in regulating perceptual switching. Sponheim et al. (2023) conducted resting-state MEG analysis and examined the relationship between peak alpha frequency within the occipital cortex and BR percept duration. They found that peak alpha frequency was correlated with percept duration, indicating that alpha oscillations may influence the dynamics of bistable perception.

Based on these findings, it can be predicted that alpha oscillations play a crucial role in regulating the dynamics of bistable perception.

2

Effects of Interocular Grouping Demands on Binocular Rivalry

Manuscript published in the Journal of Vision

Mokri, E., da Silva Castanheira, J., Laldin, S., Landry, M., & Mendola, J. D. (2023). Effects of interocular grouping demands on binocular rivalry. Journal of Vision, 23(10), 15-15.

DOI: https://doi.org/10.1167/jov.23.10.15

2.1 Preface

The second chapter explores the effects of increasing interocular grouping demands during binocular rivalry using psychophysics. Utilizing a two-fold approach with a matched stimulus for BR and IOG, the effects of grouping were explored by increasing the number of complementary bistable patches, and changing the orientation of the central meridian division. This chapter unveils novel findings while also laying a conceptual foundation for subsequent neuroimaging studies.

Given the novelty of the grouping demands, the aim was to characterize the behavioral measures of rivalry comprehensively, providing insight into our stimuli before embarking on the MEG experiments in chapters three and four. Notably, the incidence of mixed percepts exhibited a disproportionate impact with an increase in the number of complementary bistable patches. Additionally, a trend favoring grouping along the vertical image meridian emerged in the context of two- and six-patch interocular grouping.

To ensure consistency in rivalry stimuli across chapters, understanding the effects of flicker frequencies was of high priority. Prior studies had indicated that flickering stimuli could prolong dominant percepts during interocular grouping (Knapen et al., 2007), a noteworthy observation given the potential application of flickering stimuli in neuroimaging studies (e.g., EEG and MEG) via a frequency-tagged approach. Hence, BR and IOG were presented with flicker frequencies.

Throughout the forthcoming chapter, emphasis is placed on the disproportionate impact on mixed percepts compared to their dominant counterparts. While increasing interocular grouping demands led to enhanced stability in dominant percept duration and predominance, a concurrent increase in mixed percept duration was observed under higher order grouping conditions.

The second chapter also introduces the topic of individual differences, a theme that is further explored in subsequent chapters. Within the framework of binocular rivalry with interocular grouping, correlations in switch rates and percept durations across rivalry conditions are examined. Notably, individuals who exhibit fast switching tendencies during BR also tend to display rapid switching behaviors during IOG, and vice versa for slow switchers. This finding lends support to the notion of common neural mechanisms underlying BR and IOG, a concept that will be thoroughly investigated in later chapters focusing on neuroimaging studies of rivalry.

2.2 Abstract

Binocular rivalry (BR) is a visual phenomenon in which perception alternates between two non-fusible images presented to each eye. Transition periods between dominant and suppressed images are marked by mixed percepts, where participants report fragments of each image being dynamically perceived. Interestingly, BR remains robust even when typical images are subdivided and presented in complementary patches to each eye, a phenomenon termed interocular grouping (IOG). The objective of the present study was to determine if increasing grouping demand in the context of BR changes the perceptual experience of rivalry. In 48 subjects with normal vision, mean dominant and mixed percept durations were recorded for classic BR and IOG conditions with increasing grouping demands from two, four, and six patches. We found that, as grouping demands increased, the duration of mixed periods increased. Indeed, durations of dominant and mixed percepts, as well as percentage of time spent in dominant or mixed state, differed significantly across conditions. However, durations of global dominant percepts remained relatively stable and saturated at about 1.5 seconds, despite the exponential increase in possible mixed combinations. Evidence shows that this saturation followed a nonlinear trend. The data also indicate that grouping across the vertical meridian is slightly more stable than for the horizontal meridian. Finally, individual differences in speed of alternation identified during BR were maintained in all interocular grouping conditions. These results provide new information about binocular visual spatial integration and will be useful for future studies of the underlying neural substrates and models of binocular vision.

2.3 Introduction

Binocular rivalry (BR) refers to the alternating periods of dominance and suppression experienced when each eye is presented with sufficiently dissimilar monocular input (Blake, 1989; Blake & Logothetis, 2002; Tong, Meng & Blake, 2006; Sutoyo & Srinivasan, 2009). During visual dichoptic presentation (i.e., separately to each eye) of two non-fusible images, subjects report periods of alternation between perceptual awareness of each image. Periods of alternating percepts can be characterized as near complete visibility of one image, termed the dominant percept, whereas the second image is suppressed from conscious perception. When subjects experience a perceptual switch, the previously suppressed image becomes dominant in visibility. During BR, the stimuli presented to each eye remain unchanged, however, the perceptual awareness of the images cycle between instances of dominance and suppression. Furthermore, during these periods of transition, subjects experience instances of partial visibility of patches from both images, termed mixed percepts. In recent years, more importance has been attributed to measuring mixed percepts experimentally and determining their theoretical role in binocular vision models (Said & Heeger, 2013; Katyal, Engel, He, & He, 2016, Sheynin, Proulx, & Hess, 2019; Bock, Fesi, Baillet, & Mendola, 2019).

Although early models of BR focused primarily on reciprocal inhibition between monocular neurons (i.e., V1 neurons that receive input from one eye only) (Blake, 1989), a wealth of subsequent evidence has supported a role of binocular neurons as well (e.g., Logothetis, Leopold, & Sheinberg, 1996; Wilson, 2003; Said & Heeger, 2013). Findings that highlight the likely functional role of binocular neurons reveal that modifications of BR stimuli to disrupt monocular information still yield robust alternations of perceptual dominance. In one such demonstration, the entire image is exchanged between the eyes at a fast rate, but normal perceptual rivalry remains intact (e.g., Logothetis et al., 1996; see also Christiansen, D'Antona, & Shevell, 2017). Likewise, another important type of rivalry, and the focus of the present work, is interocular grouping (IOG). In IOG, complementary patches from two intact images are presented to each eye, requiring combinatorial processing between the visual inputs from each eye to achieve a unified percept of the global image (Kovács, Papathomas, Yang, & Fehér, 1996). Early observations in visual psychophysics revealed that complementary concentric circles and parallel

lines (Figure 2.1A) yielded not only periods of alternations of so called "eye-based" monocular images but also unified percepts requiring grouping between the monocular inputs from the two eyes (Diaz-Caneja, 1928; translated by Alais, O'Shea, Mesana-Alais, & Wilson, 2000). In this way, evidence from IOG experiments provide compelling evidence that binocular neurons contribute to perceptual dominance and suppression in the context of BR.

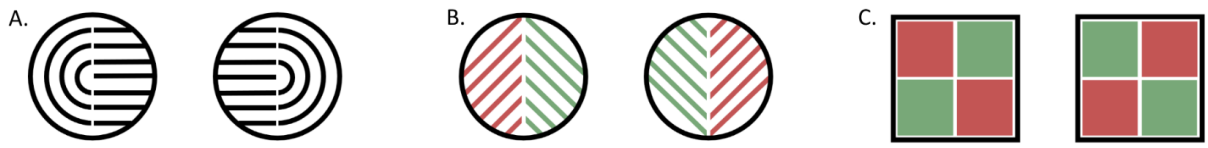

Figure 2.1 Example of interocular grouping stimuli adapted from literature review. A. Reproduction of Diaz-Caneja stimuli (1928), where stimulus flicker altered interocular grouping during BR (Knapen et al., 2007). **B.** Reproduction of visual stimuli presented by Sutoyo and Srinivasan (2009). **C.** Reproduction of visual stimuli presented by Golubitsky et al. (2019) showing four quadrant interocular grouping (see Discussion section).

Different proposals have been made to explain IOG. On the one hand, higher level stimulus pattern integration argues against monocular eye-dominance accounts of alternation during BR, as outlined in the previous paragraph (Kovács et al., 1996). Conversely, some proponents of lower-level eye-of-origin theory claim that simultaneous eye-based dominance of local patches of the stimulus could drive alternating percepts during IOG (as might be implemented by horizontal connections between monocular neurons in V1) (Lee & Blake, 2004). In their view, coordinated dominance between difference regions of the retinotopic representation (local zones that correspond to local patches of the stimulus) as opposed to dominance based on the representation of the entire stimulus could explain IOG. However, recent functional magnetic resonance imaging (fMRI) findings support the idea that IOG rivalry primarily occurs between binocular neurons with larger receptive fields in higher level areas (Buckthought, Kirsch, Fesi, & Mendola, 2021). In sum, the observation that individuals experience coherent percepts when viewing intermingled patchwork of rivalrous images highlights the importance of spatial integration mechanisms for the experience of BR.

In the context of BR with suprathreshold stimuli, mixed percepts rarely appear as a fusion or superimposition of the right and left eye stimuli (a plaid in the case of gratings). Instead, patches of partial visibility of each image are commonly reported (Kovács et al., 1996) and are also referred to as piecemeal rivalry (Alais & Melcher, 2007; Skerswetat, Bex, & Baron-Cohen, 2022). In the case of IOG, one would expect that periods of mixed percepts would be substantially increased if monocular eye-based rivalry was the primary mechanism. Alternatively, if binocular neurons are the primary substrate, then Gestalt principles of good continuation and global consistency may result in mixed percepts that minimally differ from classic BR. Accordingly, for both BR and IOG, characterizing mixed percepts is interesting, not only because they mark the intermittent transition period between cycles of dominance but also because they may represent a distinct mode of binocular integration that is crucial to the combination of information from both eyes during IOG. In fact, previous reports indicate that levels of inhibition in some cortical areas may increase during mixed percepts (e.g., Katyal at al., 2016). If IOG provides a more challenging environment for binocular integration to occur, we aimed to ask if mixed percepts would be selectively affected by increasing IOG demands.

In recent years, tristability models of BR (i.e., alternations among three percepts) have emerged (Riesen, Norcia, & Gardner, 2019; Qiu, Caldwell, You, & Mendola, 2020). This view proposes alternations between each of the monocular inputs, as well as some type of mixed percept arising from the combination of the dichoptic stimuli. It is acknowledged, that the mixed percepts elicited in these two studies are reflective of binocular fusion as opposed to piecemeal percepts. The model of tristability is relevant because it highlights mixed percepts as a distinct perceptual state of interest with its own relative stability. This emergent viewpoint follows in part from neurophysiological evidence linking intermittent periods of mixed percepts to a distinct neural signature of intermodulation frequencies when the images are frequency tagged during neuroimaging studies (Katyal et al., 2016; Bock et al., 2019). This outcome emphasizes the role of binocular neurons marked by the integration of monocular inputs, although these studies looked at intermodulation frequencies during BR only, and the same is not known for IOG. We aimed to explore the notion of tristability in classic BR and IOG with the inclusion of mixed percepts as a stable perceptual state. We believe that an indication of tristability in our study would find relatively proportional probability of transitions between dominant-to-dominant percepts, as well

as dominant-to-mixed states (i.e., participants transitioning from a dominant red percept to either a dominant green, or a mixed percept).

Alternation rates have long been important in the characterization of BR and other bistable percepts. This is defined as the number of dominant perceptual alternations between each eye's stimuli over a defined time (Brascamp, Klink, & Levelt, 2015). Interestingly, there are many recent findings highlighting individual differences in switch rates observed during rivalry. The idea that switch rate is partially heritable is supported by twin studies (Miller et al., 2010; Shannon, Patrick, Jiang, Bernat, & He, 2011) and studies that found neural differences between fast and slow switchers (Fesi & Mendola, 2015; Bock et al., 2019). In addition, there is evidence that rivalry dynamics change with age, are affected by different neurological conditions or other previous experience (Scocchia, Valsecchi, & Triesch, 2014; Robertson, Ratai, & Kanwisher, 2016; Ye, Zhu, Zhou, He, & Wang, 2019). Finding a strong correlation between the behavioural measures of BR and IOG (i.e., alternation rate, and durations of dominant and mixed percepts), would indicate a similar underlying neural mechanism.

In the current study, we compared the effects of increasing the number of patches distributed to each eye by dividing our classic BR image with orthogonal gratings into five different IOG conditions with two-, four-, and six-patch conditions (Figure 2.2). Grouping across the horizontal meridian was compared with grouping across the vertical meridian. Reports of mixed percepts as well as coherent dominance/suppression were obtained throughout all conditions. Whereas previous studies have used similar but isolated stimuli (Figures 2.1A and 2.1B), our design sought to systematically alter the location and number of image divisions while importantly maintaining the same visual percept for participants between classic BR and our five IOG conditions. Finally, in this study, we used flickering stimuli primarily to accommodate the separate magnetoencephalography experiments conducted with a subset of subjects (not reported here). We already know that dichoptic flicker alone does not cause rivalry. However, it is interesting that flickering stimuli have been shown to increase the duration of dominant percepts during interocular grouping with the use of flicker rates from 10 to 24 Hz (Knapen, Paffen, Kanai, & van Ee, 2007). For that reason, we also compared two rates of dichoptic flicker ranging between 5 and 12 Hz, to test for any large facilitatory effect on grouping when the higher flicker rate was used.

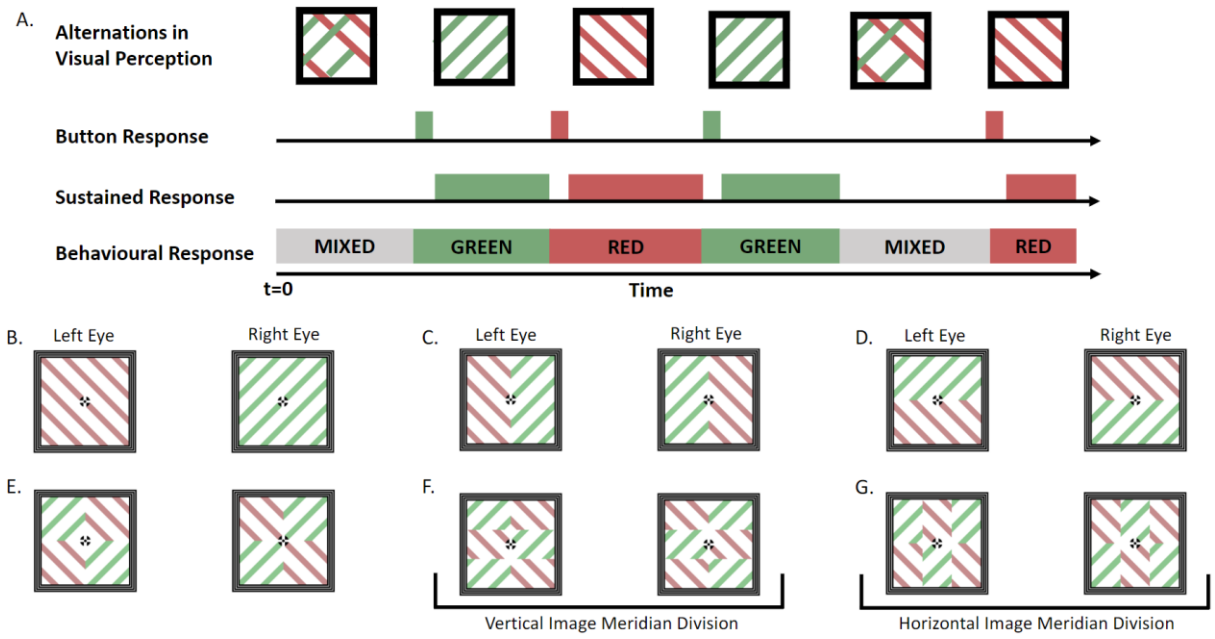

Figure 2.2 Experimental design and BR stimuli with increasing interocular grouping demands. A. Experimental design to capture behavioral responses for alternations in percepts during BR and interocular grouping. Subjects were asked to report with a two-button press-and-hold response when viewing dominant percepts. Mixed percepts were inferred from periods of no responses. Illustration is shown over the time course of the visual presentation of rivalrous images. **B**. BR with dichoptic presentation of stimuli. **C.** Interocular grouping with two patches divided along the vertical meridian of each classic BR image. **D**. Interocular grouping with two patches divided along the horizontal meridian of each classic BR image. **E**. Interocular grouping with four patches divided along the vertical and horizontal meridian of each classic BR image. **F**. Interocular grouping with six patches divided along the vertical meridian of each classic BR image. **G**. Interocular grouping with six patches divided along the horizontal meridian of each classic BR image.

2.4 Methods

Participants

Participants recruited for inclusion reported normal or corrected normal vision and no known visual disorders. Contact lenses were allowed for visual acuity correction, but not glasses because of the prism glasses required for testing. We screened participants for visual impairments in acuity and stereo vision based on two assessments: the Logarithmic Visual Acuity chart (Early Treatment Diabetic Retinopathy Study [ETDRS] 2000 series chart; Precision Vision, Woodstock, IL), and the Titmus Stereoacuity Test (Stereo Optical, Chicago, IL). Participants completed these assessments in a well-lit room at the distance recommended by the testing manufacturer. Each eye was tested independently in visual acuity due to the dichoptic nature of BR. For each eye, visual acuity cut-offs for inclusion were 20/40 and no more than two lines of difference between eyes to avoid an underlying eye dominance. The median value for both right and left eyes was 20/20. For the stereo test, the inclusion criterion was set at 7/9, which corresponds to an angle of stereopsis of 60 seconds at 16 inches. The median results of the stereo vision test for the subject pool were 9/9. Out of the 61 participants recruited, nine did not meet the vision test criteria for inclusion and were excluded. The remaining 52 participants performed the experiment. Four participants were later excluded from the analysis due to testing values that were invalid for reasons beyond the scope of the experiment and were deemed not to represent the intended perceptual rivalry of the current study. For the remaining 48 participants, rare runs where they reported 100% mixed perception, periods of dominance below ~100ms (7 frames on the 60 Hz display), and self-reports of loss of fusion due to glasses fogging were removed. The final subject pool was N = 48, including two authors (EM and JM); 33 were females (M = 25.1 years, SD = 5.1 years).

Experimental Design

BR was achieved with the use of a black opaque divider placed between the two eyes and prism lenses 12 diopters in strength to overlay the images seen by each eye. When fusion was achieved by the participant on the fixation screen, the participant was instructed to self-initiate each testing block. All participants were guided through an unrecorded practice session (45 seconds for BR and IOG conditions) before the experimental conditions began.

Throughout the experiment, participants were instructed to report alternations in dominant percepts (red or green) using a two-button press-and-hold design. Specifically, when the majority (80% or more) of the image was perceived to be red, participants were instructed to press the right-sided button at the onset of the dominant red perception and to continuously hold the key down throughout the stability of this percept. Alternatively, they were instructed to press and hold the left key for green percepts. When neither red, nor green was perceived as perceptually dominant, participants were instructed to withhold a response, indicating the experience of a mixed percept (Figure 2.2A). These instructions were identical for BR and IOG conditions.

Stimuli

Images were shown using Psychtoolbox-3 (Brainard, 1997; Kleiner, Brainard, & Pelli, 2007) and MATLAB 2016a (MathWorks, Natick, MA), as illustrated in Figures 2.2B to 2.2G, with color codes in RGBA values for red [0.5 0 0 0.2] and green [0 0.4 0 0.2]. Pilot testing was conducted with five participants to achieve approximately balanced ratios for the proportion of time spent viewing red and green percepts. A fixation mark designed as a combination between a bullseye and crosshair was chosen to promote the stability (Thaler, Schütz, Goodale, & Gegenfurtner, 2013) required for interocular grouping.

The stimuli shown had a visual angle of 6.67 (6° 41' 0.83'), with a viewing distance of 47 cm and stimuli size of 5.5 × 5.5 cm. The interocular orientation difference between red and green gratings was set at 90° for all conditions. The experimental design used stimulus-based tagging for two dichoptically presented flicker regimes that were compatible with a 60 Hz display. Flicker frequencies followed a slow and a fast regime of 5 and 6.67 Hz and 10 and 12 Hz, respectively. The green gratings were tagged at frequencies of 6.67 or 12 Hz, with corresponding frequencies of 5 or 10 Hz for red. Throughout the experiment, the images were counterbalanced for the color and orientation of gratings shown to each eye to limit the effects of adaptation.

The experiment was comprised of seven conditions, each shown twice in 4-minute runs divided into four blocks of 1 minute. The order of conditions shown was counterbalanced and randomized among participants. Specific conditions were BR, two-patch vertical IOG (2VM), two-patch horizontal IOG (2HM), four-patch IOG (4), six-patch vertical IOG (6VM), and six-patch horizontal IOG (6HM).

2.5 Results

Effect of Flicker Frequencies

In the Methods section, we explained how all stimuli consisted of red or green gratings, and, because we intended to use this experimental design for brain imaging, we also used stimulus-based tagging for two dichoptically presented flicker regimes (e.g., Bock, Fesi, Da Silva Castenheira, Baillet, & Mendola, 2023). The slow flicker regime used frequencies at 6.67 Hz and 5 Hz, whereas the fast flicker regime used 12 Hz and 10 Hz. Hence, we plotted the mean durations of dominant (red or green) percepts for BR and all IOG conditions combined and separately for slow and fast flicker frequencies (Figure 2.3). Dominance durations are computed as the average duration of red and green percepts. Overall, results showed that rivalry was slightly slower (longer percept durations and decreased alternation rate) for the slow flicker condition, as indicated by a Welch *t*-test that revealed a significant different difference between flicker speed for both BR (slow, 1.96 s; fast, 1.79 s; $t = 2.32$; $df = 368$; $p = 0.02$) and IOG (slow, 1.52 s; fast, 1.46 s; $t = 2.35$; $df = 1828.6$; $p = 0.02$). Next, mean durations of the mixed percepts were considered for BR and IOG. In this case, a Welch two-sample *t*-test was not significant for BR (slow, 1.08 s; fast, 1.06 s; $t = 0.21$; $df = 364.04$; $p = 0.8$) but was significant for IOG (slow, 2.39 s; fast, 2.21 s; $t = 2.8$; $df = 1816.6$; $p = 0.005$). Next, we examined alternation rate, which was computed as the number of perceptual alternations per second. Mean alternation rates were slightly higher for both BR and IOG with the faster flicker rate. Welch two-sample *t*-test was significant for BR (slow, 0.40 Hz; fast, 0.43 Hz; $t = -2.57$; $df = 366.09$; $p = 0.01$) and for IOG (slow, 0.32 Hz; fast, 0.34 Hz; $t = -3.40$; $df = 1828.9$; $p = 0.0007$). As observed across the results in Figures 2.3A to 2.3C, flicker frequency had a greater impact during BR, where the slower regime produced longer dominant percept durations and slower alternation rates; however, during IOG, increasing grouping demands led to a reduction in differences between the mean results, with the largest differences obtained during IOG2 with trends that mimicked BR. These results show that we obtained stable rivalry for both rates of flicker with only minor differences between them (considered further in the Discussion section). In all of the following analyses, with the exceptions of Tables 2.1 to 2.4, slow and fast flicker were combined in Figures 2.4 to 2.7.

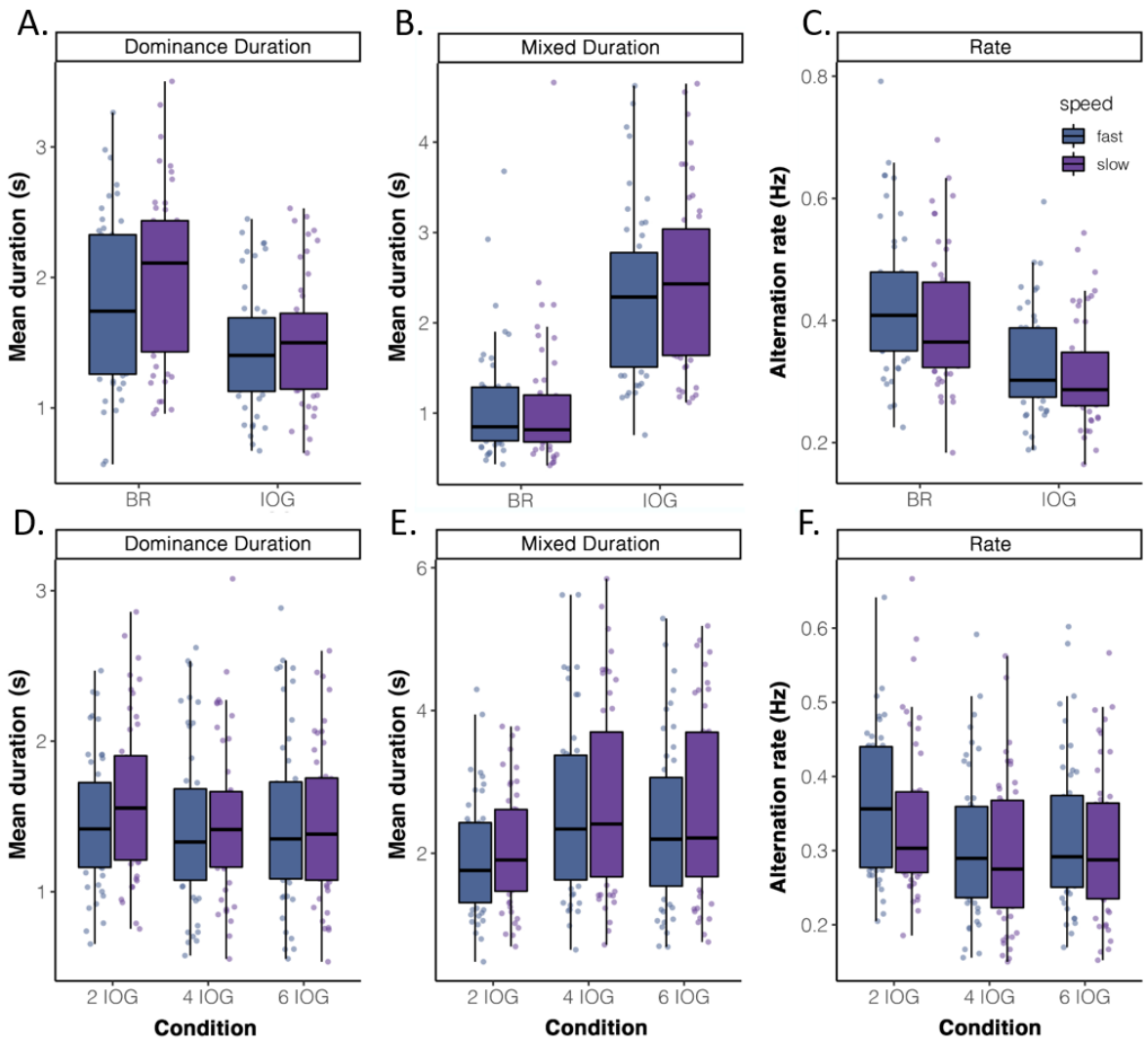

Figure 2.3 Comparison of flicker frequencies. **A–C**. Mean duration values for dominant and mixed percepts and alternation rate for BR and IOG. **D–F**. Mean duration values for dominant and mixed percepts and alternation rate for increasing grouping demands during IOG. Dominant percepts are plotted as mean values for red and green responses. Black lines are the median values, and the dots represent participant data.

Table 2.1 Multiple linear regression analysis between binocular rivalry and interocular grouping for mean dominant percept durations. Mean dominant percept duration was computed as the average time each dominant percept (red or green) was held by participants.

Mean Dominant Percept Duration BR vs IOG			
Predictors	*Estimates*	*CI*	*p*
(Intercept)	1.84	1.70 – 1.98	**<0.001**
Number of divisions	-0.15	-0.17 – -0.13	**<0.001**
Flicker rate [fast]	-0.19	-0.24 – -0.13	**<0.001**
Number of divisions * Flicker rate [fast]	0.07	0.04 – 0.09	**<0.001**
Random Effects			
σ^2		0.13	
τ_{00}		0.23	
ICC		0.63	
N		48	
Observations		2201	
Marginal R^2 / Conditional R^2		0.049 / 0.652	

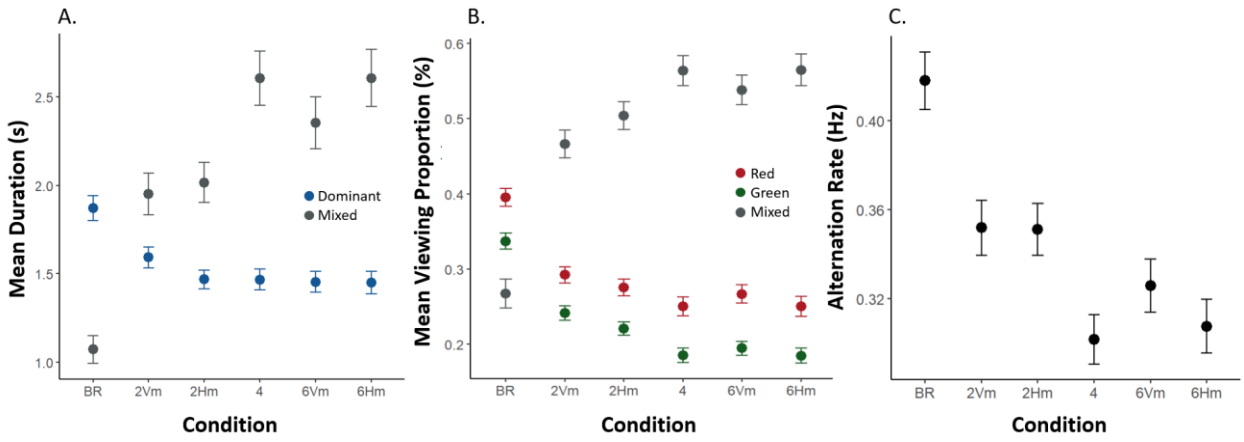

Figure 2.4 Mean duration and proportion of viewing time for BR and interocular grouping. **A**. Mean durations of percepts plotted for BR and IOG conditions. Duration of percepts is plotted as the mean duration for red and green percepts. **B**. Mean proportion of viewing time for red, green, and mixed percepts across BR and IOG conditions. **C**. Alternation rates plotted for each condition. Error bars plotted in all three graphs are 95% confidence intervals.

Effect of Increasing Interocular Grouping Demands

Percept Durations

The mean duration of each sequential percept corresponds to perceptual stability in conscious perception of alternating percepts. Here, we computed mean percept durations for red and green percepts (labeled dominant), as well as mixed percepts (Figure 2.4A). Dominant percepts are most stable (longer duration) for classic BR (1.87, *SD* = 0.69), with a mean duration of nearly 2 seconds, and mixed percepts lasting on average just over 1 second (BR = 1.07, *SD* = 0.77). In contrast, for all the IOG conditions, the mean duration of dominant percepts (∼1.5 s) was shorter than BR (2VM = 1.59, *SD* = 0.58; 2HM = 1.47, *SD* = 0.53; 4 = 1.47, *SD* = 0.56; 6VM = 1.45, *SD* = 0.58; 6HM = 1.45, *SD* = 0.61), and less than the mean duration of mixed percepts for each IOG condition (2VM = 1.95, *SD* = 1.17; 2HM = 2.02, *SD* = 1.13; 4 = 2.61, *SD* = 1.48; 6VM = 2.35, *SD* = 1.44; 6HM = 2.61, *SD* = 1.53). This was found to be a significant difference with the results shown in Table 2.1. However, it is notable that the dominant percepts remained very similar in duration even as grouping demands increased dramatically. In contrast, mixed percepts increased modestly as grouping demands increased. In addition, we see that mixed percepts are slightly longer for 2HM and 6HM (Figure 2.4A) than the image meridian division of 2VM and 6VM. In sum, between classic BR and interocular grouping conditions, there was an inversion of the duration for the most predominant type of percept (i.e., dominant or mixed) as seen in Figure 2.4A, with the experience of BR favoring longer dominant percepts, whereas IOG resulted in longer durations of mixed percepts.

We performed a multiple linear regression analysis to examine whether there is an interaction between grouping demands and percept duration. There was a significant interaction in regression analysis with increasing grouping demands during IOG ($p < 0.001$; estimate = −0.12; confidence interval [CI], −0.15 to −0.09) and meridian division orientation ($p < 0.001$; estimate = −0.27; CI, −0.38 to −0.17), as reported in Table 2.2, favoring grouping in images divided along the vertical meridian. Therefore, grouping was affected by both the increase in number of patches and the orientation of their division. To determine whether mixed percepts differed between BR and IOG, we performed a multiple linear regression analysis that showed a main effect between the two conditions in Table 2.3 ($p < 0.001$; estimate = −1.35; CI, −1.51 to −1.19). Participants spent significantly longer periods viewing mixed percepts during IOG conditions.

Table 2.2 Multiple linear regression analysis for increasing interocular grouping demands across the number and orientation of image division. Mean dominant percept duration was computed as the average time each dominant percept (red or green) was held by participants. Increasing interocular grouping demands was defined as moving from IOG2, IOG4, to IOG6. Orientation of image division was either along the vertical or horizontal meridian.

Mean Dominant Percept Duration Meridian Divisions			
Predictors	*Estimates*	*CI*	*p*
(Intercept)	1.81	1.66 – 1.97	**<0.001**
Number of divisions	-0.12	-0.15 – -0.09	**<0.001**
Flicker rate [fast]	-0.28	-0.39 – -0.18	**<0.001**
Meridian division [horizontal]	-0.27	-0.38 – -0.17	**<0.001**
Number of divisions * Flicker rate [fast]	0.10	0.05 – 0.14	**<0.001**
Number of divisions * Meridian division [horizontal]	0.09	0.04 – 0.14	**<0.001**
Flicker rate [fast] * Meridian division [horizontal]	0.16	0.01 – 0.31	**0.040**
(Number of divisions * Flicker rate [fast]) * Meridian division [horizontal]	-0.04	-0.11 – 0.03	0.222
Random Effects			
σ^2		0.11	
$\tau_{00\ Sub\_ID}$		0.23	
ICC		0.68	
N_{Sub_ID}		48	
Observations		1470	
Marginal R^2 / Conditional R^2		0.018 / 0.683	

Table 2.3 Multiple linear regression analysis between binocular rivalry and interocular grouping for mean mixed percept durations and alternation rate. Mean mixed percept duration was computed as the average time each mixed percept was held by participants.

Mean Mixed Percept Duration BR vs IOG			
Predictors	*Estimates*	*CI*	*p*
(Intercept)	2.42	2.17 – 2.67	**<0.001**
Condition [Binocular rivalry]	-1.35	-1.51 – -1.19	**<0.001**
Flicker rate [fast]	-0.18	-0.27 – -0.09	**<0.001**
Condition [Binocular rivalry] * Flicker rate [fast]	0.17	-0.05 – 0.40	0.124
Random Effects			
σ^2		0.98	
$\tau_{00\ Sub\_ID}$		0.73	
ICC		0.43	
N_{Sub_ID}		48	
Observations		2201	
Marginal R^2 / Conditional R^2		0.118 / 0.493	

Percept Predominance

The next step was computing the percentage of time each of the three possible percepts was reported, combining the two runs (slow and fast flickering rates) for each condition. The proportion of viewing time was calculated by taking the total duration of each condition measured in frames and dividing it by the total duration that participants indicated red, green, or mixed percepts. The predominance results provide a global view of the rivalry experience across the whole of the experiment and are plotted separately for red grating dominant, green grating dominant, or a mixed percept, for classic BR and each grouping condition (Figure 2.4B). The pattern of results is similar to the percept durations seen in Figure 2.4A. For classic BR, a dominant percept was perceived approximately 70% of the time. During BR, participants experienced the three percepts in the following viewing proportions: BR red = 0.40 (*SD* = 0.12); BR green = 0.34 (*SD* = 0.11); and BR mixed = 0.27 (*SD* = 0.19). During IOG conditions, the viewing proportions of the red grating (2VM = 0.29, *SD* = 0.11; 2HM = 0.27, *SD* = 0.11; 4 = 0.25, *SD* = 0.12; 6VM = 0.27, *SD* = 0.12; 6HM = 0.25, *SD* = 0.12) were seen slightly more often that green (2VM = 0.24, *SD* = 0.09; 2HM = 0.22, *SD* = 0.09; 4 = 0.19, *SD* = 0.09; 6VM = 0.19, *SD* = 0.09; 6HM = 0.18, *SD* = 0.09) which may be due to a small residual advantage in visibility, or even a bias at more cognitive levels. For the remaining viewing proportions, the proportions of mixed percepts

were BR = 0.27 (*SD* = 0.19); 2VM = 0.47 (*SD* = 0.18); 2HM = 0.50 (*SD* = 0.18); 4 = 0.56 (*SD* = 0.19); 6VM = 0.54 (*SD* = 0.19); and 6HM = 0.56 (*SD* = 0.20), seen as a piecemeal percept, which was in line with previous studies that recorded mixed percepts. Sheynin et al. (2019) reported a proportion of mixed percepts for a subset of their participants with normal vision at approximately 42%. Given that our stimuli differed in color, spatial frequency, and size, our results are reasonably comparable with their findings. When IOG is next considered, it is evident that mixed percepts are perceived for a significantly longer period (Figure 2.4B), in the range of approximately 45% to 55%. Dominant percepts were perceived significantly less than for classic BR. In comparison, Kovács et al. (1996) originally reported 60% dominant and 37% mixed viewing, with the remaining time spent viewing fused percepts, although direct comparison is somewhat challenging due to differences in the stimuli used. As our grouping demands increased, there was a rather modest increase in mixed percepts from IOG2 to IOG6 (Figure 2.4B). However, it is notable that we see a plateau that is better modeled by a nonlinear, second-order polynomial function, rather than a linear function in the percentage of viewing time for mixed percepts, even as the number of patches increases, and the number of possible mixed percepts increases exponentially (further considered in the Discussion section). Finally, we also found that rivalry was slightly more stable when grouping was required across the vertical meridian compared with the horizontal meridian, defined by orientation of the central image division.

Alternation Rate

Alternation rate was measured in hertz as the number of alternations in dominant percepts (red and green) per second. In our study, this measure did not include the button responses for mixed percepts. Higher alternation rates are indicative of faster switching between red and green dominant percepts experienced by the participant and are often cited as "fast switcher" in rivalry literature (e.g., Fesi & Mendola, 2015; Bock et al., 2019). The alternation rate was calculated by dividing the total duration of time spent viewing each condition by the number of red and green button responses (indicated switch of percept). We found that classic BR created the fastest rivalry experience (BR = 0.42, *SD* = 0.13), and IOG always results in a slower mean rate of dominance alternations (2VM = 0.35, *SD* = 0.12; 2HM = 0.35, *SD* = 0.12; 4 = 0.30, *SD* = 0.11; 6VM = 0.33, *SD* = 0.12; 6HM = 0.31, *SD* = 0.11) as shown in Figure 2.4C. In other words, rivalry was

slowed down under conditions of interocular grouping because subjects spent more time in (mixed percept) transitions periods.

Furthermore, the multiple linear regression analysis shown in Table 2.4 was performed to investigate the relationship between increasing grouping demands and alternation rate. This analysis resulted in a significant interaction between alternation rate and the number of patches in IOG ($p < 0.001$, estimate = 0.03 Hz; C, −0.03 to −0.02). We observed a decrease in alternation rate as the grouping demands increased.

Table 2.4 Multiple linear regression analysis between binocular rivalry and interocular grouping for alternation rate. Alternation rate was defined as the number of switches between dominant percepts per second. It was computed by dividing the total number of alternations between dominant percepts by the duration of the experiment.

Alternation Rate BR vs IOG			
Predictors	*Estimates*	*CI*	*p*
(Intercept)	0.38	0.35 – 0.40	**<0.001**
Number of divisions	-0.03	-0.03 – -0.02	**<0.001**
Flicker rate [fast]	0.03	0.02 – 0.04	**<0.001**
Number of divisions * Flicker rate [fast]	-0.01	-0.01 – -0.00	**0.026**
Random Effects			
σ^2		0.01	
τ_{00}		0.01	
ICC		0.57	
N		48	
Observations		2201	
Marginal R^2 / Conditional R^2		0.085 / 0.608	

Individual Differences in Switch Rates and Percept Durations

We performed correlation analyses between the BR and IOG conditions to observe the relationship between conditions for percept durations (dominant and mixed) and alternation rate. The correlations for alternation rate between conditions was robust and high in the positive direction, as shown by the *R* values in Figure 2.5C. This indicates that fast switchers for BR were also faster switchers during IOG. Although rate is traditionally used as a primary measure to gauge rivalry dynamics, we also investigated the correlations between both mean durations for dominant and mixed percepts (i.e., the duration percepts were held). The correlations between conditions for

dominant percept durations (Figure 2.5A) and mixed percept durations (Figure 2.5B) were also found to be strong and positive as shown by the *R* values shown in Figure 2.5. All correlations were found to be significant after false discovery rate (FDR) correction when using the p.adjust function in R (R Foundation for Statistical Computing, Vienna, Austria). Within IOG, a strong positive relationship was also found among the conditions. Simply put, relationships were strongest for images that were closer in their number of divisions (i.e., IOG2 and IOG4, or IOG4 and IOG6), whereas conditions with greater dissimilarity (i.e., IOG2 and IOG6, or BR to IOG4/IOG6) had comparatively decreased *R* values. Taken together, the alternation rate, mean duration for dominant, and mean duration for mixed percepts provide an overall view of the rivalry dynamics experienced by participants and highlight the strong positive correlations found (Figure 2.5) among the conditions. A visual of the scatter plots that produced the correlation results in Figure 2.5 are shown in the Appendix (Figure A.1) for BR and IOG2 conditions.

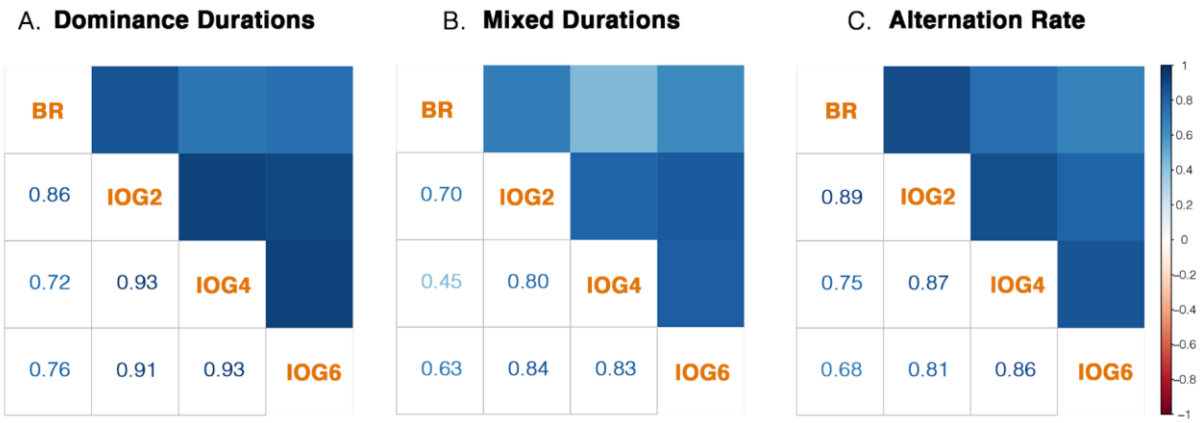

Figure 2.5 Correlation matrix with *R* values plotted of mean values for participants depicting relationship between BR and interocular grouping. A. Mean duration (seconds) of dominant (red and green) percepts. **B.** Mean duration (seconds) of mixed percepts. **C.** Alternation rate (Hz). All correlations were statistically significant after FDR correction.

The results in Figure 2.5 were calculated for 95% CIs, with the following results. For dominant percept durations, BR-IOG2 = 0.73 to 0.90, BR-IOG4 = 0.57 to 0.79, BR-IOG6 = 0.61 to 0.83, IOG2-IOG4 = 0.89 to 0.95, IOG2-IOG6 = 0.83 to 0.94, and IOG4-IOG6 = 0.90 to 0.96 (Figure 2.5A). For mixed percept durations, BR-IOG2 = 0.59 to 0.79, BR-IOG4 = 0.26 to 0.57, BR-IOG6 = 0.47 to 0.72, IOG2-IOG4 = 0.68 to 0.88, IOG2-IOG6 = 0.73 to 0.91, and IOG4-IOG6

= 0.73 to 0.89 (Figure 2.5B). For alternation rate, BR-IOG2 = 0.83 to 0.92, BR-IOG4 = 0.49 to 0.79, BR-IOG6 = 0.56 to 0.84, IOG2-IOG4 = 0.64 to 0.89, IOG2-IOG6 = 0.70 to 0.90, and IOG4-IOG6 = 0.82 to 0.94 (Figure 2.5C).

In a further analysis, illustrated in Figure 2.6, we sought to separately evaluate whether dominant or mixed percepts were better correlated with alternation rates across BR and IOG. During BR, we found a strong negative correlation between both the mean dominant percept duration and alternation rate ($R = -0.55$, $t = -4.5204$, $df = 46$, $p = 4.307\text{e-}05$) and mixed percept duration and alternation rate ($R = -0.48$, $t = -3.6803$, $df = 46$, $p = 0.0006097$), plotted in Figure 2.6A. However, this was not the case during IOG (Figure 2.6B), where only the duration of mixed percepts was found to show a significant negative correlation with alternation rate ($R = -0.84$, $t = -10.426$, $df = 46$, $p = 1.062\text{e-}13$), whereas there was a nonsignificant relationship with the duration of dominant percepts and alternation rate ($R = -0.21$, $t = -1.4628$, $df = 46$, $p = 0.1503$). Fast switchers in both BR and IOG conditions tended to have shorter mixed percepts, but for dominant percepts fast switchers were significantly quicker only during BR, and not IOG, whereas slow switchers tended to have longer durations of mixed percepts.

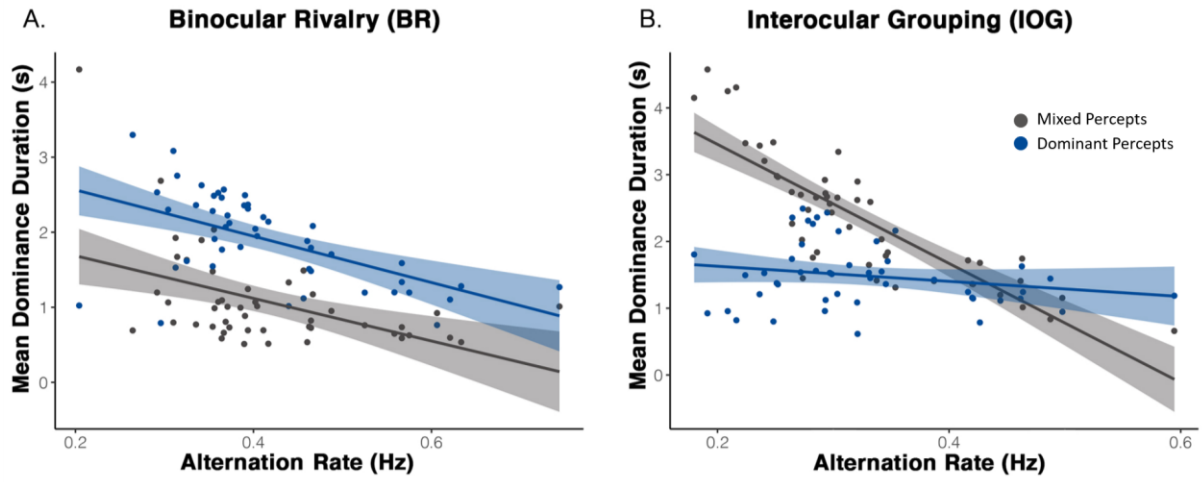

Figure 2.6 Scatterplot depicting correlations between the alternation rate and mean duration of mixed percepts, with linear lines of best fit. A. BR alternation rate and mean duration of dominant and mixed percepts. **B.** Interocular grouping alternation rate and mean duration of dominant and mixed percepts.

Transition Probabilities between Perceptual States as an Indication of Tristability

As previously proposed by Riesen et al. (2019) and Qiu et al. (2020), models of tristability during classic BR and IOG were tested. Our analysis used transition probabilities between perceptual states during rivalry. Transition probabilities between perceptual states reported by participants were computed by comparing the current percept reported and their prior state of perception. With the inclusion of mixed percepts as a behavioral response, participants were able to report three different percepts: red, green, and mixed (Figure 2.7). When viewing a percept, there was the possibility of transitioning to either of the two different states, such that a participant viewing mixed could report the transition toward either a red or a green percept. For this reason, the arrowed lines leaving a percept in Figure 2.7 are equal to the value of 1 (i.e., the arrows leaving a green percept toward both a red and mixed percept) and point in the direction of the percepts reported. For the purposes of this computation, stable percept periods were defined as those lasting more than 100ms in duration to avoid mislabeling the transitions between dominant to dominant as including a mixed period when participants were shifting between response keys.

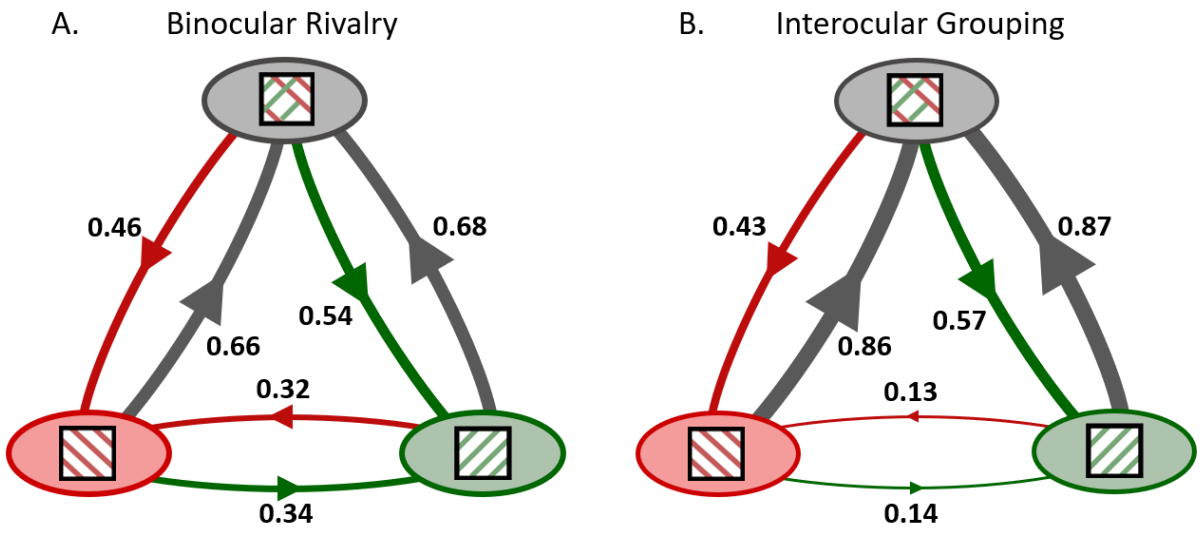

Figure 2.7 Transition probabilities between perceptual states during rivalry. A. Results for BR. **B.** Combined results for all conditions of interocular grouping. Lines between perceptual states are drawn to scale of the mean probability of values of transition. Arrows point toward percepts reported from the previous state.

For both BR and IOG, there are similar transition probabilities when moving from a mixed to dominant percept, with a slight preference toward green. These values are taken to be 0.46 (*SE* = 0.008) and 0.43 (*SE* = 0.003) from mixed to red and 0.54 (*SE* = 0.008) and 0.57 (*SE* = 0.003) from mixed to green for BR and IOG, respectively. When viewing a red percept, participants had a greater tendency to transition to a mixed percept, with probabilities of 0.66 (*SE* = 0.017) for BR and 0.86 (*SE* = 0.005) IOG, whereas it was less often reported to move between red to green with values of 0.34 (*SE* = 0.017) for BR and 0.14 (*SE* = 0.005) for IOG. When experiencing green, a similar trend was observed with transition probabilities of BR and IOG going to mixed of 0.68 (*SE* = 0.017) and 0.87 (*SE* = 0.005), with a decline of values observed moving to red at 0.32 (*SE* = 0.017) and 0.13 (*SE* = 0.005) for BR and IOG, respectively.

Importantly, between BR and IOG, there was a difference in the transition probabilities of moving between dominant-to-dominant percepts. During BR, participants reported moving between red and green roughly a third of the time, whereas this value was greatly reduced during IOG. In addition, the results between IOG conditions did not vary greatly for dominant-to-dominant transition probabilities from red to green (IOG2 = 0.16, IOG4 = 0.13, IOG6 = 0.13) and from green to red (IOG2 = 0.15, IOG4 = 0.12, IOG6 = 0.12). This result allows us to understand the tristable nature of the rivalry dynamics experienced by participants during BR. In contrast, there was far greater likelihood of participants reporting mixed percepts after transitioning from either red or green percepts during IOG (Figure 2.7B).

We found no evidence that flicker rate impacted the nature of this tristability during BR. Both flicker regimes yielded similar transition probabilities. For mix to red (slow, 0.47; fast, 0.45), mix to green (slow, 0.53; fast, 0.55), red to mix (slow, 0.66; fast, 0.66), green to mix (slow, 0.69; fast, 0.67), red to green (slow, 0.34; fast, 0.34), and green to red (slow, 0.31; fast, 0.33).

Finally, a related phenomenon known as switchbacks was also calculated. Switchbacks represent the experience of going from a dominant to mixed and back to the previously reported dominant state (i.e., red, mix, red perceptual reports). The probability of switchbacks from red–mix–red was as follows: BR = 0.07, IOG2 = 0.11, IOG4 = 0.13, and IOG6 = 0.12. Similarly, for green–mix–green, BR = 0.11, IOG2 = 0.21, IOG4 = 0.27, and IOG6 = 0.27. Thus, a trend was observed for higher switchback probability during IOG when compared with BR. This result further supports the evidence for a tristable regime observed during BR with its lower probability of switchbacks.

2.6 Discussion

Our study on visual rivalry sought to explore the behavioral outcomes (i.e., mean dominant and mixed durations, alternation rate) when the number of complementary grouped patches during interocular grouping was systematically increased, from classic BR to two, four, and six image divisions. Classic BR resulted in the longest mean dominant percept durations, which were roughly twice as long as the mean for mixed percepts. This trend was reversed for the grouping conditions (Figure 2.4A), with longer mixed percept lengths relative to the dominant percepts. In fact, the mean dominant durations for IOG showed remarkable stability as the number of complementary grouped patches increased; apart from 2VM (1.59 s), the grouping conditions of 2HM, 4, 6VM, and 6HM ranged from only 1.45 to 1.47 seconds. This is an important result, because it highlights the stability of dominant percepts as the demands of interocular grouping increase. In contrast to dominant percept durations, as grouping demands increased, the mean mixed percept duration increased from the two- to four-patch grouping conditions. A nonlinear trend was observed when moving from the four- to six-patch conditions, better modeled by a nonlinear, second-order polynomial function than a linear equation. We thus found that alternation rates decreased with increased grouping demands and showed that individual differences in switch rates for classic BR are maintained with IOG. Finally, the preponderance of mixed percepts in IOG resulted in a departure from the classic BR pattern that better resembles tristability, with a dominant (red/green) percept equally likely to transition to mixed or dominant (green/red). In IOG, dominant percepts usually transition to mixed before dominance is again established.

Impact of Flicker Rate in the Experience of Rivalry

The design of our study sought to test whether altering the dichoptic flicker regime between slow (5 and 6.67 Hz) and fast (10 and 12 Hz) frequencies affected the experience of BR and interocular grouping. In both BR and IOG, we observed similar trends; modest increases in both dominant and mixed percept duration for slow flicker compared with fast flicker (Figure 2.3). These results slightly extend the findings by Knapen et al. (2007) to lower frequency regimes; they previously showed that that flickering images (>10 Hz) increased interocular grouping compared with static images. We were able to determine that slower rates of flicker did not adversely disrupt

IOG and may even stabilize it. This is of practical importance for neuroimaging studies of visual rivalry that rely on frequency tagging below 10 Hz (e.g., Tononi, Srinivasan, Russell, & Edelman, 1998; Srinivasan, Russell, Edelman, & Tononi, 1999; Cosmelli et al., 2004; Kamphuisen, Bauer, & van Ee, 2008; Sutoyo & Srinivasan, 2009; Jamison, Roy, He, Engel, & He, 2015; Katyal et al., 2016; Roy, Jamison, He, Engel, & He, 2017; Bock et al., 2019). The difference noted between our slow (5 and 6.67 Hz) and fast (10 and 12 Hz) was significant but small in magnitude for the measures of mean durations and alternation rate. Therefore, a wide range of frequencies appears to provide adequately long durations of perceptual stability between alternations, which can be advantageous in steady-state visually evoked potential neuroimaging studies.

Importance of Mixed Percepts

Although a few previous studies of IOG exist, none of them measured mixed percepts as systematically as the current study (Knapen et al., 2007; Sutoyo & Srinivasan, 2009; Golubitsky, Zhao, Wang, & Lu, 2019). Our study was designed to explicitly measure the experience of mixed percepts, without adding additional high cognitive demands to traditional two-button response studies. We were able to further characterize mixed periods in their frequency, duration, proportion of viewing time, correlation to switch rates, and transition probabilities. The periods where (ungrouped) portions from images shown independently to each eye are visible represent ambiguity and competition within the visual system prior to the resolution of coherent visual perception. Although the perceptual experience of BR was well mimicked during IOG, fundamentally the two visual illusions differ. During BR, alternations took place between monocularly driven stimuli, and the perception of mixed percepts represented periods where both images demonstrated partial visibility. In contrast to this, the experience of IOG involves each eye being shown a version of a so-called "static" mixed percept, and it is up to the neural mechanisms of the visual system to elicit the seamless experience of dominance and suppression as is the case during BR. It is thus important to mention that, although we observed an inversion in the durations of dominant and mixed percepts between BR and IOG, dominant durations during IOG were significantly longer than mixed percepts during BR (non-overlapping error bars in Figure 2.4A). These periods of dominance during IOG may represent durations where combinatorial processing between binocular driven neurons is occurring. We note in passing that the mixed percepts observed during IOG may entail competition between monocular images as well as various

ungrouped binocular combinations, and thus the processing is not identical to that during BR. Comparing the tagged intermodulation frequency signals physiologically recorded for mixed percepts during BR with IOG would be informative in future studies (see Katyal et al., 2016; Bock et al., 2019).

For IOG, it is interesting that the visual system "unscrambles" the mixed monocular inputs to mimic classical BR alternation experience so robustly. This highlights some of the Gestalt principles of similarity in color, continuity in oriented gratings, and pattern completion to drive perception toward a unified image. We observed a distinct dissociation between the majority of percepts perceived by participants between BR and IOG. For BR, dominant red/green percepts were reported in an approximate 2:1 ratio over mixed percept for their duration (Figure 2.4A) and approximately a third of viewing proportion (Figure 2.4B). This trend was reversed during IOG with an increasing duration of mixed percepts as the conditions increased in grouping demands, as well as an increase in the proportion of mixed percept viewing. To emphasize the remarkable stability of grouping mechanisms as demands increased, we observed a nonlinear trend in total mixed viewing proportion that plateaued below 0.6 (Figure 2.4B) even as the number of divisions was increased from two to six patches. This was previously modeled by Kovács et al. (1996) as the possible number of combinations that can be viewed based on the assumption that perception alternates randomly in each complementary patch (i.e., between red and green). The authors proposed that the probability of a uniform percept (p_u) can be modeled by the equation $p_u = 2 \times 1/2^n$, where n is the number of bistable patches. During the IOG4 conditions, where participants viewed a superimposed rivalrous quadrant with four bistable patches, $p_u = 2 \times 1/2^4$ results in 0.125 (12.5%). This result was pushed even further during IOG6, where $p_u = 0.003125$ (3.125%) and p_m (where m = proportion of mixed percepts) can be modeled as $p_m = 1 - p_u = 0.96875$ (96.875%). Clearly, this model would not explain our observation that participants never exceeded a group mean of 60% viewing proportions for mixed percepts as grouping demands linearly increased.

Several previous studies on IOG limited stimuli to two or four patches (Knapen et al., 2007; Sutoyo & Srinivasan, 2009; Golubitsky et al., 2019). Our results correspond with these findings, despite differences in stimulus parameters that could promote global percepts. The seminal paper by Kovács et al. (1996) reported mixed proportions of 37% for BR and 50% for IOG, with limited evidence of binocular fusion. Subsequently, about of 40% viewing time spent

in mixed periods has been cited during rivalry by Alais & Melcher (2007), and Sheynin et al., (2019). These results are in line with our findings from two-patch IOG, but we observed a further increase in the relative proportion of mixed percepts as the grouping demands increased. Moreover, we found that there was a strong negative correlation between alternation rate and duration of mixed percepts (Figure 2.6B) during IOG, but durations of dominant percepts were remarkably stable at approximately 1.5 seconds. This suggests to us that the factors and mechanisms determining a switch from *dominance to suppression* may differ from a switch from *suppression to dominance* (Bock et al., 2023). The former mechanism that determines the duration of dominance appears minimally affected by grouping demands and may rely more heavily on ventral stream visual areas (e.g., Sandberg, Bahrami, Lindelov, Overgaard, & Rees, 2011; Sandberg et al., 2014, Bock et al., 2023). The later mechanism, which establishes dominance and may be more reliant on dorsal stream visual areas according to some evidence, appears more vulnerable to grouping demands.

Effect of Increasing Grouping Demands

We defined difficulty in grouping as the number of divisions and complementary bistable patches used to elicit IOG during rivalry. Throughout the experiment, it was observed that participants viewed dominant percepts with greater ease during the two-patch IOG conditions, as opposed to the four- and six-patch IOG (Figures 2.3 and 2.4). Of interest, participants qualitatively described the experience of rivalry during higher order grouping conditions (e.g., IOG6) to build up in nature toward a dominant percept. They reported mixed percepts to be dynamically perceived, whereas the complementary bistable patches would flip toward a coherent percept and be stable in perception during the report of a dominant percept, similar to the experience of dominance during BR. Some subjects reported awareness of a gradual "wave" of dominance so that spreading of coherency occurred sequentially for adjacent patches. Interestingly, as we increased grouping demands during IOG, an observable difference was present between IOG2 to IOG4 and between IOG4 to IOG6. We found the experience of rivalry to be slowed in the four-patch condition when compared with IOG2, due to the reduced alternation rates, and increase in mixed percept durations. The same cannot be said of the transition from four to six bistable patches, which led us to hypothesize that grouping along both the vertical and horizontal meridian must be resolved for a global uniform percept. We can thus predict that the gatekeeping step in the

alternation rate during IOG was the resolution of conflict across both the vertical and horizontal meridian. We could further hypothesize that increasing the number of complementary patches beyond what was tested may not have as great of an effect on alternation rate as the initial vertical and horizontal conflict resolution.

Interocular Grouping across the Horizontal versus Vertical Image Meridian

We observed a difference in grouping across the vertical and horizontal meridians of the visual field that lead to a preference in what we defined as IOG stimuli divided across the vertical image meridian. The results presented in Table 2.2 indicated a significant effect ($p < 0.001$) for the predictor of image orientation division (i.e., vertical or horizontal) during IOG2 and IOG6 on the mean duration of dominant percepts. Our findings can be related to a previous neuroimaging study (Large, Culham, Kuchinad, Aldcroft, & Vilis, 2008) that posits a two-stage model of spatial integration in the visual hierarchy of higher tier visual areas. Namely, visual representations for upper and lower visual representations are processed in the lateral occipital (LO) *prior* to integration across left and right visual hemifields. Similarly, Larsson and Heeger (2006) found a role for visual areas LO1 and LO2 in integration of shape information for the entire contralateral visual hemifield, including both upper and lower quadrants. Tootell, Mendola, Hadjikhani, Liu, and Dale (1998) hypothesized that information was processed in multiple stages, first in the contralateral visual field and then across the vertical meridian as the receptive fields increase in size and extend to ipsilateral visual field, in areas such as LO. With this model and the two-stage model proposed by Large et al. (2008), we could expect a difference between IOG grouping demands across the vertical or horizontal meridian and slower rivalry dynamics when increasing the number of bistable patches to IOG4. This was shown to be true for Golubitsky et al. (2019), who found differences in the perceptual reports between IOG2 and IOG4 patch conditions, although they had a limited subject pool of $n = 3$. For the condition labeled 2VM in our study, they found more reports of all red and green percepts during their 2-second IOG presentation experiment, whereas the 2HM stimuli produced more monocular percepts, meaning less evidence grouping during rivalry. The diagonal condition they used resembled our IOG4 condition and showed results similar to those for 2HM. This could be interpreted as grouping across the 2HM condition being a limiting factor in a two-step process. Our results are similar, with participants viewing more dominant (i.e., longer mean duration of dominant percepts during IOG2V as

opposed to IOG2H) and less mixed percepts (i.e., shorter mean duration of mixed percepts during IOG6V as opposed to IOG6H) during the IOG stimuli with vertical image meridian divisions.

We note in passing additional anatomical and physiological evidence for how visual quadrants are combined that may impact vertical vs horizontal IOG grouping (Saint-Amour, Lepore, Lassonde, & Guillemot, 2004; Knyazeva, Fornari, Meuli, & Maeder, 2006). A particular area of interest is the lateral occipital visual cortex, previously found to be important for integration of information during interocular grouping with fMRI in the 2HM condition (Buckthought et al., 2021). The current behavioral results would predict a noticeable change in fMRI results between IOG2 and IOG4 due to the demands of integration across both the vertical and horizontal image meridian. When information from within and between hemifields is integrated, we could thus expect similar results as grouping demands increase from four to six patches.

Effects of Collinearity and End-Stopping

Another important factor that may explain our results is the well-known faciliatory (excitatory) effects of colinear oriented stimuli in visual cortex (Polat & Sagi, 1993; Polat, 1999; Cass & Alais, 2006). As has been previously hypothesized, collinear facilitation may rely on different mechanisms involving both lateral connectivity within V1 and extra-striate feedback (Cass & Alais, 2006; Jachim, Gowen, & Warren, 2017). When we increase the number of complementary grouped patches, we would expect a decreased collinear interaction for the monocular images in the visual cortex that may weaken their representation at the level of V1. Increasing the number of divisions equally results in a smaller surface area for each of the complementary patches, which in turn increases the proportion of mid- to higher spatial frequencies presented. This outcome may shift the balance between lower and higher tier visual areas and between monocular and binocular competition, leading to greater mixed percepts and the small reduction in dominant percept durations observed. Another consideration is that, as we add patches, we increase the amount of end-stopping and potentially have a wider band of orientations (from patch edges) in the stimulus that will selectively stimulate different regions of the visual cortex. We presume that end-stopping as first presented by Hubel and Wiesel (1965) would have the opposite effect of collinearity. In primates, end-stopped neurons respond better to short as opposed to long contours (Pack, Livingstone, Duffy, & Born, 2003). The increased excitation of end-stopped neurons may have contributed to our nonlinear trends observed

as participants moved to higher order grouping conditions. Finally, it is likewise possible that the differences observed in participants between lateral and feedback connections to V1 (Jachim et al., 2017) could also account for some of the individual differences in IOG observed during our study.

Individual Differences during Classic BR and IOG

Individual differences in speed of alternation during BR have been well documented and are heritable (Miller et al., 2010; Scocchia et al., 2014). Moreover, physiological studies have also examined the distinction between fast and slow switchers (e.g., Fesi & Mendola, 2015; Bock et al., 2019) in order to better understand the sources of such trait-like behaviors. Our results show a strong positive correlation between the individual differences in alternation rates between BR and IOG. The relationship was strongest for stimuli that were most similar (i.e., BR to two patches) and decreased as the grouping demands increased (BR-IOG2, $R = 0.89$; BR-IOG4, $R = 0.75$; BR-IOG6, $R = 0.68$). This is consistent with the finding that mixed percept durations systematically increase at the group level as grouping demands increase. However, the fast switchers for both BR and IOG experienced relatively shorter mixed percept durations, whereas slower switchers had longer periods of mixed percepts. This is important because it highlights again the transition from suppression to dominance, this time as a distinction between fast and slow switchers. Fast switchers can transition to dominant percepts more easily, which may be due to lower levels of baseline inhibition in the visual system that provides stability of dominant and suppressed inhibited percepts. Further, neural mechanisms such as the balance between excitation and inhibition have already been linked to altered rivalry in the case of autistic traits where there is a hypothesized imbalance (Robertson, Kravitz, Freyberg, Baron-Cohen, & Baker, 2013; Robertson et al., 2016; Dunn & Jones, 2020).

Evidence for Tristability

BR has long been modeled as a bistable process, in line with other examples of bistable and multistable illusions (Blake & Logothetis, 2002; Rodríguez-Martínez & Castillo-Parra, 2018). However, the possibility of rivalry between more than two possible percepts has been recognized for some time (e.g., Said & Heeger 2013; Katyal et al., 2016; Riesen et al., 2019; Bock et al., 2019; Qiu et al., 2020). In fact, for specific classic BR conditions, binocular fusion or mixed

percepts may exhibit a pattern of tristability, such as for gratings with a small difference in interocular orientation (Riesen et al., 2019), as well as for luminance contrast BR stimuli (Qiu et al., 2020). These models would assume that mixed percepts have relative stability in their durations and alternate in conjunction with the other percepts. In addition, a tristable illusion would entail approximately equal probabilities of transitioning to either of the two other percepts from the current perceptual state (Riesen et al., 2019). Our results for BR have an indication for tristability among red, green, and mixed percepts; however, this was not observed during interocular grouping. We show here specifically that switching through a period of mixed percepts was not mandatory for BR, whereas for IOG we found little evidence of transitions directly from one dominant percept to the other.

This could point toward evidence for a difference in the mechanisms of alternation between the two visual illusions. Monocular competition may be more prevalent overall when experiencing BR, whereas binocular integration is crucial for the experience of IOG. Taken together, our results seem indicative of a similar network that might operate differently to accommodate grouping during BR. We already have some evidence that BR and IOG share a similar overarching "rivalry network" that differs mainly in higher order visual regions that have specificity for grouping demands. fMRI studies on IOG have found increased blood-oxygen-level-dependent (BOLD) signal in higher order visual areas such as the lateral occipital (LO) area and intraparietal regions (Buckthought et al., 2021). Moreover, electroencephalogram (EEG) and transcranial magnetic stimulation (TMS) studies have highlighted the role of the parietal cortex in perceptual reversals more generally (Zaretskaya, Thielscher, Logothetis, & Bartels, 2010; Pitts & Britz, 2011). In a proposed tristable model of BR (Figure 2.8), rivalry could be occurring not only between monocular driven neurons but also with binocular driven neurons. The resolution of this conflict in earlier regions (i.e., primary visual cortex) would require a higher order visual region that received information from both pools of neurons, resulting in the results observed during BR. In particular, interocular competition may act locally in V1 to establish patches of dominant populations of neurons that feed up to higher levels and interact with binocular feature-based competition in an area such as LO. Concurrently, LO feeds back signals that bias the lower levels toward global consistency, which in turn further promotes a winner at the higher level. This cycle may repeat and might take longer in the case of IOG (during the longer mixed percepts). Such a

model might limit the piecemeal rivalry with a traditional stimulus and also allow global feature dominance to occur in IOG.

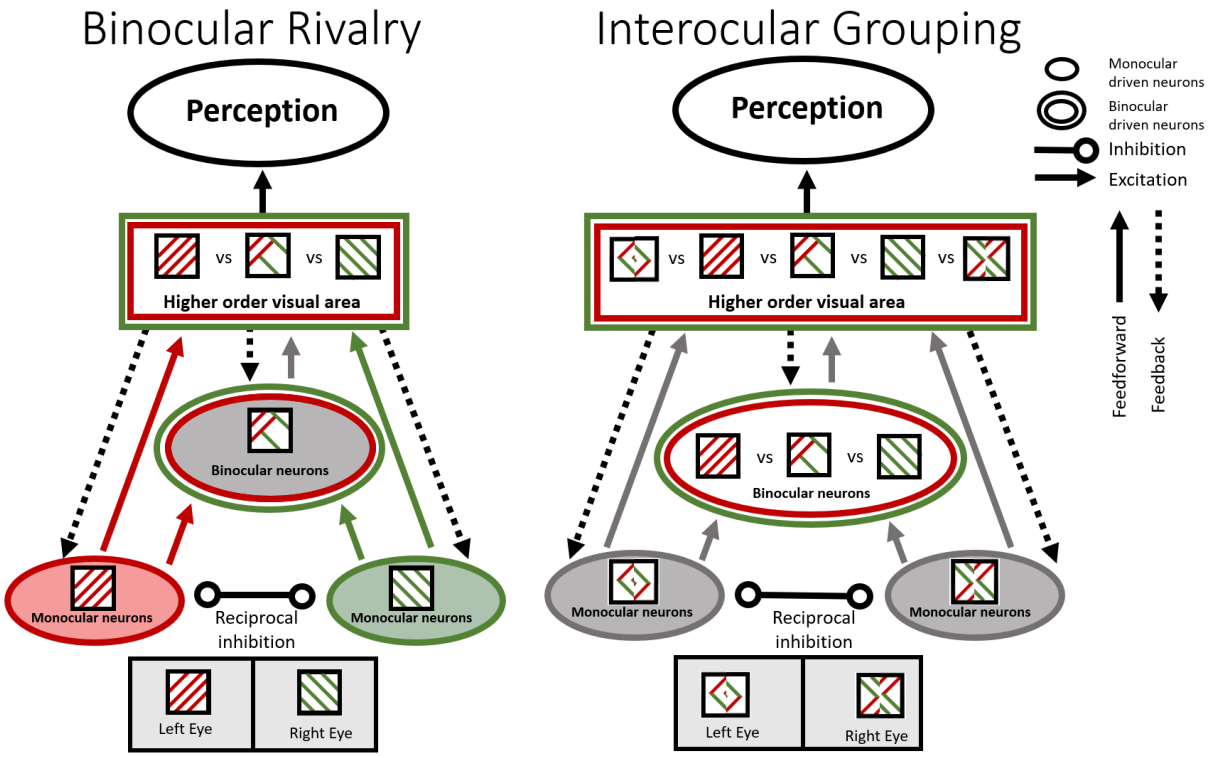

Figure 2.8 Visual model that accounts for tristable paradigm observed during BR. Schematic of competition occurring at higher level of the visual pathway, in a proposed region that received information from both monocular and binocular driven neurons. Competition in higher order visual areas results in perception of the dominant percept and feedback inhibition of suppressed percepts.

Taken together, our results illustrate the strength of the visual system in grouping dichoptic stimuli with similar color, orientation, and good continuation, even as the interocular grouping demands increased during rivalry. We found differences in grouping across the vertical and horizontal image meridian during IOG, and our results indicate a slight preference across participants for images divided along the vertical meridian. We further supported the notion of tristability during BR, which builds on models of rivalry to include rivalry between both monocular and binocularly driven neural mechanisms. Although we found mixed percepts to have an

increased predominance during interocular grouping, the visual system was robust toward its preference for uniform percepts. Finally, of interest for the study of rivalry and visual illusions, we found a strong positive correlation between behavioral results during BR and IOG conditions, indicative of a similar neural mechanism at play dictating perception.

2.7 Acknowledgements

The authors thank the helpful input of two anonymous reviewers.

Commercial relationships: none.

Corresponding author: Eric Mokri.

Email: eric.mokri@mail.mcgill.ca.

Address: Department of Ophthalmology and Visual Sciences, McGill University, Montreal, QC, Canada.

2.8 References

Alais, D., & Melcher, D. (2007). Strength and coherence of binocular rivalry depends on shared stimulus complexity. *Vision Research,* 47(2), 269–279.

Alais, D., O'Shea, R. P., Mesana-Alais, C., & Wilson, I. G. (2000). On binocular alternation. *Perception,* 29(12), 1437–1445.

Blake, R. (1989). A neural theory of binocular rivalry. *Psychological Review,* 96(1), 145.

Blake, R., & Logothetis, N. K. (2002). Visual competition. *Nature Reviews Neuroscience,* 3(1), 13–21.

Bock, E. A., Fesi, J. D., Baillet, S., & Mendola, J. D. (2019). Tagged MEG measures binocular rivalry in a cortical network that predicts alternation rate. *PLoS One,* 14(7), e0218529.

Bock, E. A., Fesi, J. D., Da Silva Castenheira, J., Baillet, S., & Mendola, J. D. (2023). Distinct dorsal and ventral streams for binocular rivalry dominance and suppression revealed by magnetoencephalography. *European Journal of Neuroscience,* 57(8), 1317–1334.

Brainard, D. H. (1997) The Psychophysics Toolbox. *Spatial Vision,* 10(4), 433–436.

Brascamp, J. W., Klink, P. C., & Levelt, W. (2015). The 'laws' of binocular rivalry: 50 years of Levelt's propositions. *Vision Research,* 109, 20–37.

Buckthought, A., Kirsch, L. E., Fesi, J. D., & Mendola, J. D. (2021). Interocular grouping in perceptual rivalry localized with fMRI. *Brain Topography*. 34(3), 323–336.

Cass, J., & Alais, D. (2006). The mechanisms of collinear integration. *Journal of Vision,* 6(9):5, 915–922.

Christiansen, J. H., D'Antona, A. D., & Shevell, S. K. (2017). Chromatic interocular-switch rivalry. *Journal of Vision,* 17(5):9, 1–16.

Cosmelli, D., David, O., Lachaux, J. P., Martinerie, J., Garnero, L., Renault, B., & Varela, F. (2004). Waves of consciousness: Ongoing cortical patterns during binocular rivalry. *NeuroImage,* 23(1), 128–140.

Diaz-Caneja, E. (1928). Sur l'Alternation binoculaire [On binocular alternation]. *Annalses d'Oculistique,* 165, 721–731.

Dunn, S., & Jones, M. (2020). Binocular rivalry dynamics associated with high levels of self-reported autistic traits suggest an imbalance of cortical excitation and inhibition. *Behavioural Brain Research,* 388, 112603.

Fesi, J. D., & Mendola, J. D. (2015). Individual peak gamma frequency predicts switch rate in perceptual rivalry. *Human Brain Mapping,* 36(2), 566–576.

Golubitsky, M., Zhao, Y., Wang, Y., & Lu, Z. L. (2019). Symmetry of generalized rivalry network models determines patterns of interocular grouping in four-location binocular rivalry. *Journal of Neurophysiology,* 122(5), 1989–1999.

Hubel, D. H., & Wiesel, T. N. (1965). Receptive fields and functional architecture in two nonstriate visual areas (18 and 19) of the cat. *Journal of neurophysiology,* 28(2), 229–289.

Jachim, S., Gowen, E., & Warren, P. A. (2017). Individual differences in the dynamics of collinear facilitation? *Vision Research,* 133, 61–72.

Jamison, K. W., Roy, A. V., He, S., Engel, S. A., & He, B. (2015). SSVEP signatures of binocular rivalry during simultaneous EEG and fMRI. *Journal of Neuroscience Methods,* 243, 53–62.

Kamphuisen, A., Bauer, M., & van Ee, R. (2008). No evidence for widespread synchronized networks in binocular rivalry: MEG frequency tagging entrains primarily early visual cortex. *Journal of Vision,* 8(5):4, 1–8.

Katyal, S., Engel, S. A., He, B., & He, S. (2016). Neurons that detect interocular conflict during binocular rivalry revealed with EEG. *Journal of Vision,* 16(3):18, 1–12.

Kleiner, M., Brainard, D., & Pelli, D. (2007). What's new in Psychtoolbox-3? *Perception,* 36(14), 1–16.

Knapen, T., Paffen, C., Kanai, R., & van Ee, R. (2007). Stimulus flicker alters interocular grouping during binocular rivalry. *Vision Research,* 47(1), 1–7.

Knyazeva M. G., Fornari E., Meuli R., & Maeder P. (2006). Interhemispheric integration at different spatial scales: The evidence from EEG coherence and FMRI. *Journal of Neurophysiology,* 96(1), 259–275.

Kovács, I., Papathomas, T. V., Yang, M., & Fehér, Á. (1996). When the brain changes its mind: Interocular grouping during binocular rivalry. *Proceedings of the National Academy of Sciences, USA,* 93(26), 15508–15511.

Large, M. E., Culham, J., Kuchinad, A., Aldcroft, A., & Vilis, T. (2008). fMRI reveals greater within-than between-hemifield integration in the human lateral occipital cortex. *European Journal of Neuroscience,* 27(12), 3299–3309.

Larsson, J., & Heeger, D. J. (2006). Two retinotopic visual areas in human lateral occipital cortex. *Journal of Neuroscience,* 26(51), 13128–13142.

Lee, S. H., & Blake, R. (2004). A fresh look at interocular grouping during binocular rivalry. *Vision Research,* 44(10), 983–991.

Logothetis, N. K., Leopold, D. A., & Sheinberg, D. L. (1996). What is rivalling during binocular rivalry? *Nature,* 380(6575), 621–624.

Miller, S. M., Hansell, N. K., Ngo, T. T., Liu, G. B., Pettigrew, J. D., Martin, N. G., & Wright, M. J. (2010). Genetic contribution to individual variation in binocular rivalry rate. *Proceedings of the National Academy of Sciences, USA,* 107(6), 2664–2668.

Pack, C. C., Livingstone, M. S., Duffy, K. R., & Born, R. T. (2003). End-stopping and the aperture problem: Two-dimensional motion signals in macaque V1. *Neuron,* 39(4), 671–680.

Pitts, M. A., & Britz, J. (2011). Insights from intermittent binocular rivalry and EEG. *Frontiers in Human Neuroscience,* 5, 107.

Polat, U. (1999). Functional architecture of long-range perceptual interactions. *Spatial Vision*. 12(2), 143–162.

Polat, U., & Sagi, D. (1993). Lateral interactions between spatial channels: Suppression and facilitation revealed by lateral masking experiments. *Vision Research,* 33(7), 993–999.

Qiu, S. X., Caldwell, C. L., You, J. Y., & Mendola, J. D. (2020). Binocular rivalry from luminance and contrast. *Vision Research,* 175, 41–50.

Riesen, G., Norcia, A. M., & Gardner, J. L. (2019). Humans perceive binocular rivalry and fusion in a tristable dynamic state. *Journal of Neuroscience,* 39(43), 8527–8537.

Robertson, C. E., Kravitz, D. J., Freyberg, J., Baron-Cohen, S., & Baker, C. I. (2013). Slower rate of binocular rivalry in autism. *Journal of Neuroscience,* 33(43), 16983–16991.

Robertson, C. E., Ratai, E. M., & Kanwisher, N. (2016). Reduced GABAergic action in the autistic brain. *Current Biology,* 26(1), 80–85.

Rodríguez-Martínez, G. A., & Castillo-Parra, H. (2018). Bistable perception: Neural bases and usefulness in psychological research. *International Journal of Psychological Research,* 11(2), 63–76.

Roy, A. V., Jamison, K. W., He, S., Engel, S. A., & He, B. (2017). Deactivation in the posterior mid-cingulate cortex reflects perceptual transitions during binocular rivalry: Evidence from simultaneous EEG-fMRI. *NeuroImage,* 152, 1–11.

Said, C. P., & Heeger, D. J. (2013). A model of binocular rivalry and cross-orientation suppression. *PLoS Computational Biology,* 9(3), e1002991.

Saint-Amour, D., Lepore, F., Lassonde, M., & Guillemot, J. P. (2004). Effective binocular integration at the midline requires the corpus callosum. *Neuropsychologia,* 42(2), 164–174.

Sandberg, K., Bahrami, B., Lindelov, J. K., Overgaard, M., & Rees, G. (2011) The impact of stimulus complexity and frequency swapping on stabilization of binocular rivalry. *Journal of Vision,* 11(2):6, 1–10.

Sandberg, K., Barnes, G. R., Bahrami, B., Kanai, R., Overgaard, M., & Rees, G. (2014) Distinct MEG correlates of conscious experience, perceptual reversals, and stabilization during binocular rivalry. *NeuroImage,* 100, 161–175.

Scocchia, L., Valsecchi, M., & Triesch, J. (2014). Top-down influences on ambiguous perception: The role of stable and transient states of the observer. *Frontiers in Human Neuroscience,* 8, 979.

Shannon, R. W., Patrick, C. J., Jiang, Y., Bernat, E., & He, S. (2011). Genes contribute to the switching dynamics of bistable perception. *Journal of Vision,* 11(3):8, 1–7.

Sheynin, Y., Proulx, S., & Hess, R. F. (2019). Temporary monocular occlusion facilitates binocular fusion during rivalry. *Journal of Vision,* 19(5):23, 1–17.

Skerswetat, J., Bex, P. J., & Baron-Cohen, S. (2022). Visual consciousness dynamics in adults with and without autism. *Scientific Reports,* 12(1), 1–15.

Srinivasan, R., Russell, D. P., Edelman, G. M., & Tononi, G. (1999). Increased synchronization of neuromagnetic responses during conscious perception. *Journal of Neuroscience,* 19(13), 5435–5448.

Sutoyo, D., & Srinivasan, R. (2009). Nonlinear SSVEP responses are sensitive to the perceptual binding of visual hemifields during conventional 'eye' rivalry and interocular 'percept' rivalry. *Brain Research,* 1251, 245–255.

Thaler, L., Schütz, A. C., Goodale, M. A., & Gegenfurtner, K. R. (2013). What is the best fixation target? The effect of target shape on stability of fixational eye movements. *Vision Research,* 76, 31–42.

Tong, F., Meng, M., & Blake, R. (2006). Neural bases of binocular rivalry. *Trends in Cognitive Sciences,* 10(11), 502–511.

Tononi, G., Srinivasan, R., Russell, D. P., & Edelman, G. M. (1998). Investigating neural correlates of conscious perception by frequency-tagged neuromagnetic responses. *Proceedings of the National Academy of Sciences, USA,* 95(6), 3198–3203.

Tootell, R. B., Mendola, J. D., Hadjikhani, N. K., Liu, A. K., & Dale, A. M. (1998). The representation of the ipsilateral visual field in human cerebral cortex. *Proceedings of the National Academy of Sciences, USA,* 95(3), 818–824.

Wilson, H. R. (2003). Computational evidence for a rivalry hierarchy in vision. *Proceedings of the National Academy of Sciences, USA,* 100(24), 14499–14503.

Ye, X., Zhu, R. L., Zhou, X. Q., He, S., & Wang, K. (2019). Slower and less variable binocular rivalry rates in patients with bipolar disorder, OCD, major depression, and schizophrenia. *Frontiers in Neuroscience,* 13, 514.

Zaretskaya, N., Thielscher, A., Logothetis, N. K., & Bartels, A. (2010). Disrupting parietal function prolongs dominance durations in binocular rivalry. *Current Biology,* 20(23), 2106–2111.

3

Neural Markers of Interocular Grouping during Binocular Rivalry with MEG

Manuscript in preparation for journal submission

Mokri, E., da Silva Castanheira, J., Landry, M., & Mendola, J. D. (in prep). Neural Markers of Interocular Grouping during Binocular Rivalry with MEG.

3.1 Preface

The third chapter transitions from psychophysics experiments to a neuroimaging study of binocular rivalry and interocular grouping. The upcoming chapter presents a frequency-tagged magnetoencephalography study, building on findings from the second chapter (Mokri et al., 2023). Interocular grouping is tested with two- and four-patch IOG images, based on limited effects observed with four- versus six-patch IOG. A subset of participants from the second chapter's psychophysics experiments underwent repeat testing with MEG. This chapter focuses on time-frequency analysis and introduces machine learning to uncover neural mechanisms between BR and IOG and perceptual states of dominance versus suppression.

Previous studies have used neuroimaging with IOG (Buckthought et al., 2021), but combining MEG and frequency-tagging for IOG is novel, extending MEG literature on BR (Tononi et al., 1998; Bock et al., 2019; Bock et al., 2023). Frequency-tagging methods were matched for dominant percepts across BR and IOG, with red gratings tagged at 5 Hz and green at 6.67 Hz. Images closely resembled those in Mokri et al., (2023), with minor adaptations. Grouping conditions included IOG2V, IOG2H, and IOG4, given smaller effects beyond four-patch grouping identified in the previous chapter. A similar two-button press-and-hold design was used to capture dominant and mixed percepts, focusing on dominant percept alternations.

Previous frequency-tagged studies of BR with EEG (Brown & Norcia, 1997; Zhang et al., 2011; Katyal et al., 2016; Spiegel et al., 2019), EEG-fMRI (Jamison et al., 2015), and MEG (Tononi et al., 1998; Bock et al., 2019; Bock et al., 2023) identified changes in power at fundamental frequencies matching perceptual alternations. This holds true for all grouping conditions, though rivalry depth is reduced during IOG. Analyzing dominance and suppression at alternation times reveals larger differences in dominance between BR and IOG. The neural mechanisms of BR and IOG share similarities, but the neural representation of dominance is stronger during BR at alternation times.

3.2 Abstract

Binocular rivalry is a visual phenomenon where two incompatible images are simultaneously presented, one to each eye, and elicit perceptual alternations between image dominance and suppression. Remarkably, binocular rivalry accommodates interocular grouping so that if portions of two globally coherent images are shown to each eye, subjects still perceive the global pattern far more often than would be expected. In this study, we recorded MEG brain activity (N = 25) while viewing classic rivalry (BR) and rivalry with interocular grouping (IOG). Our design included conditions with systematically increasing grouping demands; stimuli were divided into 2 or 4 complementary patches shown to each eye, and vertical or horizontal image meridian divisions. In all cases, participants reported their frequency and durations of dominant or mixed percepts, and stimuli consisted of flickering red or green dichoptic orthogonal gratings at 5 or 6.67 Hz, respectively. This allowed for analysis of tagged fundamentals in the SSVEF with MEG. Compared to BR, IOG produced weaker MEG power at the fundamental frequencies in early visual cortex. The reduced power for IOG in V1/V2 might be expected from less time spent perceiving/attending a coherent image, and could be due to diminished competition between monocular neurons for IOG. IOG showed early (i.e., prior to alternation), but weaker neural markers of dominance when compared to BR, while patterns of suppression were not as affected in depth nor topography. Multivariate logistic regression models highlighted differences between BR and IOG conditions, in specific regions in the early visual cortex (i.e., V1 and V2) as well as higher-order visual areas (i.e., IP and LO) that differed in the specific temporal characteristics of SSVEF responses. Further, a three-fold support vector machine (SVM) approach was used to disentangle neural correlates of dominance and suppression, demonstrating the highest decoding accuracy at the time of the report of alternation. Overall, we show evidence of a broad similarity for BR and IOG in the neural representations across an expanse of the visual system that argues for a common overarching rivalry network for both BR and IOG.

3.3 Introduction

Binocular rivalry (BR) is a visual phenomenon in which perception alternates between two non-fusible images presented to each eye. Participants experience periods of dominance and suppression between left and right eye image representations during cycles of alternation. When an image becomes dominant, it is reported with near-complete visibility, whereas the non-attended image becomes suppressed from visual awareness (Levelt 1965; Blake 1989; Alais & Blake, 2005). This phenomenon is of interest, because it represents an instance where perception changes vividly despite static image presentation. In our experiment, rivalry is achieved by using complementary colored (red or green) orthogonal gratings, with an interocular orientation difference of 90 degrees to elicit vigorous alternations (O'Shea, 1997; Baker & Graf, 2009; Cooper & Mendola, 2019). During periods of transitions between dominant percepts, participants often report a period where fragments of each image are seen, termed mixed or piecemeal percepts (Said & Heeger, 2013; Katyal et al., 2016; Bock et al., 2019. Importantly, mixed percepts are thought to represent a period of perceptual ambiguity, where image representations from each eye are competing for perceptual dominance. These periods of ambiguity will transition to the emergence of one dominant image representation.

In addition, another type of binocular rivalry, termed interocular grouping (IOG), is experienced when participants view two non-fusible images presented in bistable complimentary patches across the eyes (Kovacs et al., 1996). During IOG, the global images are subdivided into image fragments and presented dichoptically across the eyes. Nevertheless, the perception of unified global images occurs frequently and engages in rivalry. IOG is an excellent demonstration of perceptual rivalry that likely require binocular combinatorial processing. Several other factors at play during IOG include the Gestalt principles of similarity and continuity. Taken together, these two visual illusions, BR and IOG, allow us to examine the dynamics of rivalry and binocular combinatorial processing that occurs during bistable perception. Moreover, during our experiments, we varied the demands of IOG by increasing the number of patches (IOG with 2 and 4 complementary bistable patches), and by comparison of the orientation of image meridian division (vertical or horizontal). We already know that both BR and IOG produce similar dynamics of perceptual alternations (Mokri et al., 2023). We aim to examine with magnetoencephalography

(MEG) whether these two visual illusions that produce similar perceptual experiences of bistable alternations are driven by shared or different neural networks.

The introduction of interocular grouping by Kovacs et al., (1996) was notable for emphasizing the role of binocular neurons during rivalry. In contrast, previous models of binocular rivalry primarily discussed competition between monocular neurons (e.g., Matsuoka 1984; Blake 1989). Such models of solely monocular-based competition would not be able to easily explain IOG, which requires information from both eyes to be combined and stabilized for the experience of perceptual alternations that mimic BR (although see discussion). Therefore, IOG is an important example of rivalry that highlights the role of binocular neurons and the interplay between lower and higher order visual areas. The role of binocular neurons during traditional BR has been debated, and supported by data from several studies (Logothetis et al., 1996; Wilson, 2003; Said & Heeger, 2013). A finding of similarity between networks isolated with MEG during binocular rivalry and interocular grouping would strengthen the case for the importance of binocular neurons and integration of image representations beyond the primary visual cortex for BR.

In recent years, the use of frequency tagging has proven to be a useful tool when combined with EEG and MEG neuroimaging studies to isolate the evoked response from brain regions that are actively computing image representations (Brown & Norcia, 1997; Kamphuisen et al., 2008; Zhang et al., 2011). In these designs, the stimuli are flickering at specific frequencies, so that the evoked response carries this frequency throughout the visual pathways through neuronal entrainment. This technique offers a high signal-to-noise ratio (SNR) due to the ability to filter the brain response at the fundamental frequencies entrained by the tagged stimuli. This method allows researchers the ability to specifically highlight which brain regions are being entrained by the highly visible stimuli. The method also allows for a joint analysis that encompasses event-related time-locking to the behavioural responses. Frequency tagging and MEG with SSVEF has been used previously and several studies show that alternations in the visual percept are associated with fluctuations in the evoked response with a higher response for dominant images compared with suppressed (Tononi et al., 1998; Srinivasan et al., 1999; Kamphuisen et al., 2008; Zhang et al., 2011; Bock et al., 2019; Spiegel et al., 2019). Some disagreement exists in the literature regarding the topography of these signals, but the most recent studies using modern (phase-locking) methods tend to isolate posterior regions of the brain, in primary and association visual cortex. (Kamphuisen et al., 2008; Bock et al., 2019; Bock et al., 2023).

Fortunately, the use of dichoptic flicker (tags) for the left and right eye does not disrupt classic binocular rivalry. Frequency tagging can also be applied to IOG; however, it is important to note that in this case we used stimulus-based frequency tagging, where the red-coloured gratings flickered at one frequency (in both eyes) while green-coloured gratings in both eyes flickered at a second frequency, 5 Hz and 6.67 Hz, respectively. In fact, this use of flicker for IOG has been shown to modestly extend periods of dominance during IOG by lengthening periods of dominant percept duration (Knapen et al., 2007). We presume this is due to flicker frequency serving as a potential binding cue, along with the colour and orientation of the grating stimuli. We hypothesized that directly comparing BR and IOG with the neuroimaging techniques of frequency-tagged MEG will provide insight into the temporal and spatial dynamics of rivalry, allowing us to determine where and when neural markers of perceptual alternations are occurring. The benefits of MEG also include the increased spatial resolution provided over other techniques such as EEG, especially when combined with anatomical MRIs for each participant. Moreover, the temporal resolution is far superior when compared with fMRI methods.

Two distinct regions beyond the primary visual cortex have received attention due to their proposed role in bistable percepts; the parietal cortex, and the lateral occipital cortex. Evidence for a causal role for regions of the parietal lobe during perceptual alternations comes from studies employing transcranial magnetic stimulation (TMS). TMS applied over the right intraparietal sulcus (IPS) decreased binocular rivalry alternation rates by prolonging the duration of stable percepts (Zaretskaya et al., 2010). Interestingly, another study found TMS over parietal cortex to increase alternation rate (Carmel et al., 2010). Nevertheless, the right inferior parietal lobe is again identified as a possible source for the origin of perceptual alternations during binocular rivalry and other bistable percepts when recording ERPs during intermittent rivalry (Britz et al., 2009; Britz et al., 2011). Consistently, increased activation is observed in the right inferior parietal lobe immediately preceding percept reversals (Pitts & Britz, 2011). fMRI studies of binocular rivalry have emphasized multiple cortical regions of activity beyond the occipital pole with increased BOLD signal. Higher BOLD activity in the right frontal, parietal, and occipital areas have been repeatedly noted during rivalry viewing (e.g., Wilcke et al., 2009; Rees, 2007). One fMRI study used simultaneous recordings of EEG with dichoptic frequency tagged stimuli and was able to guide fMRI analysis with the SSVEPs obtained. A right-lateralized fronto-parietal network and posterior regions of the default mode network (DMN) were highlighted for resolving perception

changes during BR, and the strongest BOLD signal was observed in the right superior parietal lobule (rSPL) during perceptual transitions (Roy et al., 2017).

Unlike BR, very few neuroimaging studies exist recording brain activity during instances of interocular grouping. Only recently, was an fMRI investigation of IOG reported (Buckthought et al., 2021). In this study specific (retinotopic) visual areas in lateral occipital cortex (LO1), and inferior parietal cortex (IP0-2) were found to increase in activity during binocular rivalry with interocular grouping when compared to BR rivalry with no grouping (Buckthought et al., 2021). Interestingly, area LO1 is part of the lateral occipital complex (LOC), a higher-level visual region that has been identified for its role in human object recognition (Grill-Spector et al., 2001). Moreover, fMRI studies have indicated an increase in activity in the LOC, and a corresponding decrease in the lower-level visual area V1 during perceptual grouping (Fang et al., 2008). Grill-Spector has suggested a hierarchical organization within the LOC, with more posterior regions activated by object fragments, and anterior regions for whole objects (2001). Moreover, regions within the lateral occipital region (LO) have been found to differ in sensitivity to stimuli that cross left and right visual hemifields versus within-hemifield, and (Large et al., 2008) posited two staged model of spatial integration.

In the current study we used MEG with stimulus frequency-tagging methods to record and compare SSVEF during well-matched conditions of binocular rivalry and interocular grouping. We further compare IOG conditions with increasing grouping demands, as was also done in Chapter 2. Our design also allows for grouping across the vertical and horizontal meridans to be contrasted directly. We hypothesized that areas LO and IP might be recruited to a greater degree for IOG than BR based on previous fMRI results. We also expected that results could differ for grouping across vertical or horizontal meridians based on both behaviral and physiological data (Golubistky et al., 2019; Mokri et al., 2023; Knyazeva et al., 2006).

3.4 Methods

Participants

Twenty-five participants were included in the study with a mean age of 24.24 years (SD = 3.13 years) (16 females). The participants were screened for normal to corrected normal vision, reported no visual disorders, with no metals in their body that were MEG incompatible, and were not taking psychoactive nor psychotropic medication during the testing period. The participants were allowed to wear contact lenses for vision correction, or have previously undergone eye correction surgery, however, the use of personal glasses was not allowed due to the necessity of MEG compatible prism lenses to facilitate visual fusion. Visual acuity was assessed by the experiment prior to tested using the Logarithmic Visual Acuity chart (Early Treatment Diabetic Retinopathy Study [ETDRS] 2000 series chart; Precision Vision, Woodstock, IL), while stereo vision was evaluated using the Titmus Stereoacuity Test (Stereo Optical, Chicago, IL). Both inclusion tests were performed in a well-lit room and followed the manufacturers recommendations for the instructions provided and the testing distances. Each eye's visual acuity was independently tested to screen for interocular imbalances that could affect BR and IOG. The criteria for inclusion were set at visual acuity values of 20/40 or better in each eye, with no more than two lines of differences between the eyes. The median visual acuity for both right and left eyes within the participant pool was 20/20. The inclusion criteria for the stereo vision test were set at 7/9 targets sequentially identified which corresponds to an angle of stereopsis of 60 seconds at 16 inches. The median result was 9/9 targets correctly identified.

Further inclusion criteria for MEG analysis resulted in the exclusion of six participants tested. Prior to data collection for three participants, hardware malfunction with the digitization equipment prevented appropriate co-registration between the anatomical MRI and MEG sensor location, resulting in faulty head models. Further, during inspection of the power spectrum density (PSD) analysis, three participants did not have visible periodic peaks at the fundamental frequencies (5 Hz and 6.67 Hz) in the primary visual cortex. This resulted in our final subject pool of twenty-five participants included in the results.

The entire testing protocol was comprised of three days of rivalry experiments that included several types of bistable stimuli, and a final day where the anatomical MRI was obtained. The

initial day of psychophysics testing is reported in Mokri et al., (2023), and comprised a larger participant pool (N = 48), many of whom were deemed incompatible with MEG testing. The second day of rivalry viewing is not discussed in this chapter as different types of bistable images were presented. The frequency-tagged MEG experiment with BR and IOG stimuli was obtained on the third day of testing.

Experimental Design

The stimulus design closely followed that previously reported by Mokri et al., (2023) from the initial day of testing. Within the MEG, we facilitated the experience of BR and IOG by using a black opaque cardboard divider positioned between the two eyes, and MEG compatible prism lenses with a strength of 12 diopters. Prior to the MEG data acquisition, all participants were guided through a four-minute practice session on a laptop to ensure appropriate fusion and experience of rivalry. During the unrecorded practice, participants were reminded of the instructions for reporting their alternations in percept previously introduced on prior testing days.

The experiment tasked participants with reporting their alternations in visual perception (i.e. red, green, or mixed percepts) during BR and IOG using a two-button press-and-hold design (Figure 3.1A). They were instructed to press the corresponding button pad when they perceived the majority (>80%) of the stimuli to be either red or green. Participants were asked to both press and hold their button response throughout the duration of the experienced percept. When neither red, nor green was dominantly experienced, they were instructed to withhold a response, indicating the experience of a mixed percept. The instructions for mixed percepts implied the inclusion of both any monocularly viewed IOG stimuli, and more traditional piecemeal percepts arising from the combination rivalry images.

Each condition (i.e., BR, IOG2V, IOG2H and IOG4) was presented in two five-minute runs that were subdivided into four counterbalanced testing blocks, each lasting 75 seconds. In total, this resulted in ten-minutes of MEG data acquisition for each experimental condition. Counterbalancing was implemented for the orientation and colour of the orthogonal gratings shown to each eye to mitigate the effects of adaptation. Each experimental block started with a blank fixation-only screen where participants were instructed to fuse and self-initiate the start of rivalry image presentation.

Stimulus

BR and IOG stimuli were presented using Psychtoolbox-3 (Brainard, 1997; Kleiner, Brainard, & Pelli, 2007) and MATLAB 2021a (MathWorks, Natick, MA), as illustrated in Figures 3B-E on a VPixx projector (VPixx Technologies Inc., Saint-Bruno, QC) with a 60 Hz refresh rate. The classic BR stimulus was comprised of seven orthogonal gratings at 90-degree interocular orientation difference shown to each eye, with RGBA values of [0.5 0 0 0.35] for red and [0 0.35 0 0.35] green colours, with a visual angle of 8° 14' 0.97". The RGBA values were selected during pilot testing with the experiments to determine approximate balance in strength between red and green gratings. Equally, the use of seven orthogonal gratings was decided during pilot testing, and found to elicit rivalry and an appropriate signal strength detected on the power spectrum density analysis in the primary visual cortex. The interocular grouping stimulus was created by subdividing the BR images into two- and four-bistable complementary patches. The fixation mark was chosen to help increase the stability and reduce eye movements, which could negatively impact fusion during BR (Thaler et al., 2013). Black borders were drawn around the stimuli to provide additional cues that could aid in fusion and maintain fixation throughout the experiment. The projector was placed at a viewing distance 52 cm away from the central bridge of the prism lenses, and the inner square of the stimuli was 7.5 cm in height and width. This corresponded to a visual angle of 8° 14' 0.97" used for all image presentation during BR and IOG conditions.

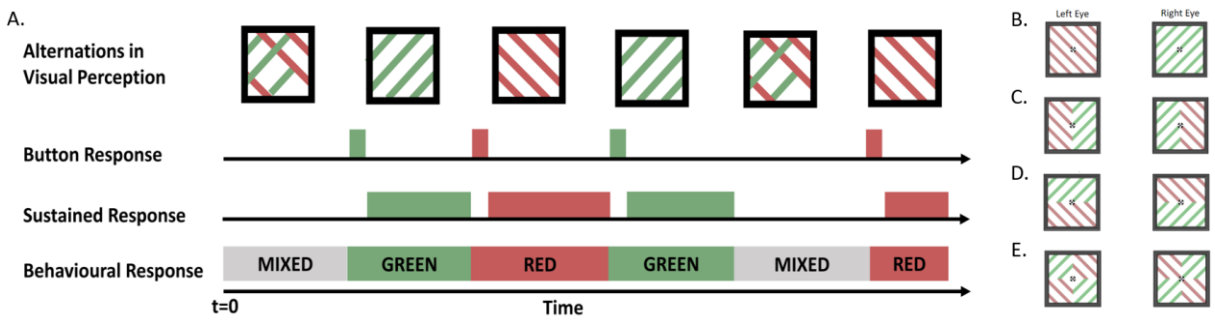

Figure 3.1 Experiment design and psychophysics results for BR and IOG conditions. A. experimental design for behavioural responses during the rivalry experience. Participants used a two-button press-and-hold response to indicate their alternations between red, green and mixed percepts. **B.** Stimulus for binocular rivalry. **C.** Stimulus for two-patch interocular grouping with a vertical image meridian division. **D.** Stimulus for two-patch interocular grouping with a horizontal image meridian division. **E.** Stimulus for four-patch interocular grouping. In all four conditions (BR, IOG2V, IOG2H and IOG4), the red orthogonal gratings were frequency-tagged at 5 Hz, and the green orthogonal gratings were frequency-tagged at 6.67 Hz.

MEG Data Collection

The MEG data acquisition was conducted in Montreal, Canada, at McGill University's McConnell Brain Imaging Centre, utilizing a 275-channel CTF/VSM MEG system (CTF MEG, British Columbia, Canada) operating at a sampling rate of 2400 Hz. Prior to MEG data acquisition, individualized head models were constructed for each participant through the digitization of approximately 100-150 points across the scalp. This process also involved recording anatomical landmarks and head-position coils using a Polhemus Fastrak system (Polhemus, Vermont, USA). To capture body-related artifacts, bipolar signals were recorded for both vertical (eye blinks) and horizontal (visual saccades) electrooculogram (EOG), in addition to electrocardiogram (ECG) signals for heartbeats. Prior to participant's data acquisition, a 2-minute empty room recording was performed to identify faulty MEG sensors and assess environmental noise levels. These empty room recordings were subsequently used during MEG source imaging to compute noise covariance. Furthermore, a T1-weighted anatomical MRI volume (1.5T Siemens Sonata) was acquired for each participant for co-registration with their MEG data, thereby enhancing spatial resolution.

MEG Data Preprocessing and Cleaning

The MEG data preprocessing, cleaning, and analysis was performed in Brainstorm (Tadel et al. 2011), which is documented and freely available for download online under the GNU general public license (http://neuroimage.usc.edu/brainstorm). The preprocessing and cleaning procedures followed the guidelines provided by Brainstorm software documentation (Tadel et al., 2011) and was similar to those reported in previous MEG frequency-tagged BR studies (Bock et al., 2019; Bock et al., 2023). The MEG recordings were downsampled from the acquisition rate of 2400 Hz to 600 Hz. Notch filters were applied at 60 Hz, 120 Hz and 180 Hz with a 3-dB notch bandwidth of 2 Hz to mitigate the interference from North American power lines and their harmonics. Additionally, a high-pass filter was set at 0.3 Hz to remove the DC offset and slow drifts of MEG sensor signals. The subject anatomy from each participant's T1-weighted anatomical MRI volume was imported, and MNI normalization was computed to derive MNI coordinates and anatomical points. During the MEG-MRI co-registration process, the furthest 5% of head points were disregarded. Co-registration was performed using the nasion fiducial (NAS), left ear fiducial (LPA), and right ear fiducial (RPA) points digitized by the experimenter during MEG data collection, along with those identified in the MRI Viewer. To enhance the alignment between the MRI and MEG sensors, an algorithm implemented in the Brainstorm software was used to refine the registration by optimizing the correspondence between head points derived from the subject's MRI and those obtained through digitization.

The data cleaning was performed by the experimenter in 20-second time windows of continuous MEG data via visual examination. Artifacts such as heartbeats, eye blinks and muscle activity were removed. Artifact detection was performed using signal-space projection (SSP) for eye blinks, cardiac artifacts, and 1-7 Hz eye movements. This criteria for removal were performed on a case-by-case basis for each individual subject, with a focus on significant components (i.e., >10%) and displaying topographies indicative of eye movements such as blinks and visual saccades (i.e., strong dipolar activity, concentrated fontal activity, concentrated activity near frontal-temporal regions). In all cases, the result of the corrections was visualized and evaluated. In addition, time-series segments exhibiting high muscle tension or movements during image presentation were identified and marked as 'bad.' Additionally, the first button press of each run was disregarded due to the uncertainty regarding the prior perceptual state. Overall, we obtained 23,926 dominant percept button responses (M = 957.04, SD = 321.88) throughout BR and IOG

conditions, with the variability attributed to individual differences in alternation rates. After preprocessing and cleaning, 79.16% of the data was retained for analysis.

MEG Frequency-Tagging

The experiments presented used frequency-tagging at two fundamental frequencies to record SSVP responses during BR and IOG. This was achieved with dichoptic flicker frequencies coded in MATLAB. Importantly, for all conditions tested, the red gratings were tagged at 5 Hz, and the green gratings at 6.67 Hz.

To ensure successful neural entrainment at the fundamental frequencies, power spectrum density (PSD) analysis using the Welch method was performed for both tagged and untagged rivalry conditions (Figure 3.2). Prior to the frequency-tagged image presentation, untagged images for BR, IOG2V, IOG2H and IOG4 were shown. The results from the untagged experiment are not discussed in this chapter further than the PSD analysis in Figure 3.2. For each participant, a PSD analysis was used on all of the 75-second testing blocks for each condition in the primary visual cortex. The frequency range was set at 0-60 Hz, mean power in V1 was computed, and a 6-second sliding window with 50% overlap was used. For each participant, the four PSD's taken from the individual 75-second testing blocks were averaged together for the individual participant average. Further, the periodic peak components of the PSD analysis for each participant were extracted using specparam methods (Donoghue et al., 2020). The frequency range for peak detection was 1-30 Hz, with peak width limits of 0.1-2 Hz, a maximum number of 10 peaks, minimum peak height of 0.02 dB, fixed aperiodic mode, a proximity threshold of 0.5 standard deviations, and the Gaussian peak model. The results for the specparam periodic peak components in V1 for all participants were averaged together in the group mean results for BR and IOG conditions shown in Figure 3.2.

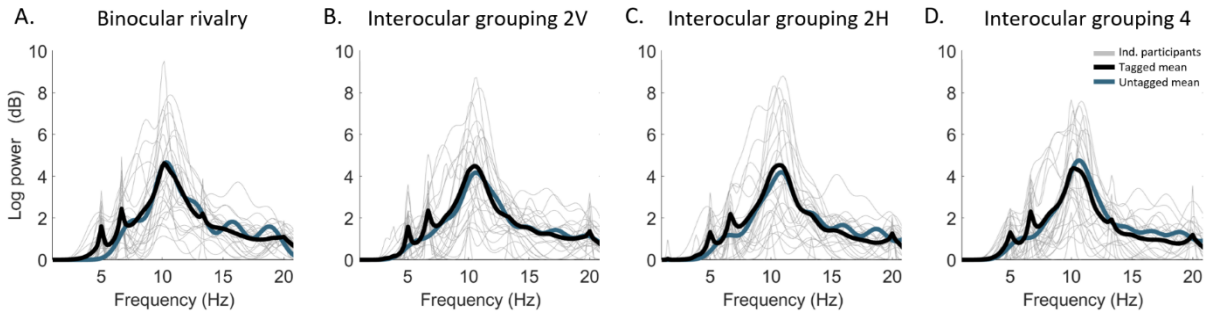

Figure 3.2 MEG frequency-tagging in the primary visual cortex during BR and IOG. Specparam methods were applied to the power spectrum density analysis in the primary visual cortex to isolate the periodic peak components. **A.** Binocular rivalry. **B.** Interocular grouping with two-patch vertical image meridian division orientation. **C.** Interocular grouping with two-patch horizontal image meridian division orientation. **D.** Interocular grouping with four-patches.

The results in Figure 3.2 confirm our methods for eliciting neural entrainment at the fundamental flicker frequencies in the primary visual cortex for all conditions. In the untagged rivalry conditions, we observed one mean peak that corresponds to the alpha band peak centered around 10 Hz. Whereas during the frequency-tagged rivalry conditions, we observed the alpha peak, in addition to two distinct peaks at 5 Hz (red grating flicker frequency) and 6.67 Hz (green grating flicker frequency). Across conditions, the power of the alpha band and fundamental frequency peaks is relatively constant. This is especially interesting when considering the differences between image presentation during BR and IOG. Additionally, smaller peaks are noticed at harmonics of the fundamental frequencies (i.e., 10, 13.34, 15 and 20 Hz) in the frequency-tagged conditions.

MEG Source Localization

The MEG source localization was performed using Brainstorm for each individual participant. This is an important step to increase spatial resolution and co-register the anatomical (T1 weighted) MRI with the MEG source space. A head model was created using the overlapping spheres method. Using both the data and noise covariance matrices, unconstrained sourced beamformer models were generated. The MRI segmentation was performed using CAT12 (Gaser et al., 2022) and SPM12 extensions in the Brainstorm software. The following parameters were selected: 15000 vertices, use spherical registration, and compute volume parcellations. The regions

of interests (ROI) were generated for each individual participant's source reconstruction. Taken from the human connectome project (HCP-MMP1) atlas (Glasser et al., 2016), 25 ROIs were created with the objective of covering the majority of the posterior cortex and the visual system (Table 4.1). Right and left hemisphere labels were combined into a single ROI for each region (i.e., left hemisphere V1 and right hemisphere V1).

Table 3.1 Regions of interest generated for each participant for scout-based MEG analysis. The abbreviation L and R refer to right and left hemispheres, respectively. The regions of interest were mapped for each participant's individual anatomy (N = 25).

ROI labels	Regions merged from HCP MMP1 atlas
V1	V1 L & V1 R
V2	V2 L & V2 R
V3	V3 L & V3 R
V3A	V3A L & V3A R
V3B	V3B L & V3B R
V4	V4 L & V4 R
V6	V6 L & V6 R
V6A	V6A L & V6A R
V7	V7 L & V7 R
V8/PIT	V8 L, V8 R, PIT L & PIT R
LO1/LO2	LO1 L, LO1 R, LO2 L & LO2 R
V4t/LO3	V4t L, V4t R, LO3 L & LO3 R
MT/MST	MT L, MT R, MST L & MST R
VMV	VMV1 L, VMV1 R, VMV2 L, VMV2 R, VMV3 L & VMV3 R
VVC	VVC1 L & VVC1 R
POS	POS1 L, POS1 R, POS2 L & POS2 R
IP0	IP0 L & IP0 R
IP1	IP1 L & IP1 R
IP2	IP2 L & IP2 R
IPS1	IPS1 L & IPS1 R
PG	PGi L, PGi R, PGp L, PGp R, PGs L & PGs R
PI	AIP L, AIP R, LIPd L, LIPd R, LIPv L, LIPv R, MIP L, MIP R, VIP L & VIP R
TPOJ	TPOJ1 L, TPOJ1 R, TPOJ2 L, TPOJ2 R, TPOJ3 L & TPOJ3 R
7	7AL L, 7AL R, 7Am L, 7Am R, 7PC L, 7PC R, 7PL L, 7PL R, 7Pm L, 7Pm R, 7m L & 7m R

MEG Event Related Analysis

The MEG data analysis was performed with Brainstorm (Tadel et al. 2011), which is documented and freely available for download online under the GNU general public license (http://neuroimage.usc.edu/brainstorm).The SSVEF signal was time-locked to the report of dominant percept alternations during BR and IOG. After preprocessing and cleaning procedures were applied, each button-press response was identified and segmented in a ten second window (i.e., five seconds prior to- and five seconds after the button press) centered around the alternation. During the segmentation process, the MEG recording was further downsampled from 600 Hz to 120 Hz and the DC offset was removed.

The Hilbert transform time-frequency analysis on the full cortex and predefined ROI scouts was performed for dominant and suppressed percepts. The analysis was performed at the specific fundamental frequencies (5 Hz and 6.67 HZ) for both dominance and suppression. This was done by filtering the matching frequency tags to behavioural reports for dominance (i.e., red responses filtered at the corresponding red grating 5 Hz frequency tag), and opposing frequencies for suppression (i.e., red response filtered at the corresponding green grating 6.67 Hz frequency tag). The Hilbert time frequency analysis was performed at the individual trial level in 10 s epochs centered around the button press, then averaged at the participant level before computing group level averages. The time series of the group level analysis was extracted between -3 to 3 seconds to minimize the edge effects. For each participant, the results were baseline normalized between the time period of -3 to 3 seconds, centered around the button press, to obtain a z-score measure of power. The baseline normalization procedures ensured consistency in scale across participants.

Multivariate Logistic Regression

We used multivariate logistic regression models to compare interocular grouping conditions with binocular rivalry based on predefined regions of interest in the occipital and parietal cortex. We contrasted BR against IOG2V, IOG2H, and IOG4. It was necessary to divide ROIs into subgroups for the model to successfully converge. We divided the ROIs mapped for each individual participant (Table 3.1) two subgroups (i.e., ROI set 1, and ROI set 2), while the ROIs from each subgroup were included as fixed effects in hierarchical logistic regression model and participants were included as random effects. The first set of regions (ROI set 1) included

early visual areas extending to mid- and higher-level regions in the visual system, broadly grouped by proximity: V1, V2, V3, V3A, V3B, V3CD, V4, V6, V6A, and V7. The second set of regions (ROI set 2) comprised higher-order areas associated with visual processing, extending to the lateral occipital and parietal cortex: LO1/LO2, LO3/V4t, MT, V8/PIT, VMV, VVC, POS, IP0, IP1, and IP2. We fitted the following models across the time series separately for dominance and suppression:

$$\text{Logit(Grouping)} = \beta 0 + S0_{\text{participants}} + \beta 1_{v1} + \beta 2_{v2} + \beta 3_{V3} + \beta 4_{V3A} + \beta 5_{v3B} + \beta 6_{V3CD} + \beta 7_{V4} + \beta 8_{V6} + \beta 9_{V6A} + \beta 10_{V7}$$

$$\text{Logit(Grouping)} = \beta 0 + S0_{\text{participants}} + \beta 1_{LO1/LO2} + \beta 2_{LO3/LO4} + \beta 3_{MT} + \beta 4_{V8/PIT} + \beta 5_{VMC} + \beta 6_{VVC} + \beta 7_{POS} + \beta 8_{IP0} + \beta 9_{IP1} + \beta 10_{IP2}$$

For null hypothesis testing, we evaluated each model against a null model, which solely comprised the intercept.

Multivariate Pattern Analysis

We used multivariate pattern classification to evaluate differences between the neural patterns from the evoked responses for dominance and suppression across time series that were time-locked to the button press for all grouping conditions. Relying on a three-fold cross-validation, our multivariate approach largely follows from the work of Bae & Luck (2018). We performed multivariate classification using the linear support vector machine (SVM) and the *fitcsvm* function in MATLAB (The MathWorks Inc., Natick (MA), USA; Version R2022a). With the three-fold cross-validation procedure, MEG times series data for trials from each grouping condition were separated into three different bins per class – i.e., three bins of trials for neural patterns related to perceptual dominance and three bins for neural patterns related to perceptual suppression. We equated trials per bins for all conditions and participants. There were 25 time series of MEG data per bin. Each time series was extracted from our Hilbert Transform time-frequency analysis on individual trials and segmented in a 10 second window centered around the button press. Next, we averaged the time series from each bin, and baseline corrected them from -5 seconds to -3 seconds prior to the button response. We then trained SVM on each time point

along the time series from -3 seconds to 3 seconds centered around the report of alternation based on multivariate patterns from the 25 ROIS previously identified. These patterns of activity were therefore included as features in our model. We trained the classifier using data from two bins (i.e., two time series related to perceptual dominance and two related to perceptual suppression), and then tested the model on the remaining ones (i.e., one time series for perceptual dominance and one for perceptual suppression). We then iterated this process such that each MEG time series was used twice for training and once for testing. We repeated this process 50 times per participant per grouping condition while randomly shuffling trials across bins for each repetition. Lastly, we averaged classification accuracy rates for each participant with smoothed values via a five-sample sliding window -- i.e., a 20ms window. This procedure allowed us to assess the classification performance across the time series.

We used one sample t-tests across the time series to determine whether classification performances were better than chance-level. We also compared classification accuracies between interocular grouping conditions using pairwise t-tests across the time series. For all analyses, we controlled for family-wise errors via random permutations and mass t-statistics for cluster size. The cluster forming threshold was set to $p < 0.05$. We performed 1000 permutations where we randomly varied the classification labels and then contrasted observed cluster sizes based on t-statistics against surrogate distributions of cluster size. Statistically significant clusters were threshold at $\geq 95\%$.

3.5 Results

Psychophysics

During the MEG recordings while participants (N = 25) experienced BR and IOG conditions, we obtained behaviourial results from participants through a two-button press-and-hold design (Figure 3.1A). These measures allowed us to record alternation rates, mean dominant and mixed percept durations, and viewing proportions during BR and IOG. The results were analyzed using the statistical software R.

Alternation rate is a commonly used metric during rivalry and bistable percept illusions that represents the rate at which participants experience changes in percepts. In our study, alternation rate is defined as the number of dominant percept alternations per second. It was computed by dividing the total number of dominant (i.e., red and green) button presses by the duration of the experiment. The results are presented in Figure 3.3A for binocular rivalry and interocular grouping: BR (M = 0.45 Hz, SD = 0.14), IOG2V (M = 0.38 Hz, SD = 0.15), IOG2H (M = 0.39 Hz, SD = 0.14), IOG4 (M = 0.33 Hz, SD = 0.15). Participants experienced faster alternation rates between dominant percepts during BR. Within IOG conditions, faster alternations were present during two-patch interocular grouping (i.e., IOG2V and IOG2H) than four-patch interocular grouping. This result indicates that a greater frequency of dominant percepts was reported during BR, with fewer alternations experienced as grouping demands increased.

In addition to rates, we analyzed percept durations indicating the length of time participants experienced dominant and mixed percepts once they were reported. The mean durations were defined as the length of time a dominant (i.e., red and green), or mixed percept was held by participants through their response. For dominant percepts (Figure 3.3B), the durations were as follows: BR (M = 1.86 seconds, SD = 0.80), IOG2V (M = 1.71 seconds, SD = 0.77), IOG2H (M = 1.73 seconds, SD = 0.96), IOG4 (M = 1.63 seconds, SD = 0.97). The results show that during the BR condition, the mean duration of dominant percepts was experienced for longer durations than IOG conditions. Within IOG conditions, dominant percept durations were reduced as grouping demands increased. Overall, we observed stability in the duration of dominant percepts between BR and IOG, as the mean duration between conditions was found to be non-significant. We further analyzed the durations of mixed percepts experienced by participants during BR and

IOG (Figure 3.3C). Mixed percept duration was obtained as the duration in time that neither red, nor green was reported between transitions in percept: BR (M = 0.66 seconds, SD = 0.38), IOG2V (M = 1.56 seconds, SD = 1.28), IOG2H (M = 1.40 seconds, SD = 0.87), IOG4 (M = 2.26 seconds, SD = 1.59). We observed that participants experienced shorter durations for mixed percepts during BR. Within IOG conditions, increasing the number of patches from two to four, resulted in an increase in the mean result for mixed percept duration. Taken together, these results indicate that the experience of mixed percepts were increased in their duration.

The final psychophysics analysis performed was focused on overall percept predominance during BR and IOG (Figure 3.3D). The computation of viewing proportions was defined as the proportion of time each percept (i.e., red, green, or mixed) was perceived throughout the experiment. This result emphasized the interaction between alternation rate and percept duration. The results were as follows: BR (red: M = 0.39, SD = 0.09, green: M = 0.36, SD = 0.08, mixed: M = 0.25, SD = 0.16), IOG2V (red: M = 0.30, SD = 0.08, green: M = 0.27, SD = 0.09, mixed: M = 0.42, SD =0.17), IOG2H (red: M = 0.31, SD = 0.09, green: M = 0.27, SD = 0.09, mixed: M = 0.42, SD = 0.17), IOG4 (red: M = 0.26, SD = 0.11, green: M = 0.22, SD = 0.09, mixed: M = 0.52, SD = 0.20). When accounting for rounding to two-decimal places, the original values for all of the viewing proportions summed to 1 for each condition. The results indicate that participants experienced greater predominance of mixed percepts as grouping demands increased from BR to IOG, and from two- to four-patch interocular grouping. Interestingly, the ratio of dominant to mixed percepts changed between BR and IOG. During BR, participants experienced a greater mean predominance of dominant (i.e., red and green) percepts, whereas IOG resulted in the opposite effect, with a greater mean predominance of mixed percepts. Throughout all conditions, we observed a slight trend for increased predominance of red percepts when contrasted with green percepts.

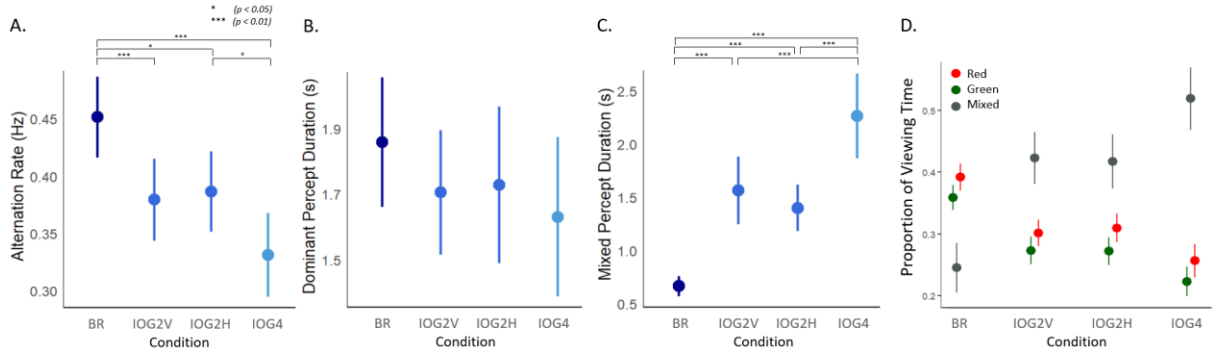

Figure 3.3 Psychophysics results for BR and IOG conditions. For all conditions, the mean result is plotted with 95% confidence intervals. **A.** Alternation rate measured in hertz for BR and IOG conditions. The alternation rate was computed by dividing the number of dominant percept alternations by the duration of the experiment. **B.** Dominant percept duration for BR and IOG conditions measured in seconds. **C.** Mixed percept duration for BR and IOG conditions measured in seconds. **D.** Proportion of percepts viewed during BR and IOG conditions. Significance results are plotted from a Welch Two Samples t-test performed in the statistical software R.

To further examine the relationship between BR and IOG conditions with regard to individual differences, Spearman correlations were performed in R for alternation rate, mean dominant percept and mixed percept durations at the individual subject level. Between BR and IOG2V the R-values are reported as follows: alternation rate = 0.90, dominant percept duration = 0.94, and mixed percept duration = 0.58. Between BR and IOG2H the R-values are: alternation rate = 0.92, dominant percept duration = 0.93, and mixed percept duration = 0.59. Between BR and IOG4 the R-values are: alternation rate = 0.68, dominant percept duration = 0.87, and mixed percept duration = 0.32. All of the correlations were found to be significant ($p < 0.05$) after false discovery rate (FDR) correction, with the exception of the correlation between BR and IOG4 mixed percept durations. These results again highlight that increasing grouping demands selectively affect mixed percept durations, whereas alternation rate and dominant percept duration were stable at the level of individual differences for all rivalrous conditions.

SSVEF Markers during MEG – Full Cortex Approach

Steady state visually evoked fields (SSVEF) were recorded during BR and IOG conditions. This was performed using frequency-tagged stimulus and time-locking the neural response to

behavioural reports. For each dominant percept alternation indicated by a button-press, the MEG recording was segmented 5 seconds prior to, and 5 seconds after the perceptual switch as described in the methods. Importantly, the perceptual states of dominance and suppression were dissociated and analyzed independently. We defined the state of *Dominance* as the SSVEF neural response of brain activity for the fundamental frequency that matched the behavioural report (i.e., 5 Hz brain activity during a red percept button-press, and 6.67 Hz brain activity during a green percept button-press). Alternatively, the state of *Suppression* was defined as the SSVEF neural response of brain activity for the fundamental frequency that was in opposition of the behavioural report (i.e., 6.67 Hz brain activity during a red percept button-press, and 5 Hz brain activity during a green percept button-press).

Full cortex Hilbert transform time-frequency analysis was performed for all conditions in Brainstorm. The time-window used for this analysis was 10 seconds, including the period of interest from -5 to 5 seconds centered around the button responses for dominant percepts. The results presented were extracted between the period of -3 to 3 seconds, centered around the button press to minimize the edge effects at the start and end of the analysis period. Displayed in Figure 3.4, the SSVEF responses were recorded at the time of alternation (time = 0 seconds). We can observe the mean change in baseline normalized power (z-score) across both rivalry conditions and perceptual states. The results provide information on the topography, magnitude, and direction of change in power at the fundamental frequencies.

During dominance (Figure 3.4A), binocular rivalry elicited the strongest and most expansive change in baseline normalized power. The increase in power at the fundamental frequency of the dominant tags is observed to peak in strength in the primary visual cortex (V1) and neighboring regions (i.e., V2 and V3). During BR, we can also observe regions within the occipital cortex (i.e., lateral occipital) and parietal cortex that correspond with mid-to-high level visual system. In comparison, when participants viewed IOG conditions, a reduction in both the magnitude, and extent of the dominance response is observed. This reduced power can be seen for two-patch IOG over the primary visual cortex and extending towards lateral occipital regions. Notably, there is a weaker response seen over parietal regions during two-patch IOG conditions when compared to BR. The decrease in magnitude and extent is even more apparent during IOG4, where we can observe a region with increased baseline normalized power mainly restricted within the primary visual cortex. To document this pattern more specifically, the magnitude of the peak

values for dominant percept power was extracted (i.e., the strongest SSVEF response observed during dominance): BR = 1.45 z-score, IOG2V = 1.22 z-score, IOG2H = 1.19 z-score, and IOG4 = 0.92 z-score.

In order to determine whether the difference in magnitude for baseline normalized changes in power were significant between conditions, statistical analyses were performed with a focus on the primary visual cortex due to its robust response to frequency-tagging. The SSVEF response within V1 was isolated for dominance during BR and IOG conditions. The baseline normalized z-scored values at the time of alternation in V1 (i.e., extracted as the mean value within the entire V1 region for each participant) are as follows: BR (M = 1.10, SD = 0.84), IOG2V (M = 0.39, SD = 0.93), IOG2H (M = 0.56, SD = 1.35), IOG4 (M = 0.51, SD = 1.19). Significant differences were found with a paired t-test between BR and IOG2V ($t = 2.991$, $df = 24$, $p = 0.006$), BR and IOG2H ($t = 2.1903$, $df = 24$, $p = 0.03$), and BR and IOG4 ($t = 2.4537$, $df = 24$, $p = 0.02$). All three grouping conditions were found to differ from BR significantly after FDR correction to account for family-wise error with multiple comparisons.

Interestingly, the SSVEF signal during suppression (Figure 3.4B) indicates less of a difference between BR and IOG conditions. A decrease in baseline normalized power is observed during BR over much of the visual cortex and covers several brain regions in the posterior cortex (i.e. occipital, parietal and temporal lobes). Similar to our observations for dominance, the strongest magnitude for suppression is observed within the primary visual cortex and neighbouring regions, although with opposing z-score directionality. Overall, when comparing the SSVEF response during BR to IOG conditions, a very similar pattern in topography and magnitude is observed. The highlighted brain regions during suppression are larger, and stronger in magnitude than those observed during dominance. Specifically, within the posterior cortex, the magnitude of the peak values for baseline normalized suppressed percept power was extracted (i.e., the strongest SSVEF response observed during suppression): BR = -1.55 z-score, IOG2V = -1.43 z-score, IOG2H = -1.56 z-score, and IOG4 = -1.34 z-score.

As reported for dominance above, the SSVEF response within the primary visual cortex (V1) was isolated for suppression to further examine effects between conditions. The baseline normalized z-score values at the time of alternation in V1 (i.e., extracted as the mean value within the entire V1 region for each participant) were as follows: BR (M = -1.18, SD = 0.77), IOG2V (M = -1.08, SD = 0.87), IOG2H (M = -1.03, SD = 0.75), IOG4 (M = -0.67, SD = 0.95). When

conducting paired t-tests between BR and IOG conditions, the result was significant between BR and IOG4 ($t = -2.132$, $df = 24$, $p = 0.04$), however it was non-significant for BR and IOG2V, as well as BR and IOG2H conditions. When applying FDR correction, none of the results for differences between baseline normalized suppression power in V1 were significant across conditions.

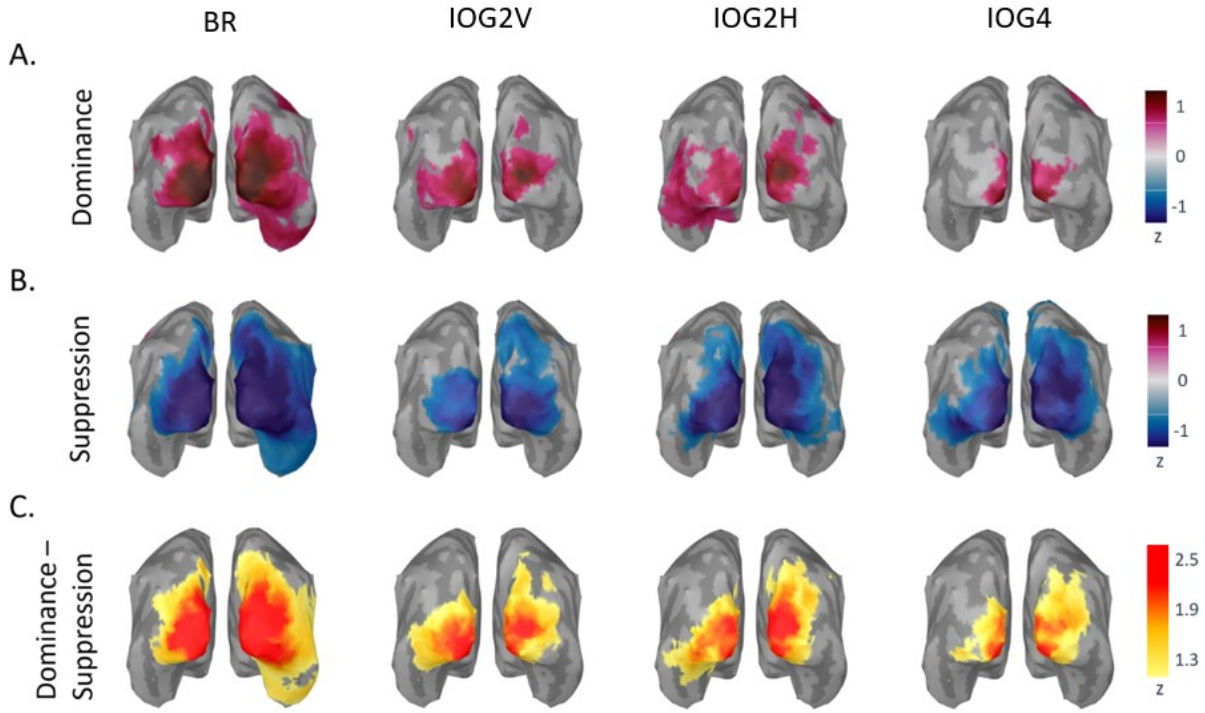

Figure 3.4 SSVEF signal for dominance and suppression during BR and IOG conditions at the time of alternation. A. Posterior cortex view of MEG source localization for dominant percepts during BR and IOG conditions at the time of alternation. **B.** Posterior cortex view of MEG source localization for suppressed percepts during BR and IOG conditions at the time of alternation. **C.** Depth of rivalry computed as dominance subtracted by suppression. All of the cortices displayed are the group mean (N = 25) projections taken at the report of a dominant percept alternation (time = 0 seconds). The results displayed are baseline normalized (z-score) between the interval of -3 to 3 seconds.

To further analyze the interaction between dominance and suppression, we compute a measure that we termed *depth of rivalry* (Figure 3.4C) computed as the difference between the SSVEF response between dominance and suppression at the time of alternation. The results indicate that participants experienced a greater depth of rivalry during BR, that peaked in the primary visual cortex and expanded across the visual system. We also observed a restricted topography, in addition to a lower depth of rivalry when participants experienced increasing grouping demands. Results indicate that this is primarily driven by the reduction in dominance experienced during IOG, whereas suppression is largely unaffected. At the time of alternation, the strongest SSVEF response for depth of rivalry was extracted: BR = 2.85 z-score, IOG2V = 2.45 z-score, IOG2H = 2.75 z-score, and IOG4 = 2.25 z-score.

In order to further investigate SSVEF differences between rivalry conditions, we performed a paired two-tailed student's t-test ($\alpha < 0.05$) in Brainstorm between binocular rivalry and interocular grouping conditions. For each participant, the baseline normalized (z-score) MEG power was compared between BR and IOG conditions within the period of 0 to 500ms after the report of a dominant percept alternation. During the onset of perceptual dominance, significant clusters with stronger power were observed during binocular rivalry (Figure 3.5 A-C). As grouping demands increased, a larger significant cluster was present for BR versus IOG4 that extended from V1 to mid-level visual areas. During suppression, no significant difference was observed between BR and IOG conditions within the primary visual cortex. (Figure 3.5 D-F).

Bonferroni correction was applied to account for multiple comparisons and reduce the likelihood of type 1 errors. The correction followed the formula $\alpha_{corrected} = \alpha_{original} / m$, where $\alpha_{original} = 0.05$ and $m = 6$ (number of comparisons performed), resulting in $\alpha_{corrected} = 0.0083$. This result reinforces the conclusion that signal magnitude was greater during BR than for any IOG condition for dominant percepts.

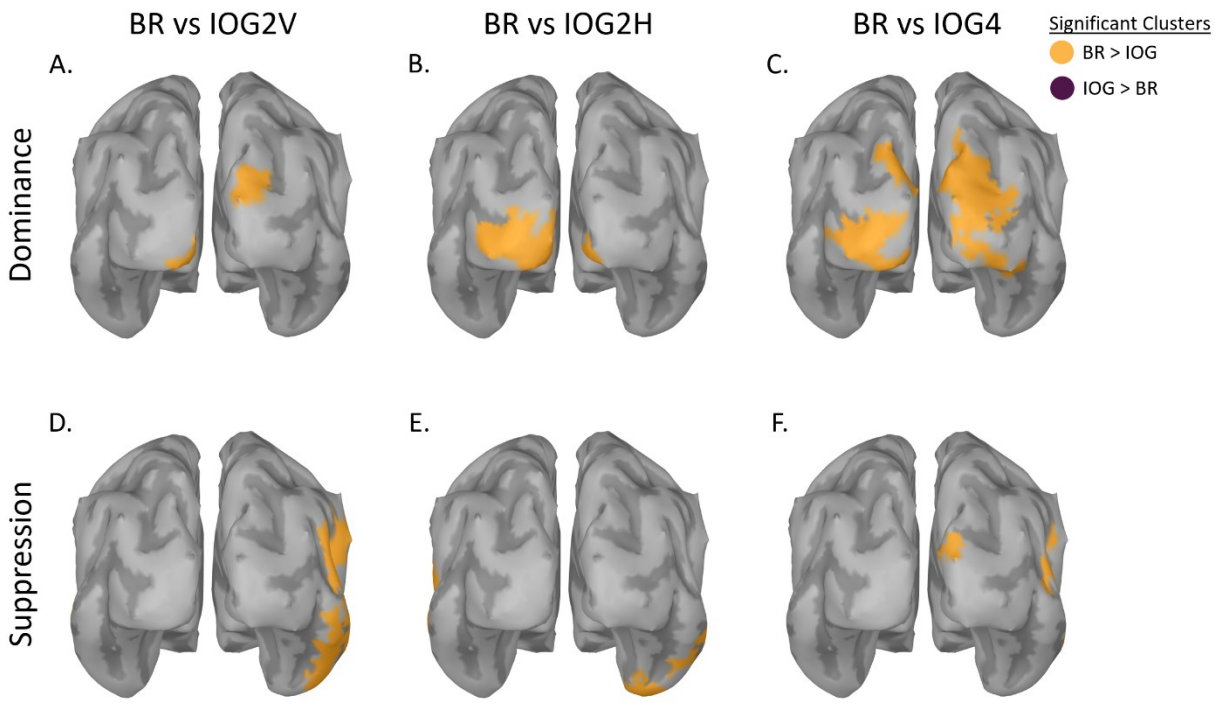

Figure 3.5 SSVEF analysis between BR and IOG conditions from 0 to 500ms after perceptual alternations. A. Dominant percepts SSVEF t-test results for BR versus IOG2V conditions. **B.** Dominant percepts SSVEF t-test results for BR versus IOG2H conditions. **C.** Dominant percepts SSVEF t-test results for BR versus IOG4 conditions. **D.** Suppressed percepts SSVEF t-test results for BR versus IOG2V conditions. **E.** Suppressed percepts SSVEF t-test results for BR versus IOG2H conditions. **F.** Suppressed percepts SSVEF t-test results for BR versus IOG4 conditions. Between rivalry conditions, a paired two-tailed student's t-test was performed (N = 25) in Brainstorm across the mean z-scored SSVEF responses between 0 to 500ms. A posterior view of the cortex is shown, with a significance threshold of $\alpha < 0.05$ with Bonferroni correction applied, and a minimum cluster size of 20.

SSVEF Markers during MEG – Regions of Interest Approach

To gain further insight into the mechanisms of alternation within the visual system, we performed time-frequency Hilbert transform analyses on scouts generated from the Human Connectome Project (HCP) atlas. Matching the analysis period from the full cortex Hilbert Transform analysis, a 10 second time window was used, including the period from -5 to 5 seconds around the button responses for dominant percepts. The results were extracted from the -3 to 3 seconds interval, centered around the button press, to minimize edge effects at the beginning and end of the analysis period. These 25 regions of interest spanned the majority of the posterior cortex including the occipital, parietal, and temporal brain regions. Over a period of three seconds prior to, and three seconds after a report of a dominant percept alternation, changes in baseline normalized power were recorded for dominance and suppression (Figure 3.6). The results are centered around the button press, indicating the report of a new dominant percept (i.e., red or green). We hypothesize that the neural correlates of the alternation occur prior to their report, with a relative delay attributed to reaction time. Although our methods did not record this precisely, we note that the response time for our participants to switch between dominant percept responses (i.e., red-to-green, and green-to-red) was 230ms on a BR replay control task presented on a prior testing day.

The SSVEF signal for dominant percepts was compared between BR and IOG conditions across ROIs (Figure 3.6A). Across all conditions, we can observe waxing and waning of the SSVEF indicated by the directionality of baseline normalized power. Prior to an alternation for BR, the dominant percept frequency tags were negative, indicating the previous suppressed state. We can then observe its transition to dominance that tends to peak around the report of alternation. During the report of alternation, marked by the dashed line at time equal to zero, an increase in baseline normalized power is observed to span across the visual system. The strongest markers of power tended to be recorded in the early visual cortex, and BR exhibited the strongest dominance markers (i.e., larger magnitude of positive z-score results). Temporally, the duration of the positive baseline normalized results during BR is visible approximately 0.5 seconds prior to, and extending to 2 seconds after a switch. This SSVEF response is in line with the bevavioural results for dominant percept durations reported in Figure 3.3B. Comparatively during IOG, earlier and weaker peaks in dominant percept SSVEF are observed (i.e., prior to the alternation across nearly

all ROIs during IOG4). The duration of the positive response is clearly reduced during IOG4 in particular.

The SSVEF response during suppression (Figure 3.6B) is notable for the similarity between BR and IOG conditions across ROIs. The strongest changes in baseline normalized power for suppression are generally observed in the early visual cortex, and decrease in ROIs located within the parietal cortex. Similar to dominance, we observed a transition in directionality of the baseline normalized power that indicated the transition from a previous dominance state (that peaked approximately two seconds before the button press). The maximal negative values for the suppressed percept are observed around the moment of button press for the majority of ROIs across both BR and IOG conditions. During BR, the decrease in SSVEF response for the suppressed percept extends between 0.5 seconds prior, and 2 seconds after the switch. Temporally, a leftward shift is observed during IOG conditions, with the largest changes in SSVEF response for suppression between -1 to 1 seconds around the report of alternation.

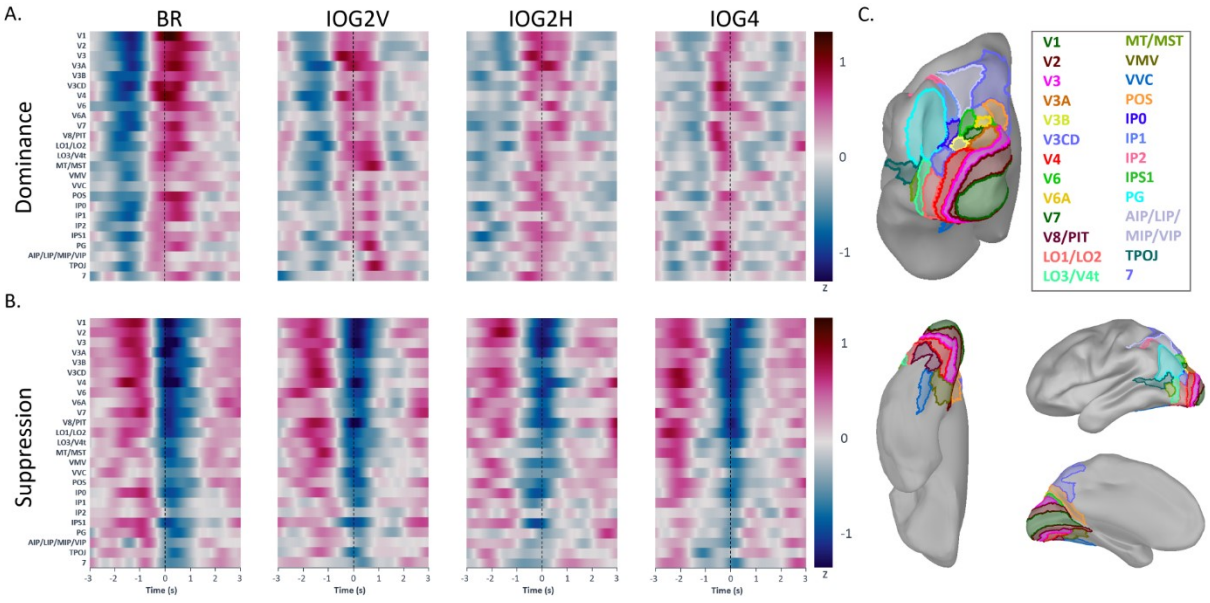

Figure 3.6 Hilbert Transform time-frequency analysis for BR and IOG conditions across regions of interest. A. Group mean (N = 25) analysis for dominant percepts during BR and IOG using Hilbert transform time-frequency methods. **B.** Group mean (N = 25) analysis for suppressed percepts during BR and IOG using Hilbert transform time-frequency methods. **C.** Visualization for the regions of interest across the posterior cortex. The results are time-locked to the behavioural

report of an alternation in dominant percept (time = 0 seconds) indicated by the dashed line and span from -3 to 3 seconds around the alternation. The results are baseline normalized (z-score) between -3 to 3 seconds.

Multivariate Logistic Regression – between Rivalry Conditions

We used multivariate logistic regression analyses to further characterize distinct interactions between predefined visual regions of interest (ROIs) in the occipital and parietal cortex under binocular rivalry (BR) and interocular grouping (IOG) conditions (Figure 3.7). The visually defined ROIs (Table 3.1) were mapped to each participant's individual source space and grouped into two sets for the analysis. The first group included early visual areas extending to mid- and higher-level regions in the visual system, broadly grouped by proximity: V1, V2, V3, V3A, V3B, V3CD, V4, V6, V6A, and V7. The second group comprised higher-order areas associated with visual processing, extending to the lateral occipital and parietal cortex: LO1/LO2, LO3/V4t, MT, V8/PIT, VMV, VVC, POS, IP0, IP1, and IP2 (Figure 3.6C shows their topography on the cortex).

Overall, more temporal clusters with significant differences ($p < 0.05$) between BR and IOG conditions were identified in the first group of ROIs. For interactions between both dominant and suppressed SSVEF markers, significant clusters were consistently identified between BR and grouping conditions approximately 1000ms before and after an alternation in dominant percept (top panels in Figures 3.7A-C). Further inspection of the coefficient magnitudes (β) revealed that the primary visual and extrastriate cortex exhibited the largest contributions to the model at significant time points. These findings indicate a distinct architecture in spatial and temporal results between BR and IOG conditions, suggesting differences in neural markers of bistable perception in the early visual cortex.

The second group of ROIs (bottom panels in Figures 3.7A-C) showed fewer differences and a reduction in significant clusters. In the multivariate analysis of these ROIs, BR and IOG2V exhibited the greatest similarity in neural markers of bistable perception, with a limited presence of significant clusters across both dominant and suppressed time-series. Interestingly, the LO and IP regions showed increased magnitude of coefficients (β) in the multivariate logistic regression model between BR and IOG4 for dominance around 800 to 1000ms after the perceptual switch.

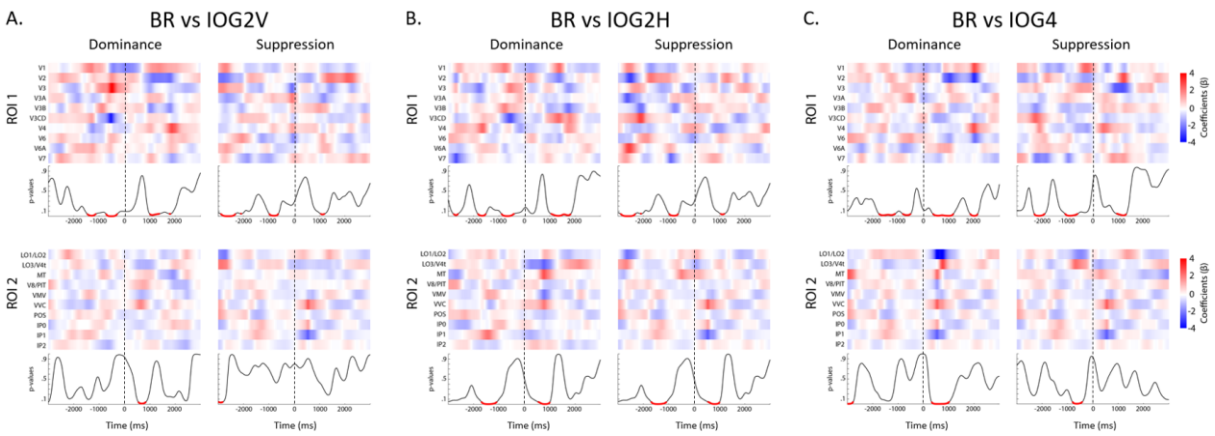

Figure 3.7 Multivariate logistic regression between BR and IOG conditions. The results of a multivariate logistic regression analysis are plotted between BR and IOG. The coefficient values for two subsets of ROIs are plotted for both dominance and suppression, in addition to a significance measure of p-values from -3000 to 3000ms centered around the button press for the report of a dominant percept alternation. A vertical dashed line is plotted at time = 0 seconds to indicate the button response. **A.** Binocular rivalry versus two-patch interocular grouping with a vertical image meridian division. **B.** Binocular rivalry versus two-patch interocular grouping with a horizontal image meridian division. **C.** Binocular rivalry versus four-patch interocular grouping.

Machine Learning Analysis – Distinguishing between Dominance and Suppression

We next used support vector machine (SVM) multivariate analysis to classify the neural correlates of dominance versus suppression during BR and IOG conditions (Figure 3.8A-D). The SVM model was first trained with SSVEF responses for both dominant and suppressed Hilbert Transform time-frequency analysis across all 25 predefined regions of interest (Table 3.1). Decoding accuracy was then determined with regard to distinguishing between dominant and suppressed responses. Interestingly, overall, similar temporal dynamics in decoding accuracy were observed for both BR and IOG conditions. Centered around the report of a percept alternation (i.e., time = 0ms), a peak in decoding accuracy was observed across all rivalry viewing conditions. This peak in accuracy began to increase approximately 500ms prior to the switch and persisted during the onset of the dominant percepts.

During BR (Figure 3.8A), the significant window of decoding accuracy between dominant and suppressed neural markers extended from 3000ms prior to the switch to nearly 2000ms after

the switch. In contrast, during IOG conditions, reduced clusters of significant decoding accuracy were observed. For IOG2 conditions (Figure 3.8B and 3.8C), significant clusters of decoding accuracy were only present from -3000ms to approximately -1000ms, followed by another peak in decoding accuracy with a significant temporal cluster from approximately -1000ms to 1000ms centered around the switch. The IOG4 condition (Figure 3.8D) demonstrated a further reduction in significant clusters, with a smaller peak in decoding accuracy observed approximately between -2000 to -1000ms prior to a switch, and the second peak between -1000 to 500ms after the switch.

Our final analysis examined the pair-wise differences in decoding accuracy between BR and each of the IOG conditions, as well as between the IOG conditions. Significant differences in decoding accuracy are reported across the time-series with a horizontal bar. Interestingly, we obtained confirmatory evidence that the depth of rivalry is stronger for BR than for any IOG condition. More specifically, between BR and both IOG2 conditions, stronger decoding accuracy was observed for BR prior to button press between -2000 to -500ms (Figures 3.8E and 3.8F). In contrast, between BR and IOG4, stronger decoding accuracy was found during BR after the switch between 0 and 1000ms (Figure 3.8G). However, between IOG conditions, no significant differences in decoding accuracy were observed (Figures 3.8H-J).

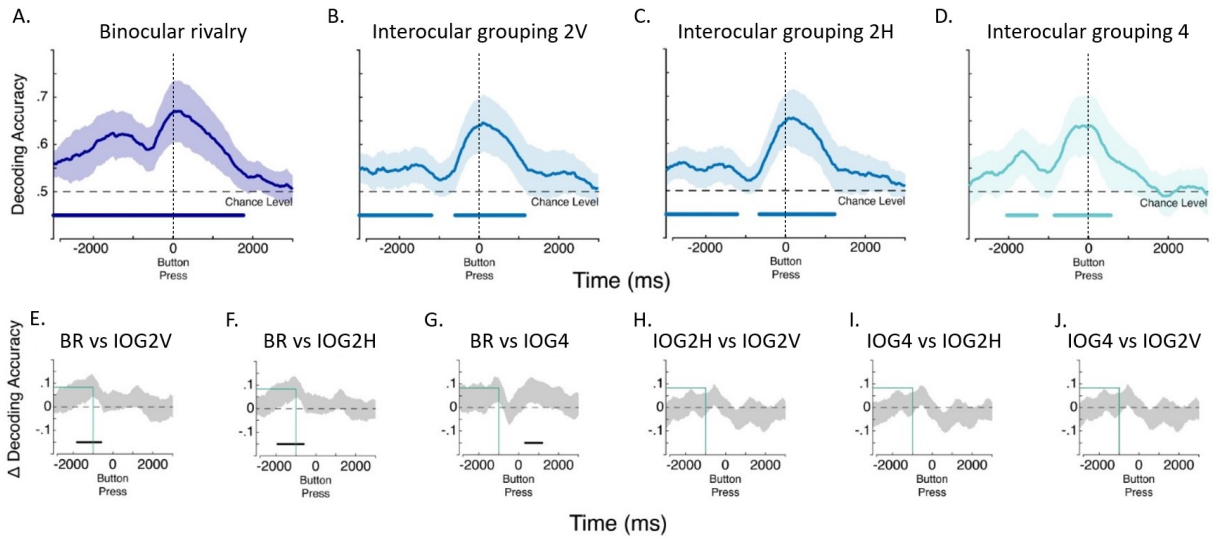

Figure 3.8 Decoding neural markers of dominance versus suppression during BR and IOG conditions. The results are plotted for a decoding analysis using a linear SVM model between BR and IOG conditions. The model was tasked with decoding between dominance and suppression, using results from a Hilbert Transform time frequency analysis across 25 ROIs. The decoding accuracy was recorded for all participants between -3000 to 3000ms centered around the button press for a dominant percept alternation. The mean decoding result is plotted, with a shaded region that represents the 95% confidence interval. A horizontal line is plotted at 0.5 decoding accuracy, representing chance level. A black vertical dashed line is plotted at t = 0ms, indicating the button press in panels A-D. A green line is plotted at t = -1000ms in panels E-J. **A.** Binocular rivalry. **B.** Two-patch interocular grouping with a vertical image meridian division. **C.** Two-patch interocular grouping with a horizontal image meridian division. **D.** Four-patch interocular grouping. **E.** The difference in decoding accuracy between binocular rivalry and two-patch interocular grouping with a vertical image meridian division. **F.** The difference in decoding accuracy between binocular rivalry and two-patch interocular grouping with a horizontal image meridian division. **G.** The difference in decoding accuracy between binocular rivalry and four-patch interocular grouping. **H.** The difference in decoding accuracy between two-patch interocular grouping with a horizontal image meridian division and two-patch interocular grouping with a vertical image meridian division. **I.** The difference in decoding accuracy between four-patch interocular grouping and two-patch interocular grouping with a horizontal image meridian division. **J.** The difference in decoding accuracy between four-patch interocular grouping and two-patch interocular grouping with a vertical image meridian division.

3.6 Discussion

The current experiment aimed to uncover the neural correlates of binocular rivalry (BR) and interocular grouping (IOG) using a combination of frequency-tagging and MEG. This aim sought to uncover both the temporal and spatial dynamics of rivalry conditions through an event-related analysis of the SSVEF response across the visual system. By recording SSVEF during bistable perception with a perceptually matched stimulus and dichoptic flicker frequencies tagged to image properties (i.e., red gratings in each eye tagged at 5 Hz and green gratings in each eye tagged at 6.67 Hz), we identified a similar neural network in posterior cortex during both BR and IOG. However, notable differences in the depth of rivalry were observed as grouping demands increased, specifically in the early visual cortex. The results from the multivariate logistic regression highlighted specific ROIs both in the early visual cortex, and higher-level visual regions (i.e., LO and IP) that contributed to differentiating the neural correlates of BR and higher order grouping conditions.

The behavioural results demonstrated robust stability in dominant percept durations even when the visual system faced increased interocular grouping demands. In contrast, the durations and predominance of mixed percepts increased under higher-order grouping conditions, leading to a decrease in alternation rate between dominant percepts experienced during IOG conditions. This suggests that while the visual system can maintain stable dominant percepts once established, the complexity of grouping affects the frequency and nature of the alternations process. The psychophysics results replicate the findings previously reported in the second chapter (Mokri et al., 2023). In both experiments, we observed a fundamental difference in the experience of rivalry between BR and IOG conditions. During BR conditions, dominant percepts are more prevalent than mixed percepts. In contrast, during IOG conditions, mixed percepts have greater predominance over dominant percepts.

The SSVEF response recorded in the occipital and parietal cortex was generally stronger in magnitude during BR compared to IOG. This difference was primarily driven by increased power during perceptual dominance in the early visual cortex. Specifically, the SSVEF markers for dominance were more pronounced in magnitude during the onset of perceptual dominance during BR (Figure 3.5A-C), while the markers for suppression showed greater similarity between

BR and IOG conditions (Figure 3.5D-E). During higher-order grouping conditions, the SSVEF response for dominance was progressively reduced in magnitude and observed earlier in time relative to the perceptual switch. These findings suggest that the neural mechanisms underlying perceptual dominance and suppression during bistable perception are distinct and supported by different mechanisms (Bock et al., 2023).

The multivariate logistic regression models further revealed distinct neural mechanisms between BR and IOG conditions beyond the early visual cortex, highlighting specific brain regions (i.e., LO and IP) that differed in SSVEF response with specific temporal markers. We observed significant differences between BR and IOG conditions during the onset of the dominant percept (i.e., 0 to 1000ms after the button response). Specifically, between BR and our highest order grouping condition (IOG4), we observed a multivariate interaction with the lateral occipital and intraparietal regions that distinguished rivalry conditions during the onset of perceptual dominance. Our SVM approach uncovered distinct neural correlates between dominant and suppressed SSVEF signal that peaked in decoding accuracy at the report of perceptual alternation across all conditions.

The results presented for this study focused on the SSVEF response with MEG during dominant percept transitions in BR and IOG. Future work is planned and aimed at investigating the neural correlates associated with mixed percepts, specifically examining the role of intermodulation frequencies during periods of perceptual ambiguity (Katyal et al., 2016; Bock et al., 2019).

Binocular Rivalry and Interocular Grouping

Our findings present evidence for broad similarities in the neural underpinnings of bistable perception between BR and IOG. To our knowledge, this is the first frequency-tagged MEG experiment on interocular grouping, and we present novel findings that expand the current literature on this bistable visual phenomenon. Overall, we observed the strongest SSVEF markers of bistable perception in the posterior cortex, primarily originating from the early visual cortex (V1) during both BR and IOG. This supports previous literature using frequency-tagged MEG in binocular rivalry, showing SSVEF responses primarily in the occipital and parietal cortex (Kamphuisen et al., 2008; Bock et al., 2019; Bock et al., 2023). Between BR and IOG conditions,

we observed a reduction in the depth of rivalry during perceptual alternations during the experience of IOG. This was primarily characterized by a reduced SSVEF response for perceptual dominance during IOG. Unlike the widespread topography of perceptual dominance observed during BR, higher-order grouping conditions exhibited a reduction in both the spatial topography and magnitude of the SSVEF response when compared on the same scale as BR. This reduction became more pronounced as we moved from two- to four-patch interocular grouping conditions. Additionally, during the onset of dominant perception between 0 to 500ms after the switch, significant spatial clusters were identified that distinguish BR and IOG conditions, primarily in the early visual (V1 and V2) and extrastriate cortex, with the largest differences observed as interocular grouping demands increased.

The observation that BR elicited a stronger SSVEF signal for dominance in the early visual cortex can be partially attributed to the entrainment and activation of monocular neurons in V1 (Hubel & Wiesel, 1968; Blasdel & Fitzpatrick, 1984; Dougherty et al., 2019). In contrast, coherent dominant percepts experienced during IOG very likely require visual processing from binocular neurons in visual regions that receive sensory information from both eyes. We interpret this difference by suggesting that the experience of dominant percepts during BR has contributions from both monocular and binocular neurons, whereas IOG only has contributions from binocular neurons. Additionally, SSVEF markers of dominance demonstrated a temporal shift with increasing interocular grouping demands, with the peak dominance response occurring prior to the report of alternation in several regions of interest during IOG. The significance of this finding is not obvious to us, but might possibly relate to a different balance between feed-forward and feed-back influences.

Surprisingly, the SSVEF response for suppression showed striking similarities in topography, magnitude, and temporal dynamics between BR and IOG conditions (Figure 3.4B and 3.6B). We interpret these results as indicative of a broader neural mechanism governing suppression in (bistable) perception, which is distinct from the mechanisms of perceptual dominance. We hypothesize that this mechanism involves both monocular and binocular neurons.

To further disentangle the intricate interactions between brain regions and their temporal characteristics, we utilized multivariate methods to compare BR and IOG conditions (Figure 3.7). This analysis explored multivariate processing across different brain regions (Westlin et al, 2023), organized into two sets of ROIs. These analyses highlighted interactions in the visual system,

extending to areas within the lateral occipital (LO) and intraparietal (IP) cortex. The multivariate models revealed distinct patterns of connectivity and activation specific to each perceptual condition. These results underscore the complex interactions between brain regions in the visual system that govern bistable perception.

Increasing Interocular Grouping Demands

Our experimental design allowed an investigation of grouping demands across different orientations of the central image meridian (i.e., IOG2V versus IOG2H) and increased the number of complementary bistable patches by dividing traditional BR images (i.e., IOG2 versus IOG4). While previous studies have reported a preference for perceptual grouping across images divided with vertical meridian divisions (Golubitsky et al., 2019; Mokri et al., 2023), our behavioral results here (acquired during the MEG acquisition) did not show significant differences between IOG2V and IOG2H in terms of alternation rate, mean dominant and mixed percept durations, and percept predominance. However, the participants in this study (N = 25) were drawn from a larger participant pool of naïve viewers (N = 48), where a preference for grouping during IOG2V was observed on the first day of rivalry testing (Mokri et al., 2023). Possible reasons for this discrepancy could include repeat testing on IOG stimuli across experimental days, learning effects related to grouping, and a reduced sample size. Additionally, the neural correlates of bistable perception between IOG2V and IOG2H conditions showed much similarity. This result supports a similar mechanism of perceptual grouping and depth of rivalry for grouping that is matched in the number of complementary bistable patches.

When increasing interocular grouping demands from two- to four-patch images, an increase in the duration and predominance of mixed percepts was observed. This suggests increased perceptual ambiguity in higher-order grouping conditions. The neural correlates of IOG exhibited a decrease in SSVEF magnitude, duration, and topography for dominant percepts. In contrast, the SSVEF response to suppression remained similar between two- and four-patch grouping conditions. This pattern of results seems consistent with other evidence that suggests that it is the development of dominance (rather than suppression) that is most critical for initiating a perceptual alternation. (Wilson, 2003; Brascamp et al., 2015; Bock et al., 2023).

Dominance versus Suppression

Consistent with previous findings during binocular rivalry (Brown & Norcia, 1997; Zhang et al., 2011; Jamison et al., 2015; Spiegel et al., 2019; Bock et al., 2019), we observed waxing and waning of the SSVERs at the fundamental frequencies corresponding to dominance and suppression, extending to interocular grouping conditions. These results suggest a shared neural mechanism underlying bistable perception in the visual system. We independently investigated the neural correlates of perceptual dominance and suppression throughout our analyses. This approach was guided by prior research, which revealed different mechanisms for dominance and suppression during binocular rivalry using MEG (Bock et al., 2023) and fMRI (Mo et al., 2023).

We identified distinct neural mechanisms underlying dominance and suppression through machine learning models using SVM methods, consistently observed across both BR and IOG conditions. Significant temporal clusters in decoding accuracy between dominant and suppressed states were evident throughout the time-series data, with the peak in decoding accuracy centered around the report of dominant percept alternation. This finding aligns with our observation that rivalry depth is maximally observed approximately at the report of alternation, with peaks in both dominant and suppressed SSVEF responses, albeit differing in their directionality of baseline normalized power. Notably, between BR and IOG conditions, longer temporal clusters exhibited significant decoding accuracy during BR, suggesting a more distinct dissociation between dominance and suppression. In contrast, higher-order grouping conditions (i.e., IOG4) showed fewer clusters of significant decoding accuracy, indicating greater perceptual ambiguity, which aligns with the behavioral experience of interocular grouping and the increased predominance and duration of mixed percepts.

While previous studies have reported findings of intermodulation frequencies (i.e., the summation and difference between fundamental frequencies) during binocular rivalry using EEG (Sutoyo & Srinivasan, 2009; Katyal et al., 2016) and MEG (Bock et al., 2019), we did not observe these non-linear responses in our power spectrum density and specparam analyses in the primary visual cortex across the entire duration of rivalry viewing. Our observation does not rule out the presence of these binocularly driven neurons that show intermodulation power through summation or differences between the fundamental frequencies. To gain a deeper understanding of these non-linear brain responses, future research could benefit from extending the power spectrum density analysis beyond V1 to include areas in the extrastriate cortex, which are hypothesized to contain binocular-driven neurons (Parker et al., 2007). Additionally, time-locking the SSVEF response

filtered at intermodulation frequencies to the onset of mixed percepts may provide further insights, as these transition states between dominant percepts involve partial perception of images presented to each eye. Ultimately, the power of the intermodulation frequencies was not observed to be on the same scale as the power of the fundamental frequencies in the primary visual cortex with our methods of analysis.

Individual Differences

Alternation rates during binocular rivalry demonstrate individual differences (Brascamp et al., 2015). These differences have been shown to be partially heritable and attributed to genetic factors through twin studies (Miller et al., 2010; Shannon et al., 2011). In line with the hypothesis of a shared neural mechanism that underlies multiple perceptual illusions (Carter & Pettigrew, 2003), we propose that the individual differences observed during binocular rivalry (BR) can be extended to interocular grouping (IOG). During bistable perception, significant strong positive correlations were observed between BR and IOG conditions across participants, consistent with previous findings (Mokri et al., 2023). The relationship was stronger between BR and two-patch interocular grouping conditions, while more inter-subject variability was observed when extending behavioral measures to four-patch interocular grouping. We attribute this finding to the increasing grouping demands, which introduce greater perceptual ambiguity in the visual system. This indicates that previous studies differentiating 'fast' versus 'slow' switchers during binocular rivalry (Fesi & Mendola, 2015; Bock et al., 2019) can be partially extended to conditions with interocular grouping demands. However, a weaker relationship was reported for the duration of mixed percepts between BR and IOG. This discrepancy is interpreted within the context of the fundamental differences mixed percepts between bistable viewing conditions. Traditionally, in BR, mixed percepts arise from partial visibility of right and left eye images. In contrast, our definition of mixed percepts during IOG encompasses both images viewed solely monocularly (i.e., left and right eye IOG images) and the dynamic combination of rivalry images, more commonly associated with mixed percepts during classic BR.

These findings collectively suggest that the neural mechanisms underlying bistable perception during the experience of BR and IOG share commonalities, supporting the hypothesis of a shared neural mechanism. This emphasizes the potential for a unified neural framework

governing both forms of bistable visual perception. Specifically, for mechanisms governing the maintenance of dominant perception. This implies that once a dominant percept is initiated for both BR and IOG, a similar brain network may function regardless of the specific bistable context. However, the weaker correlations observed between mixed percept durations highlight the increased complexity and variability associated with resolving perceptual ambiguity and transitions, particularly in response to grouping demands.

Further research aimed at uncovering individual differences in SSVEF responses and their correlation with percept duration, both between (i.e., individual difference in alternation rates) and within subjects (i.e., differences in percept durations experienced during BR), could provide deeper insights. With regard to within subject effects, recent studies using EEG during binocular rivalry have shown that more gradual changes in SSVEP amplitude at fundamental frequencies for dominant and suppressed percepts characterize longer visual percepts (Nie et al., 2023).

3.7 References

Alais, D., & Blake, R. (Eds.). (2005). Binocular rivalry. *MIT press.*

Bae, G. Y., & Luck, S. J. (2018). Dissociable decoding of spatial attention and working memory from EEG oscillations and sustained potentials. *Journal of Neuroscience*, 38(2), 409-422.

Baker, D. H., & Graf, E. W. (2009). On the relation between dichoptic masking and binocular rivalry. *Vision research*, 49(4), 451-459.

Blake, R. (1989). A neural theory of binocular rivalry. *Psychological review*, 96(1), 145.

Blasdel, G. G., & Fitzpatrick, D. (1984). Physiological organization of layer 4 in macaque striate cortex. *Journal of Neuroscience,* 4(3), 880-895.

Bock, E. A., Fesi, J. D., Baillet, S., & Mendola, J. D. (2019). Tagged MEG measures binocular rivalry in a cortical network that predicts alternation rate. *Plos one*, 14(7), e0218529.

Bock, E. A., Fesi, J. D., Da Silva Castenheira, J., Baillet, S., & Mendola, J. D. (2023). Distinct dorsal and ventral streams for binocular rivalry dominance and suppression revealed by magnetoencephalography. *European Journal of Neuroscience*, 57(8), 1317-1334.

Brascamp, J. W., Klink, P. C., & Levelt, W. (2015). The 'laws' of binocular rivalry: 50 years of Levelt's propositions. *Vision Research,* 109, 20–37.

Britz, J., Landis, T., & Michel, C. M. (2009). Right parietal brain activity precedes perceptual alternation of bistable stimuli. *Cerebral Cortex*, 19(1), 55-65.

Britz, J., Pitts, M. A., & Michel, C. M. (2011). Right parietal brain activity precedes perceptual alternation during binocular rivalry. *Human brain mapping*, 32(9), 1432-1442.

Brown, R. J., & Norcia, A. M. (1997). A method for investigating binocular rivalry in real-time with the steady-state VEP. *Vision research*, 37(17), 2401-2408.

Buckthought, A., Kirsch, L. E., Fesi, J. D., & Mendola, J. D. (2021). Interocular grouping in perceptual rivalry localized with fMRI. *Brain Topography*, 34, 323-336.

Carmel, D., Walsh, V., Lavie, N., & Rees, G. (2010). Right parietal TMS shortens dominance durations in binocular rivalry. *Current biology*, 20(18), R799-R800.

Carter, O. L., & Pettigrew, J. D. (2003). A common oscillator for perceptual rivalries?. *Perception*, *32*(3), 295-305.

Cooper, P. R., & Mendola, J. D. (2019). Abnormal sensory eye dominance in stereoanomalous subjects. *Journal of Vision*, 19(13), 14-14.

Cosmelli, D., David, O., Lachaux, J. P., Martinerie, J., Garnero, L., Renault, B., & Varela, F. (2004). Waves of consciousness: ongoing cortical patterns during binocular rivalry. *Neuroimage*, 23(1), 128-140.

Donoghue, T., Haller, M., Peterson, E. J., Varma, P., Sebastian, P., Gao, R., Noto, T., Lara, A. H., Wallis, J. D., Knight, R. T., Shestyuk, A., & Voytek, B. (2020). Parameterizing neural power spectra into periodic and aperiodic components. *Nature neuroscience*, 23(12), 1655-1665.

Dougherty, K., Cox, M. A., Westerberg, J. A., & Maier, A. (2019). Binocular modulation of monocular V1 neurons. *Current Biology*, *29*(3), 381-391.

Fang, F., Kersten, D., & Murray, S. O. (2008). Perceptual grouping and inverse fMRI activity patterns in human visual cortex. *Journal of vision*, 8(7), 2-2.

Fesi, J. D., & Mendola, J. D. (2015). Individual peak gamma frequency predicts switch rate in perceptual rivalry. *Human Brain Mapping*, *36*(2), 566-576.

Gaser, C., Dahnke, R., Thompson, P. M., Kurth, F., Luders, E., & Alzheimer's Disease Neuroimaging Initiative. (2022). CAT–A computational anatomy toolbox for the analysis of structural MRI data. *biorxiv*, 2022-06.

Glasser, M. F., Coalson, T. S., Robinson, E. C., Hacker, C. D., Harwell, J., Yacoub, E., Ugurbil, K., Andersson, J., Beckmann, C. F., Jenkinson, M., Smith, S. M., & Van Essen, D. C. (2016). A multi-modal parcellation of human cerebral cortex. *Nature*, 536(7615), 171-178.

Golubitsky, M., Zhao, Y., Wang, Y., & Lu, Z. L. (2019). Symmetry of generalized rivalry network models determines patterns of interocular grouping in four-location binocular rivalry. *Journal of Neurophysiology*, 122(5), 1989-1999.

Grill-Spector, K., Kourtzi, Z., & Kanwisher, N. (2001). The lateral occipital complex and its role in object recognition. *Vision research*, 41(10-11), 1409-1422.

Hillebrand, A., Tewarie, P., Van Dellen, E., Yu, M., Carbo, E. W., Douw, L., Gouw, A. A., van Straaten, E. C. W., & Stam, C. J. (2016). Direction of information flow in large-scale resting-state networks is frequency-dependent. *Proceedings of the National Academy of Sciences,* 113(14), 3867-3872.

Hubel, D. H., & Wiesel, T. N. (1968). Receptive fields and functional architecture of monkey striate cortex. *The Journal of physiology*, *195*(1), 215-243.

Jamison, K. W., Roy, A. V., He, S., Engel, S. A., & He, B. (2015). SSVEP signatures of binocular rivalry during simultaneous EEG and fMRI. *Journal of neuroscience methods*, 243, 53-62.

Kamphuisen, A., Bauer, M., & van Ee, R. (2008). No evidence for widespread synchronized networks in binocular rivalry: MEG frequency tagging entrains primarily early visual cortex. *Journal of Vision*, 8(5), 4-4.

Katyal, S., Engel, S. A., He, B., & He, S. (2016). Neurons that detect interocular conflict during binocular rivalry revealed with EEG. *Journal of vision*, 16(3), 18-18.

Kleiner, M., Brainard, D., & Pelli, D. (2007). What's new in Psychtoolbox-3? *Perception,* 36(14), 1–16.

Knapen, T., Paffen, C., Kanai, R., & van Ee, R. (2007). Stimulus flicker alters interocular grouping during binocular rivalry. *Vision Research*, 47(1), 1-7.

Knyazeva, M. G., Fornari, E., Meuli, R., Innocenti, G., & Maeder, P. (2006). Imaging of a synchronous neuronal assembly in the human visual brain. *Neuroimage*, 29(2), 593-604.

Kovács, I., Papathomas, T. V., Yang, M., & Fehér, Á. (1996). When the brain changes its mind: Interocular grouping during binocular rivalry. *Proceedings of the National Academy of Sciences*, 93(26), 15508-15511.

Large, M. E., Culham, J., Kuchinad, A., Aldcroft, A., & Vilis, T. (2008). fMRI reveals greater within-than between-hemifield integration in the human lateral occipital cortex. *European journal of neuroscience*, 27(12), 3299-3309.

Larsson, J., & Heeger, D. J. (2006). Two retinotopic visual areas in human lateral occipital cortex. *Journal of neuroscience*, 26(51), 13128-13142.

Levelt, W. J. (1965). On binocular rivalry (Doctoral dissertation, Van Gorcum Assen).

Lobier, M., Siebenhühner, F., Palva, S., & Palva, J. M. (2014). Phase transfer entropy: a novel phase-based measure for directed connectivity in networks coupled by oscillatory interactions. *Neuroimage*, 85, 853-872.

Logothetis, N. K., Leopold, D. A., & Sheinberg, D. L. (1996). What is rivalling during binocular rivalry?. *Nature*, 380(6575), 621-624.

Matsuoka, K. (1984). The dynamic model of binocular rivalry. *Biological cybernetics*, 49(3), 201-208.

Miller, S. M., Hansell, N. K., Ngo, T. T., Liu, G. B., Pettigrew, J. D., Martin, N. G., & Wright, M. J. (2010). Genetic contribution to individual variation in binocular rivalry rate. *Proceedings of the National Academy of Sciences, USA,* 107(6), 2664–2668.

Mo, C., Lu, J., Shi, C., & Fang, F. (2023). Neural representations of competing stimuli along the dorsal and ventral visual pathways during binocular rivalry. *Cerebral Cortex*, 33(6), 2734-2747.

Mokri, E., da Silva Castanheira, J., Laldin, S., Landry, M., & Mendola, J. D. (2023). Effects of interocular grouping demands on binocular rivalry. *Journal of Vision*, 23(10), 15-15.

Nie, S., Katyal, S., & Engel, S. A. (2023). An Accumulating Neural Signal Underlying Binocular Rivalry Dynamics. *Journal of Neuroscience*, *43*(50), 8777-8784.

O'Shea, R. P. (1997). Effects of Orientation and Spatial Frequency on Monocular and Binocular Rivalry. *In ICONIP* (1) (pp. 67-70).

Parker, A. J. (2007). Binocular depth perception and the cerebral cortex. *Nature Reviews Neuroscience*, *8*(5), 379-391.

Pitts, M. A., & Britz, J. (2011). Insights from intermittent binocular rivalry and EEG. Frontiers in human neuroscience, 5, 107.

Rees, G. (2007). Neural correlates of the contents of visual awareness in humans. Philosophical Transactions of the Royal Society B: *Biological Sciences*, 362(1481), 877-886.

Roy, A. V., Jamison, K. W., He, S., Engel, S. A., & He, B. (2017). Deactivation in the posterior mid-cingulate cortex reflects perceptual transitions during binocular rivalry: Evidence from simultaneous EEG-fMRI. *NeuroImage*, 152, 1-11.

Said, C. P., & Heeger, D. J. (2013). A model of binocular rivalry and cross-orientation suppression. *PLoS computational biology*, 9(3), e1002991.

Shannon, R. W., Patrick, C. J., Jiang, Y., Bernat, E., & He, S. (2011). Genes contribute to the switching dynamics of bistable perception. *Journal of Vision,* 11(3):8, 1–7.

Spiegel, A., Mentch, J., Haskins, A. J., & Robertson, C. E. (2019). Slower binocular rivalry in the autistic brain. *Current Biology*, 29(17), 2948-2953.

Srinivasan, R., Russell, D. P., Edelman, G. M., & Tononi, G. (1999). Increased synchronization of neuromagnetic responses during conscious perception. *Journal of Neuroscience*, 19(13), 5435-5448.

Sutoyo, D., & Srinivasan, R. (2009). Nonlinear SSVEP responses are sensitive to the perceptual binding of visual hemifields during conventional 'eye'rivalry and interocular 'percept'rivalry. *Brain research*, 1251, 245-255.

Tadel, F., Baillet, S., Mosher, J. C., Pantazis, D., & Leahy, R. M. (2011). Brainstorm: a user-friendly application for MEG/EEG analysis. *Computational intelligence and neuroscience*, 2011, 1-13.

Thaler, L., Schütz, A. C., Goodale, M. A., & Gegenfurtner, K. R. (2013). What is the best fixation target? The effect of target shape on stability of fixational eye movements. *Vision Research*, 76, 31–42.

Tong, F., Meng, M., & Blake, R. (2006). Neural bases of binocular rivalry. *Trends in cognitive sciences*, 10(11), 502-511.

Tononi, G., Srinivasan, R., Russell, D. P., & Edelman, G. M. (1998). Investigating neural correlates of conscious perception by frequency-tagged neuromagnetic responses. *Proceedings of the National Academy of Sciences*, 95(6), 3198-3203.

Westlin, C., Theriault, J.E., Katsumi, Y., Nieto-Castanon, A., Kucyi, A., Ruf, S.F., Brown, S.M., Pavel, M., Erdogmus, D., Brooks, D.H., Quigley, K.S., Whitfield-Gabrieli, S., & Barrett, L. F. (2023). Improving the study of brain-behavior relationships by revisiting basic assumptions. *Trends in cognitive sciences*, 27(3), 246-257.

Wilcke, J. C., O'Shea, R. P., & Watts, R. (2009). Frontoparietal activity and its structural connectivity in binocular rivalry. *Brain research*, 1305, 96-107.

Wilson, H. R. (2003). Computational evidence for a rivalry hierarchy in vision. *Proceedings of the National Academy of Sciences*, 100(24), 14499-14503.

Zaretskaya, N., Thielscher, A., Logothetis, N. K., & Bartels, A. (2010). Disrupting parietal function prolongs dominance durations in binocular rivalry. *Current Biology*, 20(23), 2106–2111.

Zhang, P., Jamison, K., Engel, S., He, B., & He, S. (2011). Binocular rivalry requires visual attention. *Neuron*, 71(2), 362-369.

4

Changes in Visual Perception Predicted by Alpha Band Power during Binocular Rivalry

Manuscript in preparation for journal submission

Mokri, E., da Silva Castanheira, J., & Mendola, J. D. (in prep). Changes in Visual Perception Predicted by Alpha Band Power during Binocular Rivalry.

4.1 Preface

The fourth chapter builds on the neuroimaging experiments from the previous chapter, using magnetoencephalography (MEG) with the same participants to study binocular rivalry with untagged stimuli. Participants viewed untagged, red and green orthogonal gratings similar to those previously used (Figure 1.1), experiencing rivalry naturally to address the shortcomings of frequency-tagging, which induces an unnatural brain state through neural entrainment.

This chapter focuses on alpha oscillations (8 – 13 Hz) and their changes relative to bistable perception during binocular rivalry. Using MEG and a two-button press-and-hold response method from previous chapters, the study examines how alpha power dynamics facilitate perceptual alternations. Recent studies highlight alpha oscillations' role in visual inhibition (Clayton et al., 2018) and their link to behavioral measures during binocular rivalry (Katyal et al., 2019; Cuello et al., 2022; Sponheim et al., 2023). Specifically, alpha power decreases in the parieto-occipital sulcus (POS) before perceptual changes in bistable tasks (Piantoni et al., 2017).

While frequency-tagging combined with EEG or MEG emphasizes early visual cortex activity (Kamphuisen et al., 2008), its methods can be debated regarding tag propagation through the visual system. Feedforward connectivity is prominent during tagged BR (Bock et al., 2023). This chapter addresses these limitations, presenting evidence of feedback connectivity from parietal to visual cortex in the alpha band prior to perceptual switches.

A control condition, binocular rivalry replay, is introduced, where perceptual switches are externally driven by software, offering insights into the temporal dynamics of alpha activity preceding perceptual alternations. Unlike traditional BR, where different images are shown to each eye, the replay condition shows the same image to both eyes, switching percepts every few seconds.

Individual differences in alpha peaks' amplitude, frequency, and shape are explored, correlating alpha activity markers with behavioral results during BR. A consistent decrease in alpha power is observed over the occipital and parietal cortex before dominant alternations in BR, occurring earlier compared to BR replay. This is contrasted with mixed percepts, where an increase in alpha power is observed prior to their report.

4.2 Abstract

Binocular rivalry (BR) is a bistable visual phenomenon where two incompatible images are simultaneously presented, one to each eye, and elicit perceptual alternations between image dominance and suppression. Alpha oscillations in visual cortex are hypothesized to be inhibitory in nature, contributing to both the emergence and stability of visual percepts. We found that the power of alpha band oscillations (8 – 13 Hz) recorded with magnetoencephalography (MEG) in the posterior cortex during rivalry viewing (N = 28) was predictive of perceptual alternations. Prior to alternation to dominant percepts, we observed a decrease in alpha band activity power over the posterior cortex, with a subsequent return after the new percept emerged. This was contrasted with periods of ambiguous mixed percepts that showed a distinct increase in alpha band activity prior to their report. Moreover, the extent of increased alpha predicted individual differences in the length of mixed percepts. Prior to each alternation, we found the earliest markers of alpha activity to be in mid-to-high level visual areas, preceding both the perceptual report, and the estimated decision time obtained from a binocular rivalry control condition. Analogous markers for a non-rivalrous control task occurred much later in time. Consistently, directed phase transfer entropy (dPTE) connectivity analysis shows feedback from higher to lower visual areas in the alpha band within the visual system prior to dominance alternations (i.e., areas IP2, IPS to V2, V3, LO1-3, MT). We thus conclude that fluctuations in the stabilizing feedback influence of alpha power may sculpt neural activity during ambiguity, and facilitate perceptual change during bistable perception.

4.3 Introduction

Binocular rivalry (BR) is a visual illusion that elicits multistable perception. It has been used to study the visual system, as it represents an instance where perception changes despite a stable unchanging retinal input. When each eye is shown a dissimilar, non-fusible image, participants report alternation in image dominance and suppression between the two stimuli (Blake 1989; Blake & Logothetis, 2002). BR has been extensively studied and characterized behaviorally, initially with a focus on the role of reciprocal monocular inhibition (Matsuoka 1984; Lehky 1988; Blake 1989), and later with more interest in how binocular neurons might contribute to the neural mechanisms of the phenomenon (Logothetis et al., 1996; Kovács et al., 1996; Wilson 2003; Said & Heeger, 2013). Recently, new details have emerged through the use of brain imaging techniques such as EEG (Pitts et al., 2010; Pitts & Britz, 2011), combinations of EEG and fMRI (Jamison et al., 2015; Roy et al., 2017) and MEG (Cosmelli et al., 2004; Kamphuisen et al., 2008; Bock et al., 2019; Bock et al., 2023). Neuroimaging studies have demonstrated that distinct neural mechanisms are involved in dominance and suppression, and a wide expanse of the visual cortex is recruited. During BR, as dominant percepts alternate, they are marked by shorter transition periods where portions of each percept may be perceived. These periods, often termed mixed percepts, are dynamically perceived and have provided new insight into visual processing. Mixed percepts, also called piecemeal percepts, are unique during rivalry as they allow partial information from each eye to be perceived (Alais & Melcher, 2007). They are also thought to represent instances of increased interocular inhibition (Katyal et al., 2016). In addition, recent tristable models of rivalry account for mixed percepts as a discrete perceptual state, in addition to the ongoing dominant percepts (Riesen et al., 2019; Qiu et al., 2020).

In order for dominant percepts to emerge, in conjunction with attention and excitability of the dominant neural representation, image suppression of the unattended stimuli is required. For this reason, we and others hypothesize that the balance of excitation and inhibition (E:I) is crucial for the experience of BR. Studies in special populations thought to display E:I imbalances such as autism (Robertson et al., 2013; Spiegel et al., 2019; Skerswetat et al., 2022) have shown altered BR dynamics, with slower alternation rates and longer mixed percepts. Theoretical computational models of rivalry have also emphasized and relied on E:I ratios. Thus, converging evidence

supports the role of inhibition within the visual system as crucial to multistable perception and alternations in percepts (Cao et al., 2021). Indeed, the balance between excitation and inhibition is crucial in everyday functioning of the visual system.

Brain activity, especially when oscillatory, is grouped into different frequency bands, each with their own properties and function. Oscillations within the alpha band (8 – 13 Hz) have been proposed to often be exerting inhibitory effects (Klimesch et al., 2007; Jensen & Mazaheri, 2010; Klimesch et al., 2012), and an even more specific hypothesis involves pulsed-inhibition of ongoing visual processing (Mathewson et al., 2011). Further, mechanisms of feedback from higher-tier to lower-tier cortical areas in the visual system have been linked to alpha oscillations (Van Kerkoerle et al., 2014), with complementary propositions that they are fundamental in inhibitory processes within the visual system (Jensen et al., 2015; Clayton et al., 2018). Alpha oscillations have been primarily reported to be stronger in strength within the parietal and occipital cortex when recorded with EEG and MEG (Chapman et al., 1984; Ciulla et al., 1999; Katyal et al., 2019). Given this background, our current focus is task related alpha activity during binocular rivalry, and this is expected to differ from alpha activity at rest.

Brain oscillations, such as those within the alpha band, represent rhythmic patterns of neural activity in the brain and are characterized by their frequency, phase, and power. Several studies have investigated the relationship between these oscillatory features and behavioral dynamics during binocular rivalry. Significant correlations were found between peak alpha *frequency* recorded with EEG electrodes over the occipital cortex during BR and alternation rate (Cuello et al., 2022). Additionally, it was reported that peak alpha frequency measured during a fixation period prior to image presentation was correlated with percept durations during BR, with faster alpha oscillations predicting shorter percept durations, particularly over bilateral occipital channels (Katyal et al., 2019). Furthermore, peak alpha frequency within the occipital cortex during resting-state MEG analysis was correlated with BR percept duration (Sponheim et al., 2023). Regarding the phase of alpha oscillations, it was found that alpha phase was coupled to higher-frequency gamma power, primarily over occipital areas (Osipova et al., 2008). Increased phase-amplitude coupling between alpha and higher gamma oscillations within visual cortical regions during non-rivalrous vision tasks was also reported (Voytek et al., 2010). Finally, changes in alpha power over parietal and occipital electrodes preceding and following perceptual reversals during a Necker cube image were observed with EEG (Piantoni et al., 2017). Consistently, that

study also found that an increase in alpha power induced through sleep deprivation resulted in prolonged percept duration. These later findings suggest that high alpha power plays a role in promoting the stability of a perceptual representation and suppressing switching to alternative percepts. What is not clear from this body of work is how unique the findings are to bistable perception, nor how the network of occipital, posterior temporal, and parietal areas interact during rivalry.

In this study, we focused on quantifying changes in alpha oscillatory power and its relationship to the experience of binocular rivalry. Recent research has highlighted the importance of parameterizing the power spectrum into both aperiodic and periodic components (Donoghue et al., 2020). Specifically, our study examined the periodic components of power in the alpha band, tracking this marker across the time series in relation to perceptual alternations during BR. Future investigations should explore the role of the aperiodic components (i.e., offset and exponent) of the power spectrum and their relationship to behavioral measures of bistable perception (Wilson et al., 2022), particularly in light of their proposed role in the excitatory-inhibitory (E:I) balance (Gao et al., 2017).

In our current experimental design, we conducted a comparison between a traditional binocular rivalry task and a matched non-rivalrous condition called BR replay. This comparison aimed to explore patterns of alpha activity associated with endogenous (internal) versus exogenous (external) mechanisms of perceptual alternations. We recorded both dominant and mixed percepts from a sizable sample with MRI guided MEG and also examined individual differences. Moreover, we applied advanced connectivity analysis to uncover the dynamic interactions between lower-, mid, and higher tier visual areas. Our focus was on investigating the role of changes in alpha oscillation power associated with changes in perceptual states. When a dominant percept is perceived, inhibition plays a crucial role in suppressing the unattended image. Subsequently, a reduction in inhibition could allow that previously suppressed image to break through and become dominant. We hypothesized that a reduction in inhibition, reflected by a decrease in alpha oscillation power, could precede alternations in dominant percepts during BR. Alternatively, we hypothesized that an increase in alpha power may precede mixed percepts, particularly when inhibition is expected to be high. During these ambiguous periods, elevated alpha power may reflect an increase in inhibition within a transiently stabilized visual system that is associated with perceptual ambiguity.

4.4 Methods

Participants

The participants included in this study reported normal to corrected normal vision, with no known visual disorders, no known metals in their body, and were not taking psychoactive or psychotropic medication. Participants were allowed to wear contact lenses or have previously undergone eye correction surgery; however, glasses were not permitted due to the necessity of MEG compatible prism lenses. Participants were screened for visual acuity and stereo vision. Visual acuity was assessed using the Logarithmic Visual Acuity chart (Early Treatment Diabetic Retinopathy Study [ETDRS] 2000 series chart; Precision Vision, Woodstock, IL), while stereo vision was evaluated using the Titmus Stereoacuity Test (Stereo Optical, Chicago, IL). Both assessments were conducted in a well-lit room and followed the manufacturer recommendations for testing distances. Each eye's visual acuity was tested independently to avoid interocular imbalances that could affect the experience of BR. The inclusion criteria were set at values for visual acuity of 20/40 or better in each eye, with no more than two lines of difference between eyes to avoid underlying eye dominance. The median visual acuity for both right and left eyes of the participant pool was 20/20. For the stereo vision test, participants were required to correctly answer 7/9 targets sequentially. This corresponded to an angle of stereopsis of 60 seconds at 16 inches for the 7th target correctly identified. The median result for the stereo vision assessment across the participant poll was 9/9. The data and results reported were obtained on the third day of visual experiments from the participant pool. The entire testing protocol included an initial day of psychophysics testing (Mokri et al., 2023), two days of MEG testing, and a final day where the anatomical MRI was obtained. A total of 31 participants participated in the study, however, due to issues with the digitization hardware on the days of data collection, 3 participants did not have appropriate head models. As a result, the final subject pool consisted of N = 28 participants, with 19 females. The mean age of the participants was 24.25 years old, with a standard deviation of 3.00 years.

Experimental Design

The experimental methods closely followed those previously reported by Mokri et al. (2023). To induce the experience of binocular rivalry (BR), we utilized a black opaque divider positioned between the two eyes, along with MEG compatible prism lenses with a strength of 12 diopters. Prior to MEG data acquisition, all participants underwent an unrecorded laptop practice session lasting approximately 5 minutes. During the practice, participants were reminded on the experimental guidelines and familiarized themselves with the reporting procedures.

The experiment required participants to report their alternations in visual percepts (red, green, or mixed) using a two-button press-and-hold design. Participants were instructed to press the corresponding button when they perceived the majority (80% or more) of the square to be either red or green, and to continuously hold the response throughout the duration of its dominance. If neither red nor green was dominantly perceived, participants were instructed to withhold a response, indicating their experience of a mixed percept. These instructions remained consistent across all testing conditions, and participants were not informed whether the testing block was BR or BR replay.

Each experimental run lasted 5 minutes and comprised four counterbalanced testing blocks, each lasting 75 seconds. Counterbalancing was implemented for the orientation and colour of the orthogonal gratings shown to each eye to mitigate the effects of adaptation. Before the start of each testing block, participants were instructed to fuse on a fixation screen and self-initiate the start of the experiment through a button press.

As a control condition for BR, a binocular rivalry replay was included, wherein perceptual alternation was externally driven by the software. During BR replay, both eyes were presented with identical stimuli matched for colour and orientation. The software switched the images to the alternative colour and orientation, artificially recreating the experience of a dominant perceptual alternation. The stimuli were programmed to change between dominant stimuli at random intervals ranging from 1.5 to 3.5 seconds, aiming to match the alternation rate observed in traditional BR during pilot testing with the experimenters. This condition was intended to serve as a 'no-rivalry' control for BR and should not have elicited mixed percepts. The BR replay condition was tagged at frequencies of 5 Hz and 6.67 Hz for red and green, respectively, and data were collected on a

separate day of MEG testing. This potential limitation is acknowledged, as we did not obtain an untagged BR replay control during the data acquisition phase.

Stimulus

Images were shown using Psychtoolbox-3 (Brainard, 1997; Kleiner et al., 2007) and MATLAB 2021a (MathWorks, Natick, MA), as illustrated in Figures 4.1A and 4.1B on a VPixx projector (VPixx Technologies Inc., Saint-Bruno, QC) with a 60 Hz refresh rate. The stimuli were comprised of 7 red or green orthogonal gratings shown to each eye. The gratings had RGBA values of [0.5 0 0 0.35] for red and [0 0.35 0 0.35] for green. The RGBA values were chosen in conjunction with testing on the experimenters to determine an appropriate balance between the strength of red and green stimuli. The grating had orientations of 45 and -45 degrees, corresponding to an interocular orientation difference of 90 degrees. The fixation mark was chosen to help increase the stability and reduce eye movements, which could negatively impact fusion during BR (Thaler et al., 2013). Black borders were drawn around the stimuli to provide additional cues that could aid in fusion and maintain fixation throughout the experiment. The projector was placed at a viewing distance 52 cm away from the central bridge of the prism lenses, and the inner square of the stimuli was 7.5 cm in height and width. This corresponded to a visual angle of 8° 14' 0.97".

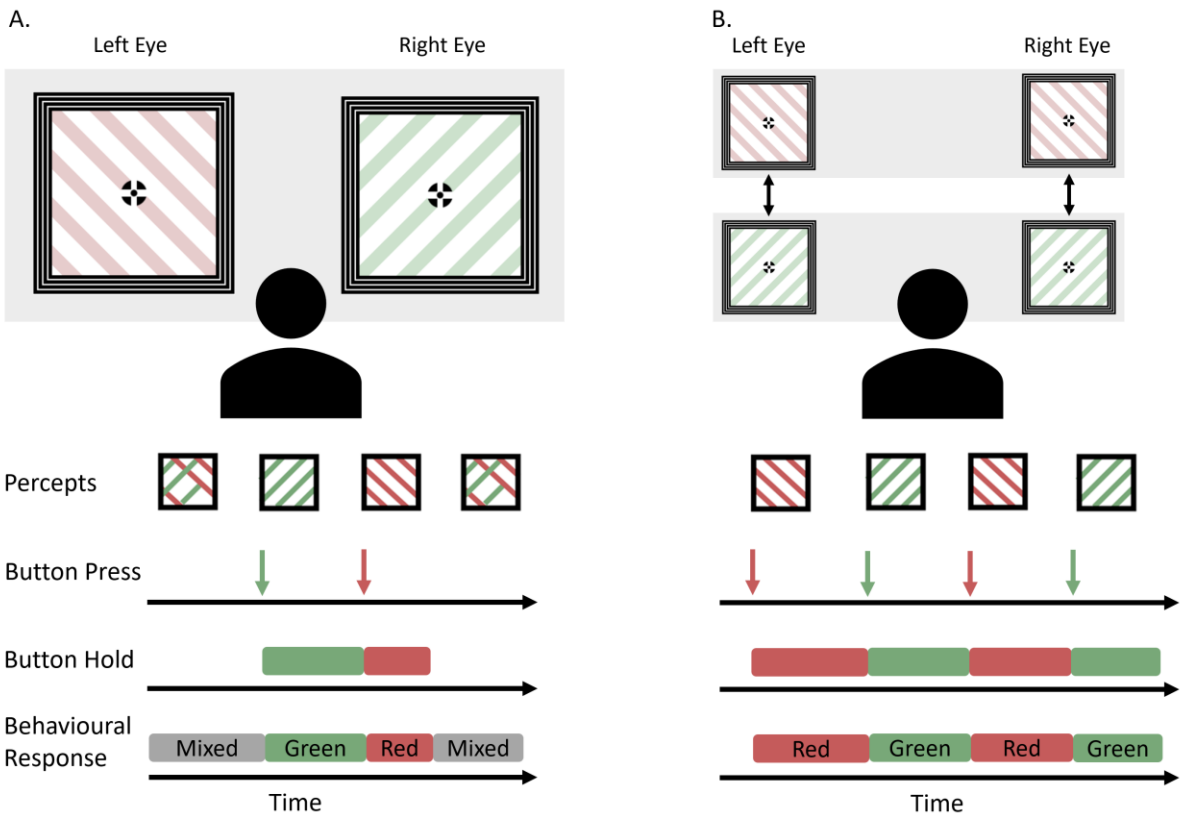

Figure 4.1 Visual stimulus and two-button press-and-hold design. A. Binocular rivalry condition where each eye is shown either a red or green orthogonal gratings with 90-degree interocular orientation difference. Perception thus alternates between red, green, and mixed percepts, which are reported through a two-button press-and-hold design. **B.** Binocular rivalry replay condition where each eye is shown either matching red or matching green orthogonal gratings. Perception alternated between red and green percepts and participants are tasked with reported their alternations with a two-button press-and-hold response.

MEG Data Collection

The MEG data acquisition was conducted in Montreal, Canada, at McGill University's McConnell Brain Imaging Centre, utilizing a 275-channel CTF/VSM MEG system (CTF MEG, British Columbia, Canada) operating at a sampling rate of 2400 Hz. Prior to MEG data acquisition, individualized head models were constructed for each participant through the digitization of approximately 100-150 points across the scalp. This process also involved recording anatomical landmarks and head-position coils using a Polhemus Fastrak system (Polhemus, Vermont, USA).

To capture body-related artifacts, bipolar signals were recorded for both vertical (eye blinks) and horizontal (visual saccades) electrooculogram (EOG), in addition to electrocardiogram (ECG) signals for heartbeats. Prior to participant's data acquisition, a 2-minute empty room recording was performed to identify faulty MEG sensors and assess environmental noise levels. These empty room recordings were subsequently used during MEG source imaging to compute noise covariance. Furthermore, a T1-weighted anatomical MRI volume (1.5T Siemens Sonata) was acquired for each participant for co-registration with their MEG data, thereby enhancing spatial resolution.

MEG Preprocessing and Cleaning

The MEG data preprocessing, cleaning, and analysis was performed in Brainstorm (Tadel et al. 2011), which is documented and freely available for download online under the GNU general public license (http://neuroimage.usc.edu/brainstorm). The preprocessing and cleaning steps for the MEG data were selected based on the guidance provided by the Brainstorm software documentation (Tadel et al., 2011) and were similar to those reported in previous studies (Bock et al., 2019; Bock et al., 2023). Initially, the MEG recordings were downsampled from 2400 Hz to 600 Hz. Notch filters at 60 Hz, 120 Hz, and 180 Hz were then applied with a 3-dB notch bandwidth of 2 Hz to mitigate the interference from North American power lines and their first two harmonics. Additionally, a high-pass filter was set at 0.3 Hz to remove the DC offset and slow drifts of MEG sensor signals. The subject anatomy from each participant's T1-weighted anatomical MRI volume was imported, and MNI normalization was computed to derive MNI coordinates and anatomical points. During the MEG-MRI co-registration process, the furthest 5% of head points were disregarded. Co-registration was performed using the nasion fiducial (NAS), left ear fiducial (LPA), and right ear fiducial (RPA) points digitized by the experimenter during MEG data collection, along with those identified in the MRI Viewer. To enhance the alignment between the MRI and MEG sensors, an algorithm implemented in the Brainstorm software was used to refine the registration by optimizing the correspondence between head points derived from the subject's MRI and those obtained through digitization.

Data cleaning was conducted on 20-second windows of the continuous MEG recordings by the experimenter, targeting artifacts such as heartbeats, eye blinks, and muscle activity. Artifact detection was performed using signal-space projection (SSP) for eye blinks, cardiac artifacts, and

1-7 Hz eye movements. The components of the projections were visually examined by the experiment and those deemed to be due to unwanted artifacts were removed. This criteria for removal were performed on a case-by-case basis for each individual subject, with a focus on significant components (i.e., >10%) and displaying topographies indicative of eye movements such as blinks and visual saccades (i.e., strong dipolar activity, concentrated fontal activity, concentrated activity near frontal-temporal regions). In all cases, the result of the corrections was visualized and evaluated. Segments exhibiting high muscle tension or movements during image presentation were identified and marked as 'bad.' Additionally, the first button press of each run was disregarded due to the uncertainty regarding the prior perceptual state. Initially, 10368 event-related responses were recorded across all participants. However, after the cleaning procedures, 8930 events were retained for analysis, representing 86.13% of the original data.

MEG Source Localization

The MEG source localization was performed using Brainstorm for each individual participant. This is an important step to increase spatial resolution and co-register the anatomical (T1 weighted) MRI with the MEG source space. A head model was created using the overlapping spheres method. Using both the data and noise covariance matrices, unconstrained sourced beamformer models were generated. The MRI segmentation was performed using CAT12 (Gaser et al., 2022) and SPM12 extensions in the Brainstorm software. The following parameters were selected: 15000 vertices, use spherical registration, and compute volume parcellations. The regions of interests (ROI) were generated for each individual participant's source reconstruction. Taken from the Human Connectome Project (HCP-MMP1) atlas (Glasser et al., 2016), 25 ROIs were created with the objective of covering the majority of the posterior cortex and the visual system (Table 4.1). Right and left hemisphere labels were combined into a single ROI for each region (i.e., left hemisphere V1 and right hemisphere V1).

Table 4.1 Regions of interest generated for each participant for scout-based MEG analysis. The abbreviation L and R refer to right and left hemispheres, respectively. The regions of interest were mapped for each participant's individual anatomy (N = 28).

ROI labels	Regions merged from HCP MMP1 atlas
V1	V1 L & V1 R
V2	V2 L & V2 R
V3	V3 L & V3 R
V3A	V3A L & V3A R
V3B	V3B L & V3B R
V4	V4 L & V4 R
V6	V6 L & V6 R
V6A	V6A L & V6A R
V7	V7 L & V7 R
V8/PIT	V8 L, V8 R, PIT L & PIT R
LO1/LO2	LO1 L, LO1 R, LO2 L & LO2 R
V4t/LO3	V4t L, V4t R, LO3 L & LO3 R
MT/MST	MT L, MT R, MST L & MST R
VMV	VMV1 L, VMV1 R, VMV2 L, VMV2 R, VMV3 L & VMV3 R
VVC	VVC1 L & VVC1 R
POS	POS1 L, POS1 R, POS2 L & POS2 R
IP0	IP0 L & IP0 R
IP1	IP1 L & IP1 R
IP2	IP2 L & IP2 R
IPS1	IPS1 L & IPS1 R
PG	PGi L, PGi R, PGp L, PGp R, PGs L & PGs R
PI	AIP L, AIP R, LIPd L, LIPd R, LIPv L, LIPv R, MIP L, MIP R, VIP L & VIP R
TPOJ	TPOJ1 L, TPOJ1 R, TPOJ2 L, TPOJ2 R, TPOJ3 L & TPOJ3 R
7	7AL L, 7AL R, 7Am L, 7Am R, 7PC L, 7PC R, 7PL L, 7PL R, 7Pm L, 7Pm R, 7m L & 7m R

MEG Event Related Analysis

The changes in alpha band activity were analyzed in relation to behavioral alternations during binocular rivalry (BR) and BR replay. Similar to an event-related potential (ERP) analysis, the power of alpha oscillations was examined in an event-related analysis time-locked to button presses. Specifically, three events were labeled for the focus of the event-related analyses: BR dominant percepts, BR mixed percepts, and BR replay dominant percepts. Red and green

perceptual reports were grouped together as dominant percepts, while reports of transitioning from red to mixed or green to mixed were categorized as mixed percepts. All three event types were segmented for further analysis within a time window of -3 to 3 seconds around the change in percept. For all event-related analyses, computations were performed at the individual trial level, and the results were subsequently averaged for each participant before calculating group mean values. Time-frequency decomposition was computed using Hilbert transform analysis, applied to both the entire cortex and predefined regions of interest. The Hilbert analyses were bandpass within the range of 8 – 13 Hz, and the mean power was extracted. The time-frequency results were baseline normalized using a z-score measure within the time range of 1 to 2 seconds, and the results obtained prior to baseline normalized are shown in the supplemental figures. This baseline period was selected in conjunction with periods of interest; -1 to 0 seconds and 0 to 1 second, as well as the psychophysics results (Figure 4.2B) characterizing the duration of BR dominant percepts (M = 1.83 seconds, SD = 0.76s, 95% CI = 1.54 – 2.13s).

The results are presented at group level means (N = 28), however, the event-related analyses were performed for each individual subject prior to the group level computations. This was done in order to account for variability in alternation rates experienced during BR, which resulted in a range of values that differed between participants for dominant and mixed percepts button responses. This method limited the overcontribution from *'fast-switchers'* that could arise if all button presses were analyzed together.

4.5 Results

Psychophysics

With the aim of further characterizing and understanding the dynamics of perceptual rivalry, we calculated results on the bevavioural aspects of BR and BR control conditions. Alternation rates, mean percept durations, and mean viewing proportions are presented in Figure 4.2. These psychophysics results were obtained from rivalry viewing during the MEG data acquisition. We also investigated whether the BR control condition was appropriately matched to traditional BR and identified behavioral patterns between dominant and mixed percepts that could inform the MEG analysis.

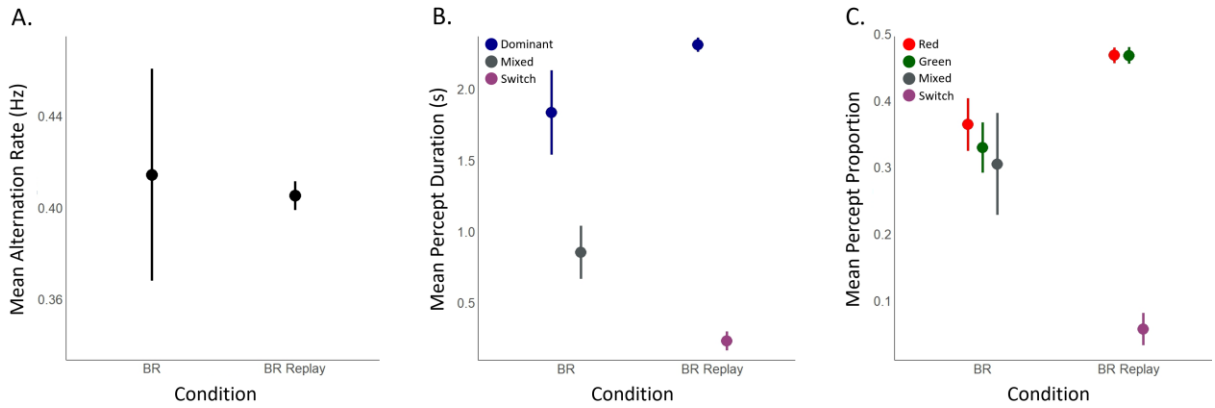

Figure 4.2 Psychophysics results for BR and BR replay conditions. A. Mean alternation rate (Hz) plotted for BR and BR replay conditions with 95% confidence intervals. **B.** Mean duration (seconds) of percepts reported for BR and BR replay conditions with 95% confidence intervals. **C.** Mean proportion of percepts experienced during BR and BR replay conditions with 95% confidence intervals.

The mean alternation rate (Figure 4.2A) indicated the frequency at which participants transitioned between dominant percepts. This measure is known to be influenced by stimulus properties, image size, and individual differences among participants. The alternation rate, measured in Hertz (Hz), was computed by dividing the total number of dominant button responses by the total duration of the experiment in seconds. For the BR condition, the mean alternation rate

was 0.41 Hz (SD = 0.12 Hz, 95% CI = 0.37 – 0.46 Hz), while for BR replay, it was 0.41 Hz (SD = 0.017 Hz, 95% CI = 0.40 – 0.41 Hz). These results indicate that the BR replay condition successfully replicated the approximate rate of transitions between dominant percepts observed during traditional BR for our participant pool. Notably, the BR condition exhibited a wider range in the 95% confidence interval and standard deviation values, highlighting the variability in alternation rates across participants.

Mean percept durations were computed for both dominant and mixed percepts (Figure 4.2B) during BR. This measure captured the durations of time each percept was held by participants throughout the experiment. For dominant percepts, the durations of both red and green percepts were averaged for a more comprehensive measure, consistent with the method used for the MEG analysis. Mixed percept duration represented the time of transitions from dominant percepts during BR when neither red nor green button responses were selected. The mean duration of dominant percepts during BR was 1.83 seconds (SD = 0.76s, 95% CI = 1.54 – 2.13s), while mixed percepts were reported with a mean duration of 0.85 seconds (SD = 0.48s, 95% CI = 0.67 – 1.04s). In contrast, the BR replay condition only measured the duration of dominant percepts, as the authentic experience of mixed percepts was fundamentally eliminated due to both eyes always being shown the same stimuli; either red or green orthogonal gratings. The mean duration of dominant percepts during BR Replay was 2.31 seconds (SD = 0.13, 95% CI = 2.26 – 2.36s). Serving as the control condition, BR replay also provides an important measure for assessing the specificities of our study's two-button press-and-hold design, the instructions provided to participants, and the stimuli presented. The mean BR replay switch time of 0.23 seconds (SD = 0.17s, 95% CI = 0.16 – 0.30s) corresponds to the mean duration it took participants to transition between dominant percept key responses. This switch time (reaction time) recorded the duration between the release of one dominant percept response and the onset of the new dominant response.

Mean percept predominance (Figure 4.2C) served as a measure of the overall viewing proportion of each percept experienced by participants throughout the experiment, offering a global view of the BR experience. This measure was calculated by dividing the total duration that each percept (red, green, or mixed) was reported by the total duration of the experiment. During BR, we observed approximately equal ratios between the three perceptual states. Red was reported with a predominance of 0.36 (SD = 0.10, 95% CI = 0.32 – 0.40), slightly higher than green, which was reported at 0.33 (SD = 0.097, 95% CI = 0.29 – 0.37). BR mixed percepts were reported with

a predominance of 0.30 (SD = 0.20, 95% CI = 0.23 - 0.38). During BR replay, the expected ratio between red and green percepts was 1:1, with a small proportion of switch time due to the transition between responses. The predominance of red was 0.47 (M = 0.47, SD = 0.030, 95% CI = 0.46 – 0.48), green was 0.47 (SD = 0.031, 95% CI = 0.46 – 0.48), and the proportion obtained for the switch was 0.057 (SD = 0.062, 95% CI = 0.033 – 0.081).

We observed meaningful perceptual stability in the mean durations and proportions of both dominant and mixed percepts during BR, warranting further investigation of the neural mechanisms of alpha oscillations with MEG. This was particularly evident when comparing traditional BR with the BR replay control, focusing on mixed percepts versus switch time. The mean duration of mixed percepts during BR was significantly longer than the switch time of BR replay, with a mean difference of 0.62 seconds observed in a paired samples t-test conducted in R ($t = 6.82$, $df = 27$, p-value = 2.54e-07). Moreover, we observed that mixed percepts during BR exhibited approximately equal predominance to the dominant states reported, highlighting their importance as a perceptual state during BR.

MEG Alpha Band Power during BR

Prior to investigating the event-related changes in alpha band activity, we explored characteristics of alpha oscillations throughout the entirety of the BR task. This preliminary analysis aimed to quantify the strength of alpha oscillatory signal and plot cortical topographies for the main sources of alpha power during the visual task.

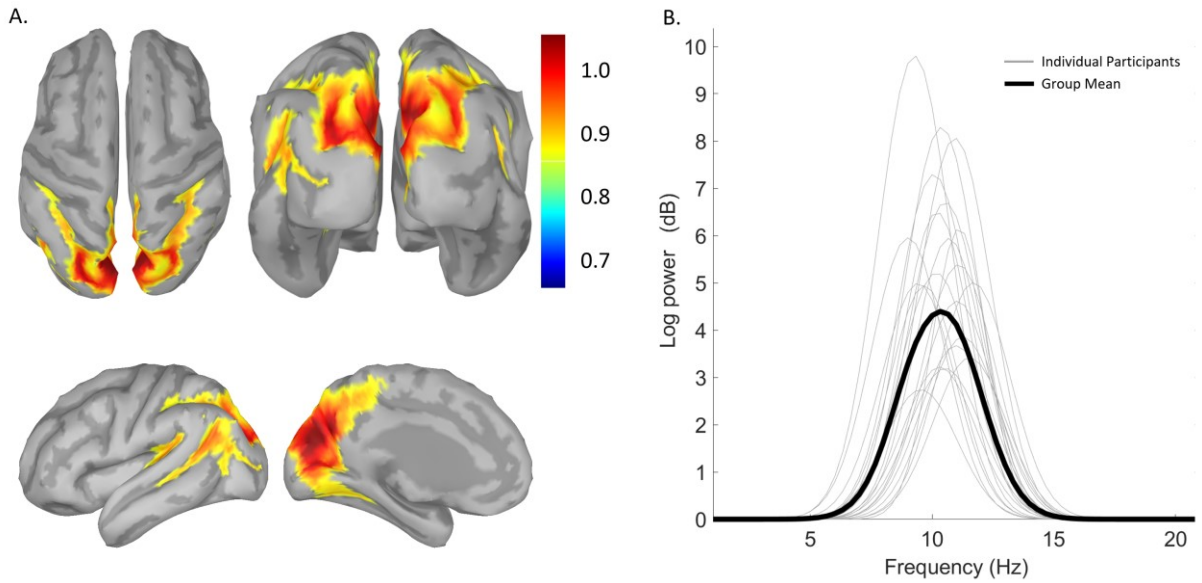

Figure 4.3 MEG alpha band topography during binocular rivalry. A. Full cortex view of the mean alpha band power during binocular rivalry across all participants. **B.** Plot displaying the isolation of the alpha peak using specparam. The peak measure was extracted from the spectral parameter results of the power spectrum density analysis. In light grey, the alpha peaks are plotted individually for all participants in addition to the group mean.

To achieve our objective of an overall measure of alpha band topography, a time-frequency decomposition using the Hilbert transform on the entirety of the recording was computed. This was done for each of the 75-second testing blocks, bandpass filtered within the range of 8 – 13 Hz, and the mean power was extracted. The mean power values from the four testing blocks were then averaged to obtain a mean BR result for each participant. Subsequently, all participants' data were projected to default anatomy space and averaged to generate a group-level result, depicted in Figure 4.3A. The displayed cortex had parameters set at a 60% smooth surface, with a colour scale threshold of 50% and a minimum cluster size of 5. Our analysis revealed the strongest alpha band power during BR in the posterior cortex, particularly in the parietal and occipital regions, with pronounced activity near and bordering the parietal-occipital sulcus (POS).

Next, we sought to further quantify the power and frequency of alpha band activity in the primary visual cortex during binocular rivalry (BR) using specparam methods to isolate periodic and aperiodic components of the power spectrum (Donoghue et al., 2020). In each of the 75-second testing blocks, we computed power spectrum density (PSD) using the Welch method, with a

window length of 3 seconds and an overlap ratio of 50%. The mean scout function was utilized to average signals from both the right and left primary visual cortices (V1). Specparam measures were then applied to each participant's PSD to isolate the periodic components, and the results were averaged together across participants. We explored a frequency range of 1 – 26 Hz, focusing on identifying a single peak corresponding to the alpha band (8 – 13 Hz) during BR. To achieve this, we set parameters to detect a single peak with a minimum height of 0.3dB and width limits of 0.5 to 3 Hz. These parameters were chosen to isolate individual alpha band peaks while excluding aperiodic activity from the power spectrum. Subsequently, we extracted only the peak measure derived from the specparam analysis, thus isolating the periodic component of the alpha band activity. The results are presented in Figure 4.3B, illustrating the mean alpha band peak in V1 across all participants. Notably, we observed individual differences in the shape, intensity, and peak frequency of alpha band activity across participants.

Full Cortex MEG Event Related Analysis

The event-related analysis aimed to investigate fluctuations in alpha band activity time-locked to behavioral responses during BR and BR replay. Both pre-stimulus and post-stimulus brain responses were incorporated into the analyses, particularly focusing on behavioural responses marking the onset of dominant percepts, centered at time zero. The objective of this analysis was not to ascertain the presence of signal within the 8 – 13 Hz range, as this could reasonably be expected with baseline activity throughout the brain. Instead, our focus was on localizing both spatial and temporal changes in alpha band power in an event-related analysis time-locked to the perceptual alternations experienced during BR.

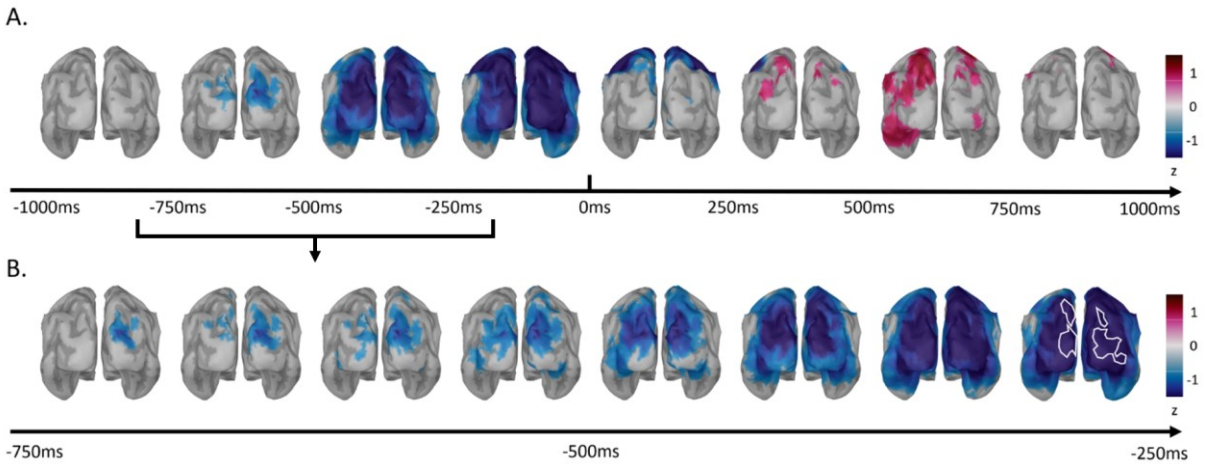

Figure 4.4 Full cortex posterior view depicting the baseline normalized (z-score) changes in alpha band power during BR dominant percepts. A. Snapshots of projected group mean cortex illustrating the changes in baseline normalized (z-score) alpha band power from -1000ms to 1000ms in 250ms intervals, centered around alternations in dominant percepts during BR at t=0. **B.** Snapshots of the projected group mean cortex illustrating the changes in baseline normalized (z-score) alpha power from -750ms to -250ms in 62.5ms intervals prior to a dominant alternation during BR. Areas of significance ($p < 0.05$) highlighted in white from the switch time of -230ms. The minimum cluster size was set at 5 and the threshold was at 50%.

Hilbert transform time frequency analysis was performed on the full cortex for dominant percepts during BR and band passed in the frequency range of 8 – 13 Hz. The analysis was performed on 6 second recordings of MEG data, segmented from -3 to 3 seconds around a button response. The results presented were then extracted between -1 to 1 second around the button press, in order to minimize the edge effects found towards the start and the end of the time-series. A posterior view of the cortex was selected in Figure 4.4 because this was where the vast majority of event related changes in both pre- and post-perceptual switch brain activity was observed. The results presented are baseline normalized through a z-score, as outlined in the methods.

We observed the first negative z-score cluster in alpha power within mid-level visual regions (V3A, V3B and V4), emerging at -750ms (Figure 4.4A). This reduction in baseline-normalized power extends over time towards the perceptual alternation, encompassing the majority of the posterior cortex. Within the initial 250ms *after* the report of a new dominant percept, the decrease in alpha power shifts towards the motor cortex. Subsequently, between 250

to 750ms, we observe a shift in power towards positive z-score clusters in parietal regions and areas lateral to the primary visual cortex. In Figure 4.4B, the initial negative cluster is evident in mid-level visual regions and expands as the alternation report approaches. This expansion is suggestive of a feedback influence as it moves across parietal regions and lateral to the primary visual cortex, eventually covering nearly all of the posterior cortex before the alternation occurs.

MEG Event Related Analysis within the Visual Cortex

The time-frequency decomposition performed using Hilbert transforms between 8 – 13 Hz was performed for all three unique events detected during the MEG experiments: BR dominant percepts, BR mixed percepts, and BR replay dominant percepts. The analyses computed the mean power within the alpha frequency range using multiple pre-defined ROIs within the visual system. However, the analysis shown in Figure 4.5 focused on the primary visual cortex. During BR dominant percepts (Figure 4.5A), the onset of negative z-score baseline-normalized power in V1 occurred at -780ms before their report. The alpha band power continued to decrease towards its trough at -175ms and returned to baseline value at 220ms after the dominant alternation. This resulted in a 1-second drop in alpha band power, primarily occurring before the alternation. In contrast, during BR replay the temporal dynamics of the alpha band drop occurred closer to the alternation, exhibiting a rightward shift in time relative to the alternation. The onset of the negative z-score is at -430ms, 350ms after what was observed during traditional BR, and peaked after the button press, at 25ms. In addition, alpha band activity returned to baseline value much later, at 590ms post-alternation. Compared to BR replay, BR shows earlier markers of alpha band activity preceding dominant percepts. It is acknowledged that the BR replay (but not BR) condition was tagged at fundamental frequencies (see methods). These frequencies were well below the alpha band. However, certain harmonics at 10 and 13.34 Hz could fall in the measured range. The introduction of these frequencies might theoretically contribute to the strong magnitude of the BR replay alpha trough, but seems unlikely, particularly as an account for the observed timing differences (see Discussion).

The pattern of results for mixed percepts during BR were entirely different than for dominant percepts. For mixed percepts, an *increase* in baseline normalized alpha band power occurred in V1 leading up to the button response for perceptual alternations (i.e., dominant-to-mixed). The peak of this alpha power occurred 530ms prior to mixed percepts. We performed a

two-tailed paired Student's t-test available through Brainstorm within the time window of -1 to 1 second to examine the changes in MEG alpha band power activity prior to dominant versus mixed percepts. At a threshold of $p < 0.05$, two significant periods of time emerged. Prior to the button press, a significant difference was present between 736.7ms to 108.3ms, encompassing a significant time cluster of 628.4ms. This period showed a higher mean alpha band power in the lead-up to mixed percepts. A shorter second significant time period was observed after the button press, between 596.7ms to 696.7ms. During this later time period, the MEG activity of dominant alpha band power was now significantly higher than for mixed percepts. It is acknowledged that the results presented are not corrected for family-wise error rate (FWER). Applying cluster correction for significant time points across the time series could offer deeper insights into the periods of significant differences.

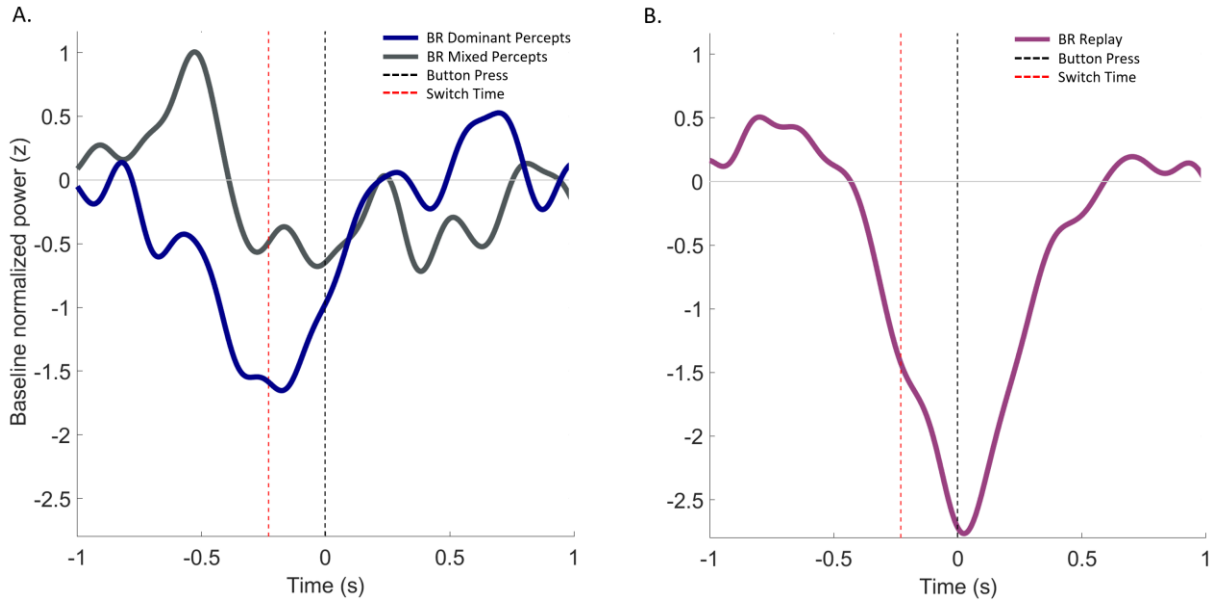

Figure 4.5 Hilbert transform analysis for BR and BR replay conditions in the primary visual cortex. A. The baseline normalized (z-score) mean alpha band power in V1 for dominant and mixed percepts is plotted during BR. **B.** The baseline normalized (z-score) mean alpha power in the primary visual cortex (V1) is plotted for dominant percepts during BR replay. The BR replay condition was frequency tagged at 5 and 6.67 Hz. The button press indicating a change in percept is marked at time = 0 seconds, and the BR replay switch time is marked at time = -0.23 seconds.

Next, to further characterize the changes in alpha band power across a broader region of the visual cortex beyond the primary visual cortex, Hilbert transform time-frequency analysis was conducted using 25 pre-defined regions of interest (ROIs) derived from each subject's individual anatomy based on the HCP atlas. These ROIs encompassed the majority of the visual system within occipital and parietal regions, as depicted in Figure 4.6C. The responses from both the right and left hemispheres were averaged for each ROI.

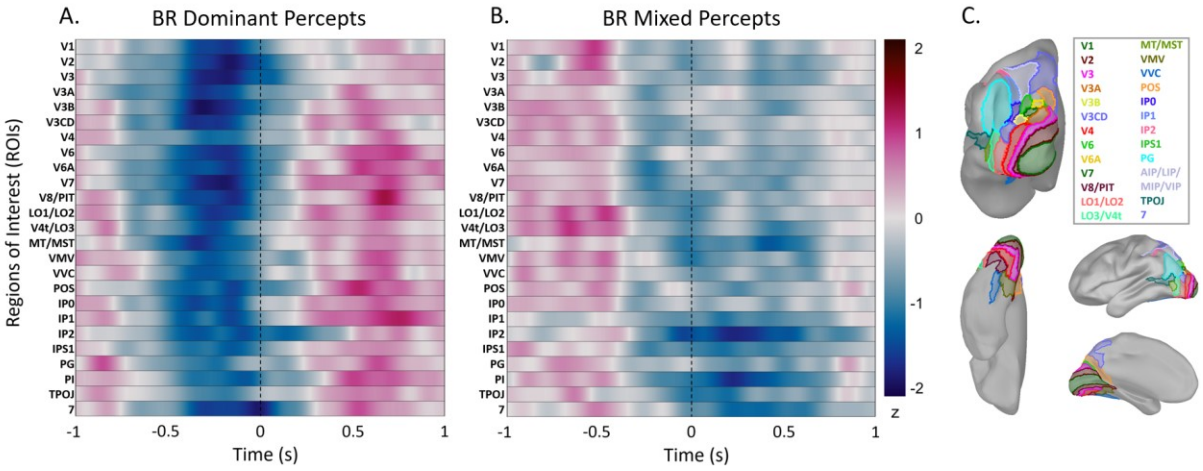

Figure 4.6 Hilbert transform analysis on alpha band power across regions of interest during BR. **A.** Hilbert transform time-frequency analysis for BR dominant percepts, centered around the perceptual report. **B.** Hilbert transform time-frequency analysis for binocular rivalry mixed percepts, centered around the perceptual report. **C.** Full cortex visualization for the regions of interest plotted in the Hilbert transform analysis.

Across the majority of regions of interest (ROI) defined in this study, we observed a generalized trend towards a decrease in alpha power preceding dominant percepts during BR (Figure 4.6A). The onset of the drop in alpha power was observed around -700ms for most regions, with troughs occurring prior to the behavioural report of dominant percepts. However, not all ROIs exhibited the same extent of change in power. Specifically, we observed a stronger drop in the early visual cortex (i.e., V1, V2, and V3), with the most pronounced negative peak recorded in V3B. Following the button press for a dominant BR percept, there was a trend for an increase in alpha band power across most visual regions. The strongest positive peak was observed over V8/PIT, with additional parietal regions showing strong peaks in POS and IP1.

In the MEG alpha band activity recorded during BR mixed percepts (Figure 4.6B), we observed a very different overall pattern. We see a trend towards increases in power prior to the perceptual report. The strongest peaks were observed over the primary visual cortex (V1) and the lateral occipital regions (LO1/LO2 and V4t/LO3). Starting approximately 300ms prior to a mixed report and persisting during the mixed state, a decrease in alpha band power was observed. The regions with the most pronounced subsequent decrease in alpha power during mixed percepts were within the parietal cortex (area IP2).

The findings related to the overall trends in alpha power changes associated with the report of dominant and mixed percepts (Figure 4.6) are observational, based on baseline normalized z-score measures. This limitation in interpretability is acknowledged, and further statistical analyses are planned.

Individual Differences

Binocular rivalry is known to exhibit robust individual differences, including variations in alternation rates. We also noted the differences in the periodic components of shape, peak, and frequency of the alpha band peak (Figure 4.3B) during BR. To investigate potential relationships between differences in alpha band activity and behavioral outcomes during BR, we conducted correlation analyses between the individual differences in alpha band power prior to alternations in percepts, and the subsequent percept duration.

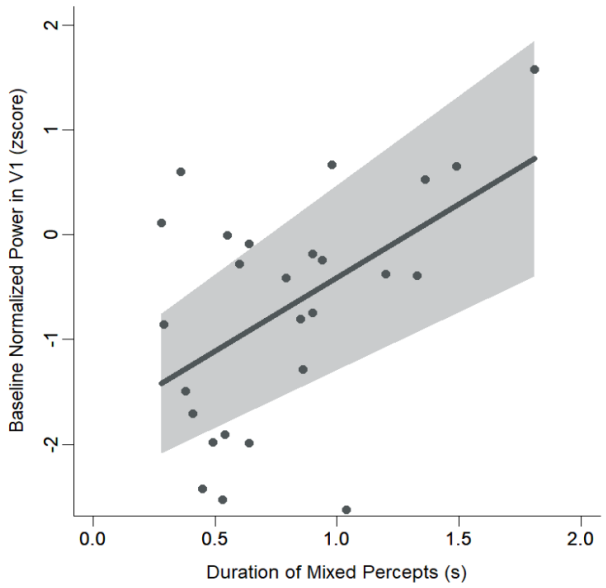

Figure 4.7 Individual differences in alpha power prior to BR mixed percepts predict their mean duration. The scatterplot illustrates the correlation between the baseline normalized power in the primary visual cortex (V1) and the mean duration of mixed percepts during BR. Each dot represents the results for individual participants. Alpha power (z-score) was measured 230ms prior to the indication of a mixed percept. The linear line of best fit is plotted with the shaded region representing the 95 percent confidence interval.

To investigate individual differences during BR in event-related alpha power and their correspondence to behavioral measures, we calculated the correlation between alpha power prior to the report of both dominant and mixed percepts and the mean duration of those percepts. While a trend was evident for dominant percepts, it was the mixed percepts that showed the strongest relationship. A significant positive correlation was found between the MEG and behavioral measures, as indicated by Pearson's product-moment correlation results using R ($t = 2.81$, $df = 24$, p-value = 0.0097, $R = 0.50$). The baseline normalized alpha power prior to the report of mixed percepts was calculated for each subject in V1 at -230ms from their Hilbert Transform time-frequency analysis (Figure 4.5A). The mean duration of mixed percepts was obtained from the behavioral results (Figure 4.2B). The results indicate that participants who demonstrated higher baseline normalized alpha power peak prior to mixed percepts, tended to view this perceptual state for longer durations. We note that prior to conducting the correlation analysis presented in Figure

4.7 (N = 26), outliers were identified using a threshold set at 3 standard deviations from the mean to ensure more representative results. This led to the identification of two participants as outliers. Importantly, even with the inclusion of these two outliers, the Pearson's product-moment correlation results remained significant and positive (p-value = 0.037).

A similar correlation analysis was conducted on dominant percept durations during BR, using the MEG baseline normalized alpha band power in V1 at -230ms prior to their report. The results exhibited trends analogous to those shown in Figure 4.7 for mixed percepts; however, no further analysis was conducted as the results were non-significant (t = 1.43, df = 26, p-value = 0.17, R = 0.27).

Alpha Band Connectivity during Binocular Rivalry

Finally, we conducted a connectivity analysis using methods of phase transfer entropy (PTE) (Lobier et al., 2014; Hillebrand et al., 2016) on the alpha band activity during BR dominant percepts. Specifically, we computed the normalized result between outgoing and incoming connectivity for each region of interest. This resulted in our directed phase transfer entropy (dPTE) results provided below which was performed in the Brainstorm software. We computed this analysis between pre-defined ROIs listed in Table 4.1, resulting in 25 x 25 matrix covering 625 pair-wise connections quantified by their strength and directionality. Our aim was to identify patterns of feedback versus feedforward connectivity between regions of interest. Specifically, we distinguished between pre-dominance and post-dominance alpha band connectivity to compare and contrast their measures.

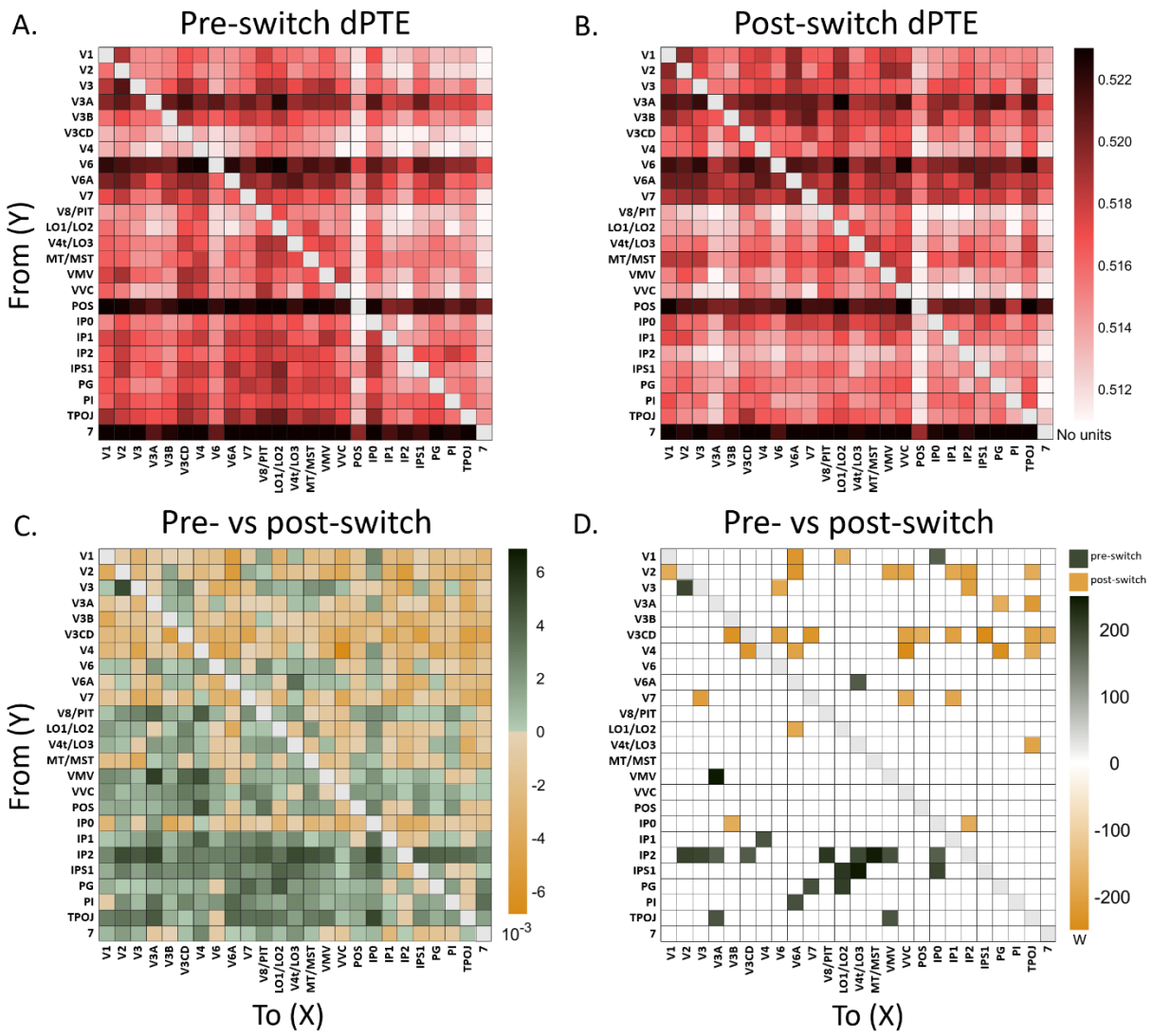

Figure 4.8 Directed phase transfer entropy (dPTE) analysis for alpha band activity during BR dominant percepts. A. Pre-button press (-1 to 0 second) dPTE alpha band activity during BR dominant percepts. **B.** Post-button press (0 to 1 second) dPTE alpha band activity during BR dominant percepts. C. Difference map between pre-button press (-1 to 0 second) and post-button press (0 to 1 second) dPTE alpha band activity results (N = 28) performed in Brainstorm. **D.** Paired permutations statistical analysis (N = 28) performed in Brainstorm using the Wilcoxon signed-rank test to compare dPTE connectivity results between pre- and post-switch BR dominance. The analysis used the Monte-Carlo approach with 10000 randomizations. The significance level was set at $\alpha = 0.05$. Green squares indicate stronger dPTE connectivity results in the pre-switch condition, whereas yellow squares indicate stronger dPTE connectivity results in the post-switch condition.

For both the pre-switch period and post switch period (Figure 4.8A-B), the dPTE results indicate that several regions exhibit stronger outgoing connections than incoming ones, including V3A, V6, POS, and 7. This can be visualized by noting the strongly consistent horizontal bands in Figure 4.8A and 4.8B. Additionally, the very weak incoming connections for POS can be noticed by the distinctly pale vertical band formed in Figures 4.8A and 4.8B. This emphasized a strong role for POS as a source of signal change that even suggests causality. We further compared the pre- versus post-switch alpha band connectivity results by computing a difference map across the dPTE results for all ROIs (Figure 4.8C). This result indicates stronger feedback connectivity (i.e., stronger magnitude in dPTE results for the direction of connectivity from regions in the parietal cortex to earlier visual areas) in alpha band activity during the pre-switch neural response. This is opposed to the results observed during post-button switch connectivity, where an increase in feedforward mechanisms is recorded (i.e. stronger magnitude in dPTE results for the direction of connectivity from regions in the early visual system to higher ordered visual and parietal areas).

Statistical analysis was computed in Brainstorm in the difference map (Figure 4.8C) to highlight dPTE results that were significant between pre- and post-switch alpha band connectivity (Figure 4.8D). The dPTE results in Figures 4.8A and 4.8B were found to have a non-normal distribution ($p < 0.05$) through a Shapiro-Wilk test performed in Brainstorm. For this reason, we chose to perform non-parametric paired-samples permutations test using the Wilcoxon signed-rank method and 10,000 random permutations with the Monte-Carlo. The significant dPTE results ($\alpha = 0.05$) are presented in Figure 4.8D. The results highlight clear feedback influences (i.e., parietal areas IP2 and IPS to lower-level visual areas V2, V3, and LO1-3, MT).

The dPTE results highlighting differences in pre- versus post-switch alpha band connectivity are observational, and the need for further statistical analysis to account for family-wise error rate (FWER) is acknowledged as a current limitation. The trends toward stronger feedback connectivity prior to, and stronger feedforward connectivity after, the perceptual alternation was most prominently observed in the difference map presented in Figure 4.8C.

4.6 Discussion

The current experiment sought to understand the influence of brain oscillations within the alpha band (8 – 13 Hz) recorded with magnetoencephalography during binocular rivalry. Through our time-frequency analysis, we consistently found a decrease in baseline normalized alpha band power to start approximately one second prior to the report of dominant percept alternations during BR. The effect was observed broadly in the visual cortex, covering occipital-temporal and parietal regions. However, the earliest markers of the decrease in power were recorded from high-to-mid-level visual areas. Further, the decrease in baseline normalized alpha band power was observed earlier in time relative to the new percept when compared to a BR replay control condition. We interpret the reduction in power of alpha band activity to reflect a decrease in inhibitory processing within the visual system, allowing for destabilization of the dominant percept, and emergence of the previously suppressed percept leading to the alternation experienced. This was in stark contrast to mixed percepts, where an increase in alpha band power was observed in visual regions prior to their report. We interpret these results within the context of inhibition (i.e., E:I) and provide evidence for top-down feedback connectivity in alpha band oscillations during binocular rivalry. Our results provide further insight into brain mechanisms at play during bistable perception. Equally, they provide support for the growing literature on the role of alpha oscillations within human visual perception.

Alpha Band Activity during Binocular Rivalry

As previously reported, a few neuroimaging studies have examined characteristics of alpha band oscillations with EEG and MEG during the experience of bistable perceptual illusions (Piantoni et al., 2017; Katyal et al., 2019; Cuello et al., 2022; Sponheim et al., 2023). In particular, during the experience of binocular rivalry, peak alpha frequency was found to be correlated to alternation rate (Cuello et al., 2022), as well as the peak alpha frequency recorded during a fixation period (Katyal et al., 2019) and during resting-state (Sponheim et al., 2023). These findings provide support for the role of alpha oscillations during bistable perception possibly as an extension of (partially heritable) trait-like influences on E:I balance. However, our current findings expand the discussion of alpha oscillations beyond their peak frequency, to consider the time-

locked task specific changes in power relative to perceptual alternations. Within this context, previous EEG findings during bistable presentation of a Necker cube-type image found that alpha power recorded from electrodes over occipital and parietal brain regions decreased prior to reversals in percept (Piantoni et al., 2017). The results we provide, generalize this effect to binocular rivalry, and offer improved spatial resolution through MEG neuroimaging methods.

In addition, by directly comparing the binocular rivalry to the replay control condition, we observed a leftward shift in the decrease of baseline normalized power of the time-frequency curve for the primary visual cortex. During the experimental condition, the decrease in alpha band activity started nearly a second prior to the alternation in dominant percept, and peaked in magnitude 175ms prior to the switch. This is contrasted to the replay condition, where the peak in decrease of the alpha band activity occurred 25ms after the switch, i.e. a peak-to-peak temporal shift of 200ms between BR and BR replay conditions. We interpret the earlier dip in alpha band power during BR to be indicative of neural processing required by the endogenous process of bistable perception. This early marker of alpha power change during BR preceded our estimate of switch time of 230ms extracted from the replay control.

Unique to BR, an increase in alpha band power was present during the initial stages of perceptual dominance (i.e., approximately 500ms after the switch) that was observed primarily in the parietal cortex (Figure 4.4A). We interpret this within the context of alpha's role in inhibition to provide a neural mechanism of perceptual dominance after the switch, further suppress the unattended image, and provide stability to the new dominant percept. Nevertheless, the dPTE results make it clear that after to switch-to-dominant the relative balance between feedback compared to feedforward influences is diminished.

In addition to the different dynamics we observed for BR replay, we also found that the change in alpha power recorded during the control condition was stronger in magnitude than the equivalent decline for BR. Several factors could contribute to this observation. During the control condition, the images viewed by participants were alternated unambiguously by the software, possibly accounting for the changes in alpha power observed due to this change. The control condition was also frequency tagged at 5 and 6.67 Hz with harmonics in the alpha band. The change in image presentation during BR replay was thus accompanied by an alternation in the harmonics (i.e., 10 and 13.34 Hz) of the coloured gratings. Specifically, the switch between red and green orthogonal gratings by the software during BR replay is hypothesized to introduce, and

equally remove, entrainment of the visual cortex to the fundamental frequencies and their respective harmonics. Nevertheless, we have no reason to suspect that this small difference in the stimuli would account for the difference in timing already discussed.

In contrast to the patterns of alpha band activity prior to dominant percept alternations, a prominent and long-lasting increase in baseline normalized power was recorded prior to mixed percepts. Often experienced as piecemeal percepts, they are thought to reflect a perceptual state of increased inhibition (Katyal et al., 2016). Mixed percepts were unique to binocular rivalry, as the control condition would not have elicited perceptual ambiguity, and this was confirmed through the psychophysics results for BR replay (Figure 4.2C). Regions within the early visual cortex (i.e. V1 and V2) and the lateral occipital (i.e., LO) had the strongest increase in alpha band power prior to mixed percepts. Given previous results in the literature that relate V1, V2, and LO with perceptual grouping and segmentation (Buckthought et al., 2021), this result emphasizes a role for competitive (E:I) neural interactions in low-to-mid tier visual areas in resolving perceptual ambiguity.

We note in passing for the sake of completeness, that the patterns in alpha band activity were observed for baseline normalized (z-score) values. Baseline normalization was applied to the time-frequency decomposition for alpha band power to provide a more robust interpretation of the results. As seen in Figure 4.3B, the MEG alpha band power recorded in the primary visual cortex varied in magnitude across participants. The variability could be attributed to several factors, with the largest contributor believed to be accounted by the distance between the MEG sensors and the participants' scalp that varied based an individual head shapes and placement in the head cap. The general trends that we present (i.e., decrease in alpha power prior to dominant percept alternations, and increase in power prior to mixed percepts) were present in the raw power prior to normalization and are presented in the Appendix (Figure A.2).

Alpha as an Inhibitor in Visual Perception

Alpha brain oscillations play diverse roles across several sensory processes, including attention, memory, and perceptual stability. In our study, we specifically examined changes in alpha band power with a focus on its role in inhibition. Previous research has consistently linked alpha oscillations to inhibitory processes within the brain (Klimesch et al., 2007; Jensen &

Mazaheri, 2010; Klimesch et al., 2012). Specifically, within the visual system, alpha oscillations are hypothesized to exert an inhibitory effect that regulates sensory input and maintains perceptual stability (Jensen et al., 2015; Clayton et al., 2018). In the context of bistable perception, such as binocular rivalry, the role of inhibition becomes particularly intricate. Bistable perception occurs when an ambiguous visual stimulus leads to alternating perceptions without any change in the actual sensory input. Our findings suggest that alpha oscillations are pivotal in modulating this perceptual alternation. We propose that increased alpha band mediated inhibition is essential for maintaining the stability of the dominant percept, whereas a decrease in alpha-band power facilitates the transition to a different percept.

Our time-frequency analysis provided robust evidence for this model. We observed that fluctuations in baseline normalized alpha band power could serve as an indicator of the level of inhibition within the visual system during bistable perception. Specifically, prior to a switch in dominant percept, we detected a dysregulation in inhibitory processing. This dysregulation appears to originate from higher-level visual areas in the parietal cortex, which plays a crucial role in integrating visual information and mediating attentional shifts, as supported by previous studies using TMS highlighting the causal role of the parietal cortex during BR (Zaretskaya et al., 2010: Carmel et al., 2010). During perceptual competition, reduced alpha band power, indicating lower inhibition, allows for increased neural activity corresponding to the competing percepts. This reduction in inhibition enables the suppressed percept to gain dominance. Following the establishment of a new dominant percept, we observed an increase in alpha band power. This increase is indicative of enhanced inhibitory control, which we hypothesize serves to stabilize the newly dominant percept by suppressing competing neural representations.

Our findings align with the hypothesis that alpha oscillations act as a gating mechanism, selectively inhibiting irrelevant or competing information to maintain perceptual coherence (Mathewson et al., 2011). This dynamic balance of inhibition and excitation, mediated by alpha oscillations, is critical for the brain's ability to process and interpret sensory information in a coherent manner. Within the larger field of bistable percepts, our findings provide insight into a distinct neural mechanism that contributes to visual perception. This mechanism, characterized by the modulation of alpha band power, could be one of many or integrated into a larger network of processes that collectively govern visual perception and perceptual stability. Previous studies have coupled oscillatory dynamics in the theta and gamma bands during BR (Doesburg et al., 2009).

This is supplemented by the observation that during EEG recording with BR, parieto-occipital alpha oscillation power decreased prior to a switch, whereas fronto-medial theta oscillation power increased before, and decreased after the alternation (Drew et al., 2022).

We observed individual differences in alpha band power prior to mixed percepts that were significantly correlated with their duration. This suggests that a "trait-like" variability in inhibitory control, as reflected by alpha oscillations, influence the experience of perceptual ambiguity during bistable perception. It has already been shown via studies of identical twins that alternation rates are a partially inherited trait (Miller et al., 2010; Shannon et al., 2011).

Moreover, our study underscores the importance of higher-level visual areas in the parietal cortex in regulating this inhibitory process. The parietal cortex is known for its role in spatial attention and sensory integration, and our results suggest it also plays a key role in managing the inhibitory dynamics that underlie bistable perception. Further, they support the previous findings during BR that have highlighted the role of the parietal cortex with transcranial magnetic stimulation (TMS) (Zaretskaya et al., 2010: Carmel et al., 2010) and intermittent presentation of BR (Pitts & Britz, 2011; Britz et al., 2011). Notably, TMS studies reporting specific regions within the parietal cortex are particularly significant, as this method offers a more causal influence on neural activity and its relationship to bistable perception during BR.

Additionally, within the larger scope of brain mechanisms, the inhibitory role of alpha oscillations contributes to the E:I ratio. The balance between excitation and inhibition within the visual system is crucial during BR. Imbalances, such as those observed in autism (Robertson et al., 2013; Spiegel et al., 2019; Skerswetat et al., 2022), have been shown to alter BR dynamics. Individuals with autism often exhibit altered excitation and inhibition ratios, leading to differences in sensory processing and perceptual stability. Our study suggests that similar mechanisms might be at play in the general population, with individual differences in alpha band power reflecting variations in excitation and inhibition ratios that affect perceptual experiences during BR and provide an account for the variability observed between individual alternation rates. Notably, our study reveals real-time changes in alpha band activity, representing fluctuations in the strength of inhibition, which may dynamically tip the scale of the E:I ratio. This underscores the intricate interplay between neural processes underlying bistable perception. Some data exists that also supports the premise that in certain contexts measures of E:I ratios show stable individual

differences, analogous to what is known for perceptual alternations rates, i.e. fast versus slow switchers (Brunel & Wang, 2003; van Pelt et al., 2012; Muthukumaraswamy et al., 2019).

The present study advances the understanding of how alpha oscillations contribute to visual perception by modulating inhibitory processes. By examining the changes in alpha band power, we provide insights into the neural mechanisms that enable perceptual stability and flexibility.

Models of Binocular Rivalry

Prevailing views of binocular rivalry have touched on diverse theories regarding bottom-up (i.e., sensory input driving perception) versus top-down (i.e., the role of selective attention) mechanisms of communication. Early accounts of BR focused on the competition between monocular neurons in the early visual cortex, emphasizing monocular inhibition (Blake, 1989; Tong, 2001). Others have proposed multistage models of BR (Wilson, 2003; Freeman, 2005), which suggest that the rivalry process involves multiple stages of neural processing, each with the potential for competitive interactions between competing percepts. Additionally, hybrid models have been proposed to reconcile these different perspectives (Tong et al., 2006). In addition to our proposition that alpha oscillation power is linked to inhibition in the visual system, the role of attention is considered. The role of attention in BR has also been extensively studied, with substantial research demonstrating the influence of attentional mechanisms on perceptual dominance (Zhang et al., 2011; Chong & Blake, 2006; Dieter et al., 2015), and efforts made to integrate attention more explicitly into models of rivalry (Li et al., 2017).

Moreover, recent studies using magnetoencephalography have shed light on the direction of communication within the brain during binocular rivalry. Previous MEG work found evidence for top-down mechanisms preceding the dominant percept, followed by an increase in bottom-up information flow during BR (Dijkstra et al., 2016). Others found more evidence for feedforward connectivity during binocular rivalry with MEG using directed phase transfer entropy (dPTE) analysis, and differentiated between neural mechanisms of dominance and suppression (Bock et al., 2023). Notably, their study utilized dichoptic frequency-tagging techniques (Brown & Norcia, 1997), which has been shown to primarily entrain and highlight activity in the early visual cortex (Kamphuisen et al., 2008). In our analysis, we employed the methods of directed phase transfer entropy (dPTE) for connectivity analysis. This approach allowed us to assess both the strength and

directionality of connections between regions of interest. Phase transfer entropy (PTE) quantifies the transfer entropy between phase time-series, such as EEG and MEG data (Lobier et al., 2014). Specifically, our analysis focused on the alpha band (8 – 13 Hz), with results normalized in Brainstorm to yield dPTE measures (Hillebrand et al., 2016). In our dPTE analysis (Figure 4.8) we observed distinct changes in the direction of communication between brain regions during different temporal phases of bistable perception. Prior to the report of dominant percepts, we observed an increase in coupling between parietal to occipital regions, suggesting top-down modulation of visual processing. However, after the button press, indicating the onset of a new dominant percept, the direction of communication increased from the early visual cortex to mid- and parietal regions, indicating a shift towards bottom-up processing. By integrating these findings with existing models of binocular rivalry, we offer a more comprehensive understanding of the dynamic interplay between bottom-up sensory input, top-down attentional modulation, and the directionality of neural communication in shaping perceptual dynamics during BR.

The experiment we present provides valuable insights into the neural mechanisms underlying binocular rivalry and the role of alpha oscillations in shaping perceptual dynamics. By leveraging advanced neuroimaging MEG techniques, we uncovered the dynamic interplay between bottom-up sensory input, top-down attentional modulation, and the directionality of neural communication during BR. Our findings support existing models of BR while also offering new perspectives on the contribution of alpha oscillations to perceptual alternations.

4.7 References

Alais, D., & Melcher, D. (2007). Strength and coherence of binocular rivalry depends on shared stimulus complexity. *Vision research*, 47(2), 269-279.

Blake, R. (1989). A neural theory of binocular rivalry. *Psychological review*, 96(1), 145.

Blake, R., & Logothetis, N. K. (2002). Visual competition. *Nature Reviews Neuroscience*, 3(1), 13-21.

Bock, E. A., Fesi, J. D., Baillet, S., & Mendola, J. D. (2019). Tagged MEG measures binocular rivalry in a cortical network that predicts alternation rate. *Plos one*, 14(7), e0218529.

Bock, E. A., Fesi, J. D., Da Silva Castenheira, J., Baillet, S., & Mendola, J. D. (2023). Distinct dorsal and ventral streams for binocular rivalry dominance and suppression revealed by magnetoencephalography. *European Journal of Neuroscience*, 57(8), 1317-1334.

Brainard, D. H. (1997) The Psychophysics Toolbox. *Spatial Vision,* 10(4), 433–436.

Brown, R. J., & Norcia, A. M. (1997). A method for investigating binocular rivalry in real-time with the steady-state VEP. *Vision research*, *37*(17), 2401-2408.

Brunel, N., & Wang, X. J. (2003). What determines the frequency of fast network oscillations with irregular neural discharges? I. Synaptic dynamics and excitation-inhibition balance. *Journal of neurophysiology*, 90(1), 415-430.

Buckthought, A., Kirsch, L. E., Fesi, J. D., & Mendola, J. D. (2021). Interocular grouping in perceptual rivalry localized with fMRI. *Brain Topography*. 34(3), 323–336.

Cao, R., Pastukhov, A., Aleshin, S., Mattia, M., & Braun, J. (2021). Binocular rivalry reveals an out-of-equilibrium neural dynamics suited for decision-making. *elife*, 10, e61581.

Carmel, D., Walsh, V., Lavie, N., & Rees, G. (2010). Right parietal TMS shortens dominance durations in binocular rivalry. *Current biology*, *20*(18), R799-R800.

Chapman, R. M., Ilmoniemi, R. J., Barbanera, S., & Romani, G. L. (1984). Selective localization of alpha brain activity with neuromagnetic measurements. *Electroencephalography and clinical neurophysiology*, 58(6), 569-572.

Ciulla, C., Takeda, T., & Endo, H. (1999). MEG characterization of spontaneous alpha rhythm in the human brain. *Brain topography*, 11, 211-222.

Chong, S. C., & Blake, R. (2006). Exogenous attention and endogenous attention influence initial dominance in binocular rivalry. *Vision research*, *46*(11), 1794-1803.

Clayton, M. S., Yeung, N., & Kadosh, R. C. (2015). The roles of cortical oscillations in sustained attention. *Trends in cognitive sciences*, 19(4), 188-195.

Clayton, M. S., Yeung, N., & Cohen Kadosh, R. (2018). The many characters of visual alpha oscillations. *European Journal of Neuroscience*, 48(7), 2498-2508.

Cosmelli, D., David, O., Lachaux, J. P., Martinerie, J., Garnero, L., Renault, B., & Varela, F. (2004). Waves of consciousness: ongoing cortical patterns during binocular rivalry. *Neuroimage*, 23(1), 128-140.

Cuello, M. T., Drew, A., San José, A. S., Fernández, L. M., & Soto-Faraco, S. (2022). Alpha fluctuations regulate the accrual of visual information to awareness. *Cortex*, 147, 58-71.

Dieter, K. C., Melnick, M. D., & Tadin, D. (2015). When can attention influence binocular rivalry?. *Attention, Perception, & Psychophysics*, *77*, 1908-1918.

Doesburg, S. M., Green, J. J., McDonald, J. J., & Ward, L. M. (2009). Rhythms of consciousness: binocular rivalry reveals large-scale oscillatory network dynamics mediating visual perception. *PloS one*, *4*(7), e6142.

Donoghue, T., Haller, M., Peterson, E. J., Varma, P., Sebastian, P., Gao, R., Noto, T., Lara, A. H., Wallis, J. D., Knight, R. T., Shestyuk, A., & Voytek, B. (2020). Parameterizing neural power spectra into periodic and aperiodic components. *Nature neuroscience*, 23(12), 1655-1665.

Dijkstra, N., van de Nieuwenhuijzen, M. E., & van Gerven, M. A. (2016). The spatiotemporal dynamics of binocular rivalry: evidence for increased top-down flow prior to a perceptual switch. *Neuroscience of consciousness*, *2016*(1), niw003.

Drew, A., Torralba, M., Ruzzoli, M., Morís Fernández, L., Sabaté, A., Pápai, M. S., & Soto-Faraco, S. (2022). Conflict monitoring and attentional adjustment during binocular rivalry. *European Journal of Neuroscience*, *55*(1), 138-153.

Freeman, A. W. (2005). Multistage model for binocular rivalry. *Journal of neurophysiology*, *94*(6), 4412-4420.

Gao, R., Peterson, E. J., & Voytek, B. (2017). Inferring synaptic excitation/inhibition balance from field potentials. *Neuroimage*, *158*, 70-78.

Gaser, C., Dahnke, R., Thompson, P. M., Kurth, F., Luders, E., & Alzheimer's Disease Neuroimaging Initiative. (2022). CAT–A computational anatomy toolbox for the analysis of structural MRI data. *biorxiv*, 2022-06.

Glasser, M. F., Coalson, T. S., Robinson, E. C., Hacker, C. D., Harwell, J., Yacoub, E., Ugurbil, K., Andersson, J., Beckmann, C. F., Jenkinson, M., Smith, S. M., & Van Essen, D. C. (2016). A multi-modal parcellation of human cerebral cortex. *Nature*, 536(7615), 171-178.

Hillebrand, A., Tewarie, P., Van Dellen, E., Yu, M., Carbo, E. W., Douw, L., Gouw, A. A., van Straaten, E. C. W., & Stam, C. J. (2016). Direction of information flow in large-scale resting-state networks is frequency-dependent. *Proceedings of the National Academy of Sciences*, 113(14), 3867-3872.

Jamison, K. W., Roy, A. V., He, S., Engel, S. A., & He, B. (2015). SSVEP signatures of binocular rivalry during simultaneous EEG and fMRI. *Journal of Neuroscience Methods*, 243, 53-62.

Jensen, O., & Mazaheri, A. (2010). Shaping functional architecture by oscillatory alpha activity: gating by inhibition. *Frontiers in human neuroscience*, 4, 186.

Jensen, O., Bonnefond, M., Marshall, T. R., & Tiesinga, P. (2015). Oscillatory mechanisms of feedforward and feedback visual processing. *Trends in neurosciences*, 38(4), 192-194.

Kamphuisen, A., Bauer, M., & van Ee, R. (2008). No evidence for widespread synchronized networks in binocular rivalry: MEG frequency tagging entrains primarily early visual cortex. *Journal of Vision*, 8(5), 4-4.

Katyal, S., Engel, S. A., He, B., & He, S. (2016). Neurons that detect interocular conflict during binocular rivalry revealed with EEG. *Journal of Vision*, 16(3), 18-18.

Katyal, S., He, S., He, B., & Engel, S. A. (2019). Frequency of alpha oscillation predicts individual differences in perceptual stability during binocular rivalry. *Human brain mapping,* 40(8), 2422-2433.

Kleiner, M., Brainard, D., & Pelli, D. (2007). What's new in Psychtoolbox-3? *Perception,* 36(14), 1–16.

Klimesch, W. (2012). Alpha-band oscillations, attention, and controlled access to stored information. *Trends in cognitive sciences*, 16(12), 606-617.

Klimesch, W., Sauseng, P., & Hanslmayr, S. (2007). EEG alpha oscillations: the inhibition–timing hypothesis. *Brain research reviews*, 53(1), 63-88.

Kovács, I., Papathomas, T. V., Yang, M., & Fehér, Á. (1996). When the brain changes its mind: Interocular grouping during binocular rivalry. *Proceedings of the National Academy of Sciences*, 93(26), 15508-15511.

Lehky, S. R. (1988). An astable multivibrator model of binocular rivalry. *Perception*, 17(2), 215-228.

Li, H. H., Rankin, J., Rinzel, J., Carrasco, M., & Heeger, D. J. (2017). Attention model of binocular rivalry. *Proceedings of the National Academy of Sciences*, *114*(30), E6192-E6201.

Lobier, M., Siebenhühner, F., Palva, S., & Palva, J. M. (2014). Phase transfer entropy: a novel phase-based measure for directed connectivity in networks coupled by oscillatory interactions. *Neuroimage*, 85, 853-872.

Logothetis, N. K., Leopold, D. A., & Sheinberg, D. L. (1996). What is rivalling during binocular rivalry?. *Nature*, 380(6575), 621-624.

Mathewson, K. E., Lleras, A., Beck, D. M., Fabiani, M., Ro, T., & Gratton, G. (2011). Pulsed out of awareness: EEG alpha oscillations represent a pulsed-inhibition of ongoing cortical processing. *Frontiers in psychology*, 2, 10619.

Matsuoka, K. (1984). The dynamic model of binocular rivalry. *Biological cybernetics*, 49(3), 201-208.

Mokri, E., da Silva Castanheira, J., Laldin, S., Landry, M., & Mendola, J. D. (2023). Effects of interocular grouping demands on binocular rivalry. *Journal of Vision*, 23(10), 15-15.

Muthukumaraswamy, S. D., Edden, R. A., Jones, D. K., Swettenham, J. B., & Singh, K. D. (2009). Resting GABA concentration predicts peak gamma frequency and fMRI amplitude in response to visual stimulation in humans. *Proceedings of the National Academy of Sciences,* 106(20), 8356-8361.

Osipova, D., Hermes, D., & Jensen, O. (2008). Gamma power is phase-locked to posterior alpha activity. *PloS one*, 3(12), e3990.

Piantoni, G., Romeijn, N., Gomez-Herrero, G., Van Der Werf, Y. D., & Van Someren, E. J. (2017). Alpha power predicts persistence of bistable perception. *Scientific reports*, 7(1), 5208.

Pitts, M. A., & Britz, J. (2011). Insights from intermittent binocular rivalry and EEG. *Frontiers in human neuroscience*, 5, 107.

Pitts, M. A., Martínez, A., & Hillyard, S. A. (2010). When and where is binocular rivalry resolved in the visual cortex?. *Journal of vision*, 10(14), 25-25.

Riesen, G., Norcia, A. M., & Gardner, J. L. (2019). Humans perceive binocular rivalry and fusion in a tristable dynamic state. *Journal of Neuroscience*, 39(43), 8527-8537.

Robertson, C. E., Kravitz, D. J., Freyberg, J., Baron-Cohen, S., & Baker, C. I. (2013). Slower rate of binocular rivalry in autism. *Journal of Neuroscience*, 33(43), 16983-16991.

Roy, A. V., Jamison, K. W., He, S., Engel, S. A., & He, B. (2017). Deactivation in the posterior mid-cingulate cortex reflects perceptual transitions during binocular rivalry: Evidence from simultaneous EEG-fMRI. *NeuroImage*, 152, 1-11.

Said, C. P., & Heeger, D. J. (2013). A model of binocular rivalry and cross-orientation suppression. *PLoS computational biology*, 9(3), e1002991.

Skerswetat, J., Bex, P. J., & Baron-Cohen, S. (2022). Visual consciousness dynamics in adults with and without autism. *Scientific reports*, 12(1), 4376.

Spiegel, A., Mentch, J., Haskins, A. J., & Robertson, C. E. (2019). Slower binocular rivalry in the autistic brain. *Current Biology*, 29(17), 2948-2953.

Sponheim, S. R., Stim, J. J., Engel, S. A., & Pokorny, V. J. (2023). Slowed alpha oscillations and percept formation in psychotic psychopathology. *Frontiers in Psychology*, 14, 1144107.

Tadel, F., Baillet, S., Mosher, J. C., Pantazis, D., & Leahy, R. M. (2011). Brainstorm: a user-friendly application for MEG/EEG analysis. *Computational intelligence and neuroscience*, 2011, 1-13.

Thaler, L., Schütz, A. C., Goodale, M. A., & Gegenfurtner, K. R. (2013). What is the best fixation target? The effect of target shape on stability of fixational eye movements. *Vision research*, 76, 31-42.

Tong, F. (2001). Competing theories of binocular rivalry: A possible resolution. *Brain and Mind*, *2*, 55-83.

Tong, F., Meng, M., & Blake, R. (2006). Neural bases of binocular rivalry. *Trends in cognitive sciences*, 10(11), 502-511.

Van Kerkoerle, T., Self, M. W., Dagnino, B., Gariel-Mathis, M. A., Poort, J., Van Der Togt, C., & Roelfsema, P. R. (2014). Alpha and gamma oscillations characterize feedback and feedforward processing in monkey visual cortex. *Proceedings of the National Academy of Sciences*, 111(40), 14332-14341.

van Pelt, S., Boomsma, D. I., & Fries, P. (2012). Magnetoencephalography in twins reveals a strong genetic determination of the peak frequency of visually induced gamma-band synchronization. *Journal of Neuroscience*, 32(10), 3388-3392.

Voytek, B., Canolty, R. T., Shestyuk, A., Crone, N. E., Parvizi, J., & Knight, R. T. (2010). Shifts in gamma phase–amplitude coupling frequency from theta to alpha over posterior cortex during visual tasks. *Frontiers in human neuroscience*, 4, 191.

Qiu, S. X., Caldwell, C. L., You, J. Y., & Mendola, J. D. (2020). Binocular rivalry from luminance and contrast. *Vision Research*, 175, 41-50.

Wilson, H. R. (2003). Computational evidence for a rivalry hierarchy in vision. *Proceedings of the National Academy of Sciences*, 100(24), 14499-14503.

Wilson, L. E., da Silva Castanheira, J., & Baillet, S. (2022). Time-resolved parameterization of aperiodic and periodic brain activity. *Elife*, *11*, e77348.

Zaretskaya, N., Thielscher, A., Logothetis, N. K., & Bartels, A. (2010). Disrupting parietal function prolongs dominance durations in binocular rivalry. *Current Biology*, 20(23), 2106–2111.

Zhang, P., Jamison, K., Engel, S., He, B., & He, S. (2011). Binocular rivalry requires visual attention. *Neuron*, *71*(2), 362-369.

5

General Discussion

5.1 Binocular Rivalry and Increasing Interocular Grouping Demands

Binocular rivalry (BR), a classic bistable perception phenomenon, involves the presentation of different images to each eye, leading to perceptual alternations between right and left eye image representation (Blake & Logothetis, 2002). Moreover, interocular grouping (IOG) is a notable extension of bistable perception, where complementary bistable patches of a divided image are presented to each eye, resulting in similar perceptual alternations (Kovacs et al., 1996). IOG builds upon binocular rivalry by subdividing the rivalrous images presented independently to each eye into complementary bistable patches. Remarkably, observers undergo periods of alternation between global dominant and suppressed percepts during IOG presentation, requiring the combination of perceptual processing from both right and left eye image representation. Within the context of bistable perception, IOG heavily emphasizes the role of binocular neurons that integrate information from both eyes. This phenomenon has been extensively studied (Knapen et al., 2007; Sutoyo & Srinivasan, 2009; Golubitsky et al., 2019; Buckthought et al., 2021). In this thesis, I introduce a novel experimental design that utilizes binocular rivalry and interocular grouping stimuli with increasing grouping demands to elicit perceptually matched dominant stimuli, specifically red or green dominant orthogonal gratings. This design enables a detailed analysis of the relationship between binocular rivalry and interocular grouping, as well as an exploration of the effects of increasing the number of image divisions and altering the orientation of the central image meridian division within interocular grouping.

Binocular Rivalry and Interocular Grouping

A well-matched comparison between binocular rivalry and interocular grouping was conducted in the experiments of Chapter Two: *Effects of Interocular Grouping Demands on Binocular Rivalry*, and Chapter Three: *Neural Markers of Interocular Grouping During Binocular Rivalry with MEG*. At the behavioral level, it was observed that IOG disproportionately affects mixed percepts. Participants experienced increased predominance, longer durations, and a higher frequency of mixed percepts during perceptual transitions. This contrasts with perceptual

dominance, where both BR and IOG elicit stable periods of dominance and suppression. It is important to note a limitation, as defined in the experimental guidelines provided to participants: mixed percepts during IOG were characterized as both monocularly viewed images and more traditional (binocular) piecemeal percepts, whereas during BR, only piecemeal percepts arising from perceptual ambiguity from the combination of images presented to each eye were defined as mixed percepts.

The MEG results from the frequency-tagged experiments of BR and IOG presented in Chapter Three revealed the neural correlates of these bistable perceptual illusions. Consistent with the behavioral experience of rivalry, the neural correlates in the steady-state visual evoked field (SSVEF) responses to dominant and suppressed percepts exhibited waxing and waning with MEG. This phenomenon, previously reported during BR (Brown & Norcia, 1997; Zhang et al., 2011; Jamison et al., 2015; Spiegel et al., 2019; Bock et al., 2019), is novel for IOG. A reduced depth of rivalry was observed between BR and IOG, mainly characterized by a reduced SSVEF response magnitude and a smaller topographic spread, primarily restricted to early visual areas during dominance for IOG. One possible explanation is related to the nature of the stimuli and the mechanisms involved in their processing. BR typically involves the dichoptic presentation of conflicting images to each eye, leading to competition between monocular neurons in early visual areas. On the other hand, the IOG stimuli encourage binocular integration and perceptual grouping across the two eyes, leading to the perception of a single coherent dominant percept. The idea that only neurons with at least partial binocular integration could be the source of SSVEF responses to the frequency-tags in IOG suggests that the neural mechanisms underlying IOG may involve a different balance of binocular integration compared to BR. In other words, the neural populations responsible for processing IOG stimuli may exhibit a higher degree of binocular integration or coherence, leading to reduced competition and shallower rivalry dynamics compared to BR. Between BR and higher-order grouping IOG4, our multivariate logistic regression models delineated distinct differences in lateral occipital (LO) and intraparietal (IP) regions for the dominant SSVEF response around 500 – 1000ms post-dominance emergence. These analyses uncovered intricate variations in patterns and interactions indicative of multivariate processing across different brain regions (Westlin et al., 2023), underlining the complex interactions governing bistable perception within the visual system.

However, despite the differences in rivalry depth for dominance, the similarity in SSVEF response magnitude and topography during suppression between BR and IOG suggests that there may be commonalities in the neural mechanisms underlying the maintenance of suppressed percepts across these two phenomena. This similarity could indicate that, despite differences in the initial processing of stimuli, similar mechanisms in the visual system may come into play to maintain the suppressed percept during both BR and IOG.

Vertical versus Horizontal Image Meridian Division

Within the visual system, the mechanisms of perceptual grouping across the central image meridians (i.e., vertical versus horizontal) during interocular grouping (IOG) are not well understood. This is partly because the functional anatomy of the representation of the vertical vs. horizontal meridian is quite different. In early visual areas, receptive fields than could span the vertical meridian would typically require interhemispheric communication via the corpus callosum. Integration across the horizontal meridian would require much shorter within hemisphere connections. Also, previous studies on IOG often utilize only one form of stimulus or the other. In the broader context of spatial integration in visual processing, previous neuroimaging research has suggested that the lateral occipital (LO) region is important for integrating visual hemifields processed at different stages (Tootell et al., 1998; Larsson & Heeger, 2006; Large et al., 2008). With this in mind, I presented an experimental design that directly compares the behavioral and neural correlates of grouping with stimuli divided either across the vertical or horizontal image meridian.

In the psychophysics experiments of Chapter Two, a perhaps surprising preference for perceptual grouping across the vertical image meridian during IOG (N = 48) was observed in both two-patch (i.e., longer mean duration of dominant percepts during IOG2V) and six-patch (i.e., shorter mean duration of mixed percepts during IOG6V) grouping conditions. This result aligns with previous studies that explored two-patch IOG between vertical and horizontal image meridian divisions (Golubitsky et al., 2019), although those studies had a smaller sample size (N = 3). However, on subsequent days of rivalry testing during the frequency-tagged MEG experiment, the behavioral measures (i.e., alternation rate, dominant and mixed percept durations, and percept

predominance) did not show significant differences between two-patch vertical and horizontal image meridian divisions (N = 25).

Furthermore, MEG results revealed considerable similarity in the neural correlates of bistable perception between IOG2V and IOG2H during repeat testing on the third day of rivalry experiments. Due to MEG compatibility, only a subset of the larger initial participant pool was tested. A potential limitation of this study is the smaller number of participants and the possible learning effects that may have emerged over the course of the three rivalry testing sessions. Additionally, the MEG analysis of SSVEF responses time-locked to the report of perceptual alternations may not be well-suited to disentangle subtle differences in grouping mechanisms that may occur at multiple stages within finer regions in the lateral occipital region (Large et al., 2008). A larger participant pool may be needed to detect the smaller effect sizes observed between the grouping conditions, in addition to finer scaled mapping of the ROIs in the lateral occipital region.

Increasing Complementary Bistable Patches

In the same vein as grouping across the vertical and horizontal image meridian, IOG has rarely been studied with a parametric design that aims to increase demands continuously. This has led to a gap in knowledge about the mechanisms of grouping between images that vary in the number of complementary bistable patches. To address this, the second and third chapters present IOG stimuli that are perceptually matched and vary in the number of image divisions.

In the second chapter, interesting effects were observed when the number of complementary bistable patches increased during interocular grouping (i.e., from IOG2 to IOG4 and IOG6). Remarkably, the mean duration of dominant percepts and their predominance demonstrated stability despite increasing interocular grouping demands. In contrast, mixed percepts were disproportionately affected, showing increased duration and predominance in higher-order grouping conditions. These results suggest that IOG conditions with increased grouping demands elicit increased perceptual ambiguity; however, once resolved, dominant percepts remain stable in perception and would appear to be supported by the same neural mechanism for perceptual dominance during BR.

During MEG testing in the third chapter, although striking similarity in neural correlates BR and IOG were observed, the SSVEF response was reduced during higher-order grouping

demands (i.e., IOG4) compared to two-patch interocular grouping (i.e., IOG2V and IOG2H). This reduction was predominantly driven by a weaker magnitude of the SSVEF response for dominant percepts, while the suppression response remained consistent in magnitude and topography. I interpret this result to indicate different neural mechanisms of dominance and suppression governing bistable perception. Specifically for dominance, the increase SSVEF response during BR can be attributed to stronger neural entrainment of monocular neurons, primarily found in V1 that represent sensory processing from right and left eye images. Whereas during IOG conditions, each eye was shown both fundamental frequency tags (i.e., 5 Hz for red orthogonal gratings, and 6.67 Hz for green orthogonal gratings). The experience of perceptual dominance during IOG required sensory processing (i.e., binocular neurons) beyond monocularly driven neurons from portions of images shown across both eyes.

5.2 Individual Differences

The alternation rate between dominant percepts during binocular rivalry differs between observers (Brascamp et al., 2015), and the distribution of dominant durations is best modelled by a gamma shaped distribution (Levelt, 1956; Fox & Herrmann, 1967). Additionally, twin studies have demonstrated that this trait-like binocular rivalry alternation rate is partially heritable (Miller et al., 2010; Shannon et al., 2011). Numerous studies have investigated individual differences and their association with alternation rates during binocular rivalry. For instance, Fesi and Mendola (2015) found an inverse relationship between peak gamma frequency in the primary visual cortex and alternation rate. In addition, Katyal et al. (2019), Cuello et al. (2022), and Sponheim et al. (2023) reported that peak alpha frequency was positively correlated with alternation rate. Moreover, research on binocular rivalry in individuals with autism spectrum disorder has revealed altered dynamics and slowed alternation rates (Robertson et al., 2013; Spiegel et al., 2019; Skerswetat et al., 2022). An imbalance in the excitation and inhibition ratio, thought to characterize autism, may contribute to these differences.

Considering these trait-like effects, I hypothesized similarities in behavioral measures (i.e., alternation rate and dominant percept duration) between binocular rivalry and interocular grouping, suggesting a shared neural mechanism in the visual system for these two forms of bistable perception. In the second chapter, a significant positive correlation was indeed found between BR and IOG for alternation rate, as well as for the duration of dominant and mixed percepts. This indicates that individuals categorized as 'fast-switchers' during BR also experienced dominant percepts during IOG at an increased alternation rate compared to 'slow-switchers'. Furthermore, mechanisms of perceptual stability (i.e., duration of dominant percepts) and perceptual ambiguity (i.e., duration of mixed percepts) were correlated between conditions. This finding was replicated in the third chapter, albeit with an overlapping participant pool.

Also, in the domain of individual differences, the fourth chapter presented significant positive correlation between participants MEG baseline normalized alpha band power prior to mixed percepts and their subsequent duration. This aligns with the role of alpha oscillations and inhibition (Klimesch et al., 2007; Jensen & Mazaheri, 2010; Klimesch et al., 2012; Jensen et al., 2015; Clayton et al., 2018), where mixed percepts reflect periods of perceptual ambiguity, where

neither monocular viewed image dominantly perceived. This result demonstrates that individuals with stronger alpha power (i.e., a proxy for increased inhibition) in the primary visual cortex prior to mixed reports experienced longer durations of mixed percepts. However, it remains unclear the degree to which such individuals with stronger alpha prior to mixed percepts are reliably slow switchers. Future research can aim to further characterize individual differences in alpha oscillations during BR and should aim to incorporate these findings within the broader scope of oscillatory brain mechanisms (i.e., gamma band activity, coupling between frequency bands) that may interact in shaping perception

Overall, drawing from literature emphasizing individual differences and trait-like characteristics of binocular rivalry, I present novel correlational evidence linking BR and interocular grouping in terms of alternation rates and percept durations, consistent across subsequent testing days. These findings collectively suggest that the neural mechanisms underlying bistable perception in both BR and IOG share commonalities. This supports the hypothesis of a shared neural mechanism, potentially involving similar oscillatory dynamics, governing both binocular rivalry and interocular grouping. Furthermore, these results bolster the idea of a unified neural framework underlying both forms of bistable visual perception.

Future research should continue to explore these dynamics to further elucidate the shared neural mechanisms of bistable perception. Investigating how individual differences in neural oscillations and connectivity patterns contribute to variability in perceptual experiences will be important to advancing our understanding of these complex visual processes.

5.3 Models of Binocular Rivalry

In the first chapter, various accounts of binocular rivalry (BR) models from the literature have been discussed. Early models focused on the competition between eyes (Blake, 1989), while subsequent studies and papers emphasized the role of binocular neurons, which integrate sensory input from both eyes (Logothetis et al., 1996; Wilson, 2003; Said & Heeger, 2013). Within this framework, interocular grouping emerged as a notable example of bistable perception, highlighting the significance of binocular combinatorial processing (Kovacs et al., 1996).

Drawing upon the current literature on binocular rivalry and the experimental findings presented in chapters two, three, and four, I propose the following conceptual model of binocular rivalry (see Figure 5.1).

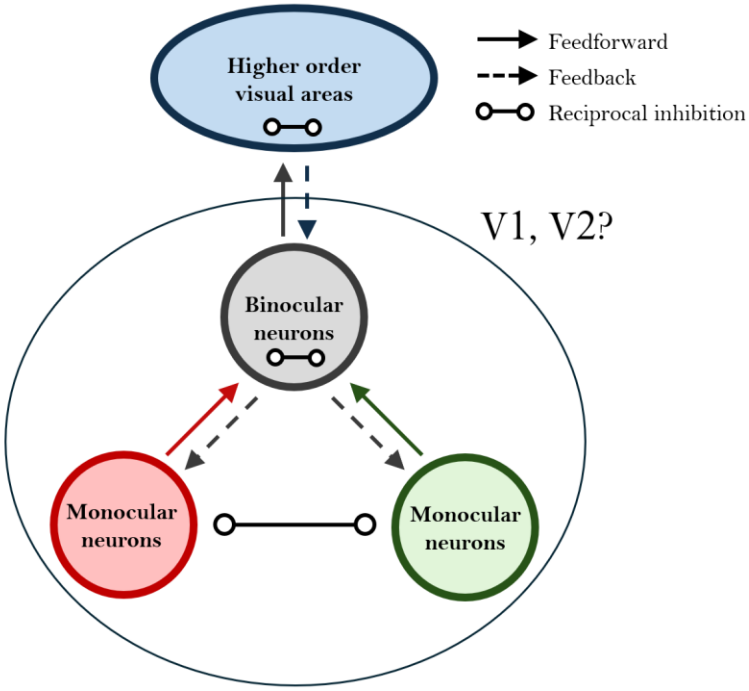

Figure 5.1 Proposed neural model of binocular rivalry and interocular grouping. The model illustrates the interaction between monocular neurons in low-level visual areas and binocular neurons that integrate and modulate sensory processing during bistable perception. It highlights how perception is dynamically resolved through the balance of excitation and inhibition signaling, facilitated by feedforward and feedback connectivity with higher-order visual areas.

The proposed neural model of binocular rivalry underscores the interplay between low-level and higher-order visual areas (i.e., extrastriate regions in the lateral occipital and intraparietal cortex) through both feedforward and feedback mechanisms of communication. Starting in the primary visual cortex (V1), reciprocal inhibition among monocular neurons (i.e., neurons receiving input from only one eye) is hypothesized, drawing on prior research (Matsuoka, 1984; Lehky, 1988; Blake, 1989). Notably, the primary visual cortex, particularly in layer 4, houses the majority of monocular neurons (Hubel & Wiesel, 1968; Blasdel & Fitzpatrick, 1984; Dougherty et al., 2019). These monocular neurons project feedforward connections to binocular neurons, where their responses are integrated and modulated. Binocular neurons (i.e., neurons receiving input from both eyes), present in both the primary visual cortex and extrastriate cortex (Parker et al., 2007), further modulate incoming information. Feedback mechanisms between binocular and monocular neurons are incorporated, aligning with previous observations of binocular modulation of monocular neurons that either increased (i.e., binocularly facilitated neurons) or decreased (i.e., binocularly suppressed neurons) their firing rates during binocular stimulation (Dougherty et al., 2019). In fact, multiple levels of (nested) reciprocal inhibition have already been proposed to explain rivalry with additional computational complexity (e.g. binocular opponent neurons) (Said & Heeger, 2013). However, our current results do not allow us to distinguish between such models.

At higher levels of visual processing, I propose that regions in the extrastriate (i.e., visual areas V3 and V4), occipital (i.e., lateral occipital), and parietal cortex (i.e., intraparietal sulcus, parieto-occipital sulcus) receive information from binocular neurons in lower-levels of visual processing (i.e., V1 and V2) and provide feedback connectivity, thereby modulating the balance between excitation and inhibition signaling. Consistent with prior research, regions within the parietal cortex are suggested to be causally related to perceptual alternations as demonstrated by intermittent binocular rivalry (BR) presentations with EEG (Pitts & Britz, 2011) and transcranial magnetic stimulation (TMS) (Carmel et al., 2010; Zaretskaya et al., 2010). Furthermore, incorporating findings from interocular grouping, fMRI results indicate increased activity in the lateral occipital (LO) and intraparietal (IP) regions during bistable perception.

In the proposed neural model, there exists an orchestrated and dynamic interaction among multiple stages of the visual pathway, as well as between dominance and suppressed perceptual states. Through the alpha band connectivity analysis in the fourth chapter, an example for both

feedback and feedforward directed coupling were observed between visual regions. Prior to alternations in dominant percepts, increased feedback connectivity in the alpha band was noted from parietal regions to early visual and extrastriate cortex, mid-level visual areas, as well as the lateral occipital. Conversely, after the alternation in dominant percept, feedforward coupling was observed from the early visual cortex to mid-level and higher order regions in the parietal cortex. Given the hypothesis of a similar neural mechanism between binocular rivalry and interocular grouping, it is suggested that similar oscillatory dynamics in the alpha band may be present during interocular grouping.

5.4 Neural Mechanisms of Perception

Understanding the neural mechanisms of bistable perception is crucial for unraveling how the brain resolves conflicting sensory information to produce a coherent perceptual experience. Bistable perception, such as binocular rivalry and interocular grouping, offers a unique window into the dynamics of perceptual decision-making and consciousness perception. Despite its importance, the neural underpinnings of bistable perception remain elusive due to the complexity of the involved processes and the interplay between various brain regions and neural circuits. Investigating the neural mechanisms of binocular rivalry provides insight into fundamental processes in the visual system, while understanding interocular grouping emphasizes higher-order perceptual processes. Together, these lines of research shed light on how the brain integrates and prioritizes sensory inputs, advancing our comprehension of visual processing and perception.

While the combination of frequency-tagging and EEG/MEG neuroimaging methods serves as a potent neuroimaging tool, its reported primary entrainment of the early visual cortex (Kamphuisen et al., 2008) and emphasis on feedforward connectivity during binocular rivalry (Bock et al., 2023) contrast with other studies extending neural correlates of bistable perception beyond early visual areas. For instance, Leopold and Logothetis (1996) recorded single-cell activity in monkeys during binocular rivalry and found the best neural correlates to be beyond V1 in the extrastriate cortex, particularly in V4. Lumer et al. (1998) identified activity in frontoparietal regions, while Sheinberg and Logothetis (1997) reported involvement of the temporal cortex. Moreover, Cosmelli et al. (2004) observed MEG activity across the extrastriate, parietal, temporal, and frontal cortex during binocular rivalry. In contrast, Frässle et al. (2014), using fMRI methods, reported frontal activity only when participants were prompted to report their percepts during binocular rivalry, which was absent during passive viewing.

These studies collectively highlight the complexity and widespread nature of neural mechanisms underlying binocular rivalry, suggesting that while frequency-tagging is effective, it might primarily capture early-stage visual processing and feedforward connectivity. This is a notable limitation given the substantial evidence pointing to the involvement of higher-order visual areas and feedback mechanisms in perceptual alternations.

In the third chapter, leveraging frequency-tagged MEG methods, SSVEF results for both dominant and suppressed percepts focused on posterior cortex regions (i.e., occipital and parietal brain regions). This observation stemmed from the MEG data indicating that the strongest change in baseline-normalized power, time-locked to behavioural reports of alternation, was predominantly present in these regions during both binocular rivalry and interocular grouping. This finding aligns with the idea that both early and mid-level visual areas play a significant role in processing visual stimuli during perceptual alternations.

To address the potential limitations of frequency-tagging, the results of an untagged binocular rivalry experiment with MEG are presented in the fourth chapter. In this experiment, the baseline-normalized alpha power time-locked to the behavioral reports of alternations was observed in its earliest markers in the extrastriate cortex and mid-level visual areas. Both the tagged and untagged MEG experiments were designed with an awareness of the presence of fundamental power in the observed frequency range being widespread and naturally occurring throughout the brain. However, the focus was on identifying regions exhibiting the greatest changes in power time-locked to perceptual switches.

This approach, while effective in capturing key regions involved in perceptual switches, could be seen as a potential limitation. It highlights the need for future experiments to explore oscillatory brain dynamics occurring at different temporal scales, spatial locations, and interactions between different frequency ranges. For example, theta-gamma frequency band coupling, as reported by Doesburg et al. (2009) during binocular rivalry, could provide further insights into the intricate neural mechanisms at play. Investigating these dynamics further may provide deeper insights into the neural mechanisms underlying perceptual alternations and bistable perception.

Future research could also benefit from combining EEG and MEG frequency-tagging, and untagged natural viewing conditions with other neuroimaging techniques, such as fMRI, to capture the full spectrum of neural activities involved in binocular rivalry and interocular grouping. Additionally, exploring how the role of different frequency bands and their interactions across various brain regions differs between individuals should uncover new aspects of how the brain processes and resolves perceptual ambiguity. By addressing these gaps, we can advance our understanding of the neural correlates of bistable perception and the broader principles of visual processing.

Conclusion & Summary

In this thesis, I began by presenting a comprehensive literature review and introduction to binocular rivalry and interocular grouping, both of which are forms of bistable perception. These visual illusions were studied together to uncover neural correlates of visual perception. Following this, I detailed three chapters that presented distinct and independent experiments incorporating psychophysics and neuroimaging methods during bistable perception. I concluded with a general discussion that incorporated findings from all three studies and outlined their significance to the existing literature.

In the second chapter, I presented a visual psychophysics experiment published in the Journal of Vision, which characterized behavioral measures of binocular rivalry under increasing interocular grouping demands. Using a perceptually matched stimulus that increased the number of divisions during interocular grouping, I found robust stability in dominant percept grouping mechanisms, while mixed percepts increased in duration and predominance with higher-order grouping demands. The predominance of mixed percepts was also highlighted by their increase in transition probabilities when alternating between percepts during interocular grouping. Remarkably, behavioral measures of rivalry were significantly correlated across conditions, indicating trait-like characteristics and similar neural mechanisms underlying both binocular rivalry and interocular grouping.

The third chapter leveraged cutting-edge frequency-tagging methods combined with magnetoencephalography (MEG) to record steady-state visually evoked field (SSVEF) during binocular rivalry and interocular grouping. The results suggest similar neural mechanisms in the topography of SSVEF time-locked responses across the cortex to perceptual alternations across conditions. However, a reduced depth of rivalry was observed with increasing interocular grouping demands. Specifically, neural correlates of perceptual dominance were reduced in magnitude, confined to a smaller topography in the occipital and parietal cortex, and occurred earlier relative to a perceptual switch during grouping conditions. This contrasted with the SSVEF response during suppression, where topography and strength were similar between binocular rivalry and interocular grouping conditions. Machine learning methods provided insight into distinct neural

mechanisms between binocular rivalry and interocular grouping, as well as during dominance and suppression.

In the fourth chapter, I explored oscillatory brain dynamics within the alpha frequency band during untagged binocular rivalry using MEG. Alpha oscillations were studied in the context of inhibition, aligning with a growing body of literature. Prior to the report of dominant percept alternations, a decrease in alpha band power was recorded in the posterior cortex, with early markers stemming from mid-level visual regions. This was compared to a binocular rivalry control condition, where a temporal delay in the decrease of alpha band power was reported. A subsequent increase in alpha band power was observed in parietal and occipital regions after the report of a dominant percept alternation, believed to facilitate the stability of the new percept and inhibition of the suppressed percept. Conversely, an increase in alpha band power was observed prior to mixed percepts, reflecting a state of increased inhibition. Additionally, alpha band power in the primary visual cortex was correlated with the duration of mixed percepts. I concluded this work with a connectivity analysis revealing greater feedback coupling before, and greater feedforward coupling after, the report of dominant percept alternations.

To conclude the thesis, I provided a scholarly discussion of the results from the previous chapters and integrated them with the existing literature on bistable perception. I discussed the limitations and future considerations of the experiments presented, highlighting potential improvements and suggesting new directions for research. Additionally, I proposed a neural model of binocular rivalry that accounts for the findings during interocular grouping. This model suggests an intricate and dynamic interaction between monocular neurons in low-level visual areas, binocular neurons that receive and integrate sensory information from both eyes, and higher-order visual areas that receive information from, and feedback to, early visual areas. This dynamic interplay between different neural circuits offers a deeper understanding of how the brain processes and resolves competing visual inputs during bistable perception, contributing to our knowledge of visual perception mechanisms.

Master References

Adrian, E. D., & Matthews, B. H. (1934). The Berger rhythm: potential changes from the occipital lobes in man. *Brain*, *57*(4), 355-385.

Alais, D., & Melcher, D. (2007). Strength and coherence of binocular rivalry depends on shared stimulus complexity. *Vision Research,* 47(2), 269–279.

Alais, D., O'Shea, R. P., Mesana-Alais, C., & Wilson, I. G. (2000). On binocular alternation. *Perception,* 29(12), 1437–1445.

Baillet, S. (2017). Magnetoencephalography for brain electrophysiology and imaging. *Nature neuroscience*, 20(3), 327-339.

Blasdel, G. G., & Fitzpatrick, D. (1984). Physiological organization of layer 4 in macaque striate cortex. *Journal of Neuroscience*, *4*(3), 880-895.

Blake, R. (1989). A neural theory of binocular rivalry. *Psychological Review,* 96(1), 145.

Blake, R., & Logothetis, N. K. (2002). Visual competition. *Nature Reviews Neuroscience*, 3(1), 13-21.

Bock, E. A., Fesi, J. D., Baillet, S., & Mendola, J. D. (2019). Tagged MEG measures binocular rivalry in a cortical network that predicts alternation rate. *Plos one*, 14(7), e0218529.

Bock, E. A., Fesi, J. D., Da Silva Castenheira, J., Baillet, S., & Mendola, J. D. (2023). Distinct dorsal and ventral streams for binocular rivalry dominance and suppression revealed by magnetoencephalography. *European Journal of Neuroscience*, 57(8), 1317-1334.

Brascamp, J. W., Klink, P. C., & Levelt, W. (2015). The 'laws' of binocular rivalry: 50 years of Levelt's propositions. *Vision research*, *109*, 20-37.

Brown, R. J., & Norcia, A. M. (1997). A method for investigating binocular rivalry in real-time with the steady-state VEP. *Vision research*, *37*(17), 2401-2408.

Buckthought, A., Fesi, J. D., Kirsch, L. E., & Mendola, J. D. (2015). Comparison of stimulus rivalry to binocular rivalry with functional magnetic resonance imaging. *Journal of Vision*, *15*(14), 2-2.

Buckthought, A., Jessula, S., & Mendola, J. D. (2011). Bistable percepts in the brain: fMRI contrasts monocular pattern rivalry and binocular rivalry. *PLoS One*, 6(5), e20367.

Buckthought, A., Kirsch, L. E., Fesi, J. D., & Mendola, J. D. (2021). Interocular grouping in perceptual rivalry localized with fMRI. *Brain Topography*, 34, 323-336.

Carmel, D., Walsh, V., Lavie, N., & Rees, G. (2010). Right parietal TMS shortens dominance durations in binocular rivalry. *Current biology*, *20*(18), R799-R800.

Chapman, R. M., Ilmoniemi, R. J., Barbanera, S., & Romani, G. L. (1984). Selective localization of alpha brain activity with neuromagnetic measurements. *Electroencephalography and clinical neurophysiology*, 58(6), 569-572.

Ciulla, C., Takeda, T., & Endo, H. (1999). MEG characterization of spontaneous alpha rhythm in the human brain. *Brain topography*, 11, 211-222.

Clayton, M. S., Yeung, N., & Cohen Kadosh, R. (2018). The many characters of visual alpha oscillations. *European Journal of Neuroscience*, 48(7), 2498-2508.

Cohen, D. (1968). Magnetoencephalography: evidence of magnetic fields produced by alpha-rhythm currents. *Science*, 161(3843), 784-786.

Cosmelli, D., David, O., Lachaux, J. P., Martinerie, J., Garnero, L., Renault, B., & Varela, F. (2004). Waves of consciousness: ongoing cortical patterns during binocular rivalry. *Neuroimage*, *23*(1), 128-140.

Cuello, M. T., Drew, A., San José, A. S., Fernández, L. M., & Soto-Faraco, S. (2022). Alpha fluctuations regulate the accrual of visual information to awareness. *Cortex*, 147, 58-71.

Diaz-Caneja, E. (1928). Sur l'Alternation binoculaire [On binocular alternation]. *Annalses d'Oculistique,* 165, 721–731.

Doesburg, S. M., Green, J. J., McDonald, J. J., & Ward, L. M. (2009). Rhythms of consciousness: binocular rivalry reveals large-scale oscillatory network dynamics mediating visual perception. *PloS one*, *4*(7), e6142.

Dougherty, K., Cox, M. A., Westerberg, J. A., & Maier, A. (2019). Binocular modulation of monocular V1 neurons. *Current Biology*, *29*(3), 381-391.

Fesi, J. D., & Mendola, J. D. (2015). Individual peak gamma frequency predicts switch rate in perceptual rivalry. *Human Brain Mapping*, *36*(2), 566-576.

Fox, R., & Herrmann, J. (1967). Stochastic properties of binocular rivalry alternations. *Perception & psychophysics*, *2*(9), 432-436.

Frässle, S., Sommer, J., Jansen, A., Naber, M., & Einhäuser, W. (2014). Binocular rivalry: frontal activity relates to introspection and action but not to perception. *Journal of Neuroscience*, *34*(5), 1738-1747.

Freeman, A. W. (2005). Multistage model for binocular rivalry. *Journal of neurophysiology*, *94*(6), 4412-4420.

Golubitsky, M., Zhao, Y., Wang, Y., & Lu, Z. L. (2019). Symmetry of generalized rivalry network models determines patterns of interocular grouping in four-location binocular rivalry. *Journal of neurophysiology*, 122(5), 1989-1999.

Gross, J. (2019). Magnetoencephalography in cognitive neuroscience: a primer. *Neuron*, *104*(2), 189-204.

Hubel, D. H., & Wiesel, T. N. (1968). Receptive fields and functional architecture of monkey striate cortex. *The Journal of physiology*, *195*(1), 215-243.

Jamison, K. W., Roy, A. V., He, S., Engel, S. A., & He, B. (2015). SSVEP signatures of binocular rivalry during simultaneous EEG and fMRI. *Journal of Neuroscience Methods*, *243*, 53-62.

Jensen, O., & Mazaheri, A. (2010). Shaping functional architecture by oscillatory alpha activity: gating by inhibition. *Frontiers in human neuroscience*, 4, 186.

Jensen, O., Bonnefond, M., Marshall, T. R., & Tiesinga, P. (2015). Oscillatory mechanisms of feedforward and feedback visual processing. *Trends in neurosciences*, 38(4), 192-194.

Kamphuisen, A., Bauer, M., & van Ee, R. (2008). No evidence for widespread synchronized networks in binocular rivalry: MEG frequency tagging entrains primarily early visual cortex. *Journal of Vision*, 8(5), 4-4.

Katyal, S., Engel, S. A., He, B., & He, S. (2016). Neurons that detect interocular conflict during binocular rivalry revealed with EEG. *Journal of Vision,* 16(3):18, 1–12.

Katyal, S., He, S., He, B., & Engel, S. A. (2019). Frequency of alpha oscillation predicts individual differences in perceptual stability during binocular rivalry. *Human brain mapping*, 40(8), 2422-2433.

Klimesch, W. (2012). Alpha-band oscillations, attention, and controlled access to stored information. *Trends in cognitive sciences*, 16(12), 606-617.

Klimesch, W., Sauseng, P., & Hanslmayr, S. (2007). EEG alpha oscillations: the inhibition–timing hypothesis. *Brain research reviews*, 53(1), 63-88.

Knapen, T., Paffen, C., Kanai, R., & van Ee, R. (2007). Stimulus flicker alters interocular grouping during binocular rivalry. *Vision Research*, 47(1), 1-7.

Kovacs, I. L. O. N. A., Papathomas, T. V., Yang, M., & Fehér, Á. (1996). When the brain changes its mind: Interocular grouping during binocular rivalry. *Proceedings of the National Academy of Sciences*, 93(26), 15508-15511.

Large, M. E., Culham, J., Kuchinad, A., Aldcroft, A., & Vilis, T. (2008). fMRI reveals greater within-than between-hemifield integration in the human lateral occipital cortex. *European Journal of Neuroscience,* 27(12), 3299–3309.

Larsson, J., & Heeger, D. J. (2006). Two retinotopic visual areas in human lateral occipital cortex. *Journal of Neuroscience,* 26(51), 13128–13142.

Lehky, S. R. (1988). An astable multivibrator model of binocular rivalry. *Perception*, *17*(2), 215-228.

Leopold, D. A., & Logothetis, N. K. (1996). Activity changes in early visual cortex reflect monkeys' percepts during binocular rivalry. *Nature*, *379*(6565), 549-553.

Levelt, W. J. (1965). On binocular rivalry (Doctoral dissertation, Van Gorcum Assen).

Logothetis, N. K., Leopold, D. A., & Sheinberg, D. L. (1996). What is rivalling during binocular rivalry?. *Nature*, *380*(6575), 621-624.

Lumer, E. D., Friston, K. J., & Rees, G. (1998). Neural correlates of perceptual rivalry in the human brain. *Science*, *280*(5371), 1930-1934.

Mathewson, K. E., Lleras, A., Beck, D. M., Fabiani, M., Ro, T., & Gratton, G. (2011). Pulsed out of awareness: EEG alpha oscillations represent a pulsed-inhibition of ongoing cortical processing. *Frontiers in psychology*, 2, 10619.

Matsuoka, K. (1984). The dynamic model of binocular rivalry. *Biological cybernetics*, *49*(3), 201-208.

Miller, S. M., Hansell, N. K., Ngo, T. T., Liu, G. B., Pettigrew, J. D., Martin, N. G., & Wright, M. J. (2010). Genetic contribution to individual variation in binocular rivalry rate. *Proceedings of the National Academy of Sciences, USA,* 107(6), 2664–2668.

Mokri, E., da Silva Castanheira, J., Laldin, S., Landry, M., & Mendola, J. D. (2023). Effects of interocular grouping demands on binocular rivalry. *Journal of Vision*, 23(10), 15-15.

Norcia, A. M., Appelbaum, L. G., Ales, J. M., Cottereau, B. R., & Rossion, B. (2015). The steady-state visual evoked potential in vision research: A review. *Journal of vision*, 15(6), 4-4.

Necker, L. A. (1832). LXI. Observations on some remarkable optical phænomena seen in Switzerland; and on an optical phænomenon which occurs on viewing a figure of a crystal or geometrical solid. *The London, Edinburgh, and Dublin Philosophical Magazine and Journal of Science*, 1(5), 329-337.

Parker, A. J. (2007). Binocular depth perception and the cerebral cortex. *Nature Reviews Neuroscience*, *8*(5), 379-391.

Piantoni, G., Romeijn, N., Gomez-Herrero, G., Van Der Werf, Y. D., & Van Someren, E. J. (2017). Alpha power predicts persistence of bistable perception. *Scientific reports*, 7(1), 5208.

Pitts, M. A., & Britz, J. (2011). Insights from intermittent binocular rivalry and EEG. *Frontiers in human neuroscience*, *5*, 107.

Qiu, S. X., Caldwell, C. L., You, J. Y., & Mendola, J. D. (2020). Binocular rivalry from luminance and contrast. *Vision Research*, 175, 41-50.

Regan, D. (1966). Some characteristics of average steady-state and transient responses evoked by modulated light. *Electroencephalography and clinical neurophysiology*, 20(3), 238-248.

Rees, G. (2007). Neural correlates of the contents of visual awareness in humans. *Philosophical Transactions of the Royal Society B: Biological Sciences*, 362(1481), 877-886.

Riesen, G., Norcia, A. M., & Gardner, J. L. (2019). Humans perceive binocular rivalry and fusion in a tristable dynamic state. *Journal of Neuroscience*, 39(43), 8527-8537.

Robertson, C. E., Kravitz, D. J., Freyberg, J., Baron-Cohen, S., & Baker, C. I. (2013). Slower rate of binocular rivalry in autism. *Journal of Neuroscience,* 33(43), 16983–16991.

Rubenstein, J. L. R., & Merzenich, M. M. (2003). Model of autism: increased ratio of excitation/inhibition in key neural systems. *Genes, Brain and Behavior*, 2(5), 255-267.

Said, C. P., & Heeger, D. J. (2013). A model of binocular rivalry and cross-orientation suppression. *PLoS computational biology*, *9*(3), e1002991.

Shannon, R. W., Patrick, C. J., Jiang, Y., Bernat, E., & He, S. (2011). Genes contribute to the switching dynamics of bistable perception. *Journal of vision*, *11*(3), 8-8.

Sheinberg, D. L., & Logothetis, N. K. (1997). The role of temporal cortical areas in perceptual organization. *Proceedings of the National Academy of Sciences*, *94*(7), 3408-3413.

Skerswetat, J., Bex, P. J., & Baron-Cohen, S. (2022). Visual consciousness dynamics in adults with and without autism. *Scientific Reports,* 12(1), 1–15.

Spiegel, A., Mentch, J., Haskins, A. J., & Robertson, C. E. (2019). Slower binocular rivalry in the autistic brain. *Current Biology*, *29*(17), 2948-2953.

Sponheim, S. R., Stim, J. J., Engel, S. A., & Pokorny, V. J. (2023). Slowed alpha oscillations and percept formation in psychotic psychopathology. *Frontiers in Psychology*, 14, 1144107.

Srinivasan, R., Russell, D. P., Edelman, G. M., & Tononi, G. (1999). Increased synchronization of neuromagnetic responses during conscious perception. *Journal of Neuroscience*, *19*(13), 5435-5448.

Sutoyo, D., & Srinivasan, R. (2009). Nonlinear SSVEP responses are sensitive to the perceptual binding of visual hemifields during conventional 'eye'rivalry and interocular 'percept'rivalry. *Brain research*, 1251, 245-255.

Tong, F., Meng, M., & Blake, R. (2006). Neural bases of binocular rivalry. *Trends in Cognitive Sciences,* 10(11), 502–511.

Tononi, G., Srinivasan, R., Russell, D. P., & Edelman, G. M. (1998). Investigating neural correlates of conscious perception by frequency-tagged neuromagnetic responses. *Proceedings of the National Academy of Sciences, USA,* 95(6), 3198–3203.

Tootell, R. B., Mendola, J. D., Hadjikhani, N. K., Liu, A. K., & Dale, A. M. (1998). The representation of the ipsilateral visual field in human cerebral cortex. *Proceedings of the National Academy of Sciences, USA,* 95(3), 818–824.

Walter, W. G., Dovey, V. J., & Shipton, H. (1946). Analysis of the electrical response of the human cortex to photic stimulation. *Nature*, 158(4016), 540-541.

Westlin, C., Theriault, J.E., Katsumi, Y., Nieto-Castanon, A., Kucyi, A., Ruf, S.F., Brown, S.M., Pavel, M., Erdogmus, D., Brooks, D.H., Quigley, K.S., Whitfield-Gabrieli, S., & Barrett, L. F. (2023). Improving the study of brain-behavior relationships by revisiting basic assumptions. *Trends in cognitive sciences*, 27(3), 246-257.

Wilcke, J. C., O'Shea, R. P., & Watts, R. (2009). Frontoparietal activity and its structural connectivity in binocular rivalry. *Brain research*, 1305, 96-107.

Wilson, H. R. (2003). Computational evidence for a rivalry hierarchy in vision. *Proceedings of the National Academy of Sciences, USA,* 100(24), 14499–14503.

Wunderlich, K., Schneider, K. A., & Kastner, S. (2005). Neural correlates of binocular rivalry in the human lateral geniculate nucleus. *Nature neuroscience*, 8(11), 1595-1602.

Yoon, Y., & Hong, S. W. (2024). The role of pattern coherence in interocular grouping during binocular rivalry: Insights from individual differences. *Vision Research*, 219, 108401.

Zaretskaya, N., Thielscher, A., Logothetis, N. K., & Bartels, A. (2010). Disrupting parietal function prolongs dominance durations in binocular rivalry. *Current Biology*, 20(23), 2106–2111.

Zhang, P., Jamison, K., Engel, S., He, B., & He, S. (2011). Binocular rivalry requires visual attention. *Neuron*, *71*(2), 362-369.

Appendix

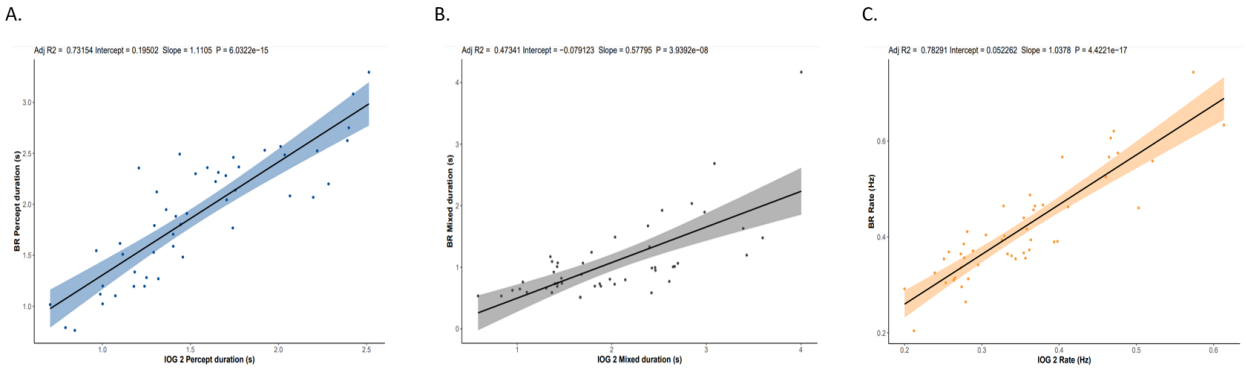

Figure A.1 Scatter plots depicting the correlation results between binocular rivalry and two-patch interocular grouping conditions. The results were presented in Chapter 2 Figure 2.5. A linear line of best fit is plotted with shaded regions representing the 95% confidence interval. The results were computed in the statistical software R. **A.** Relationship between BR and IOG2 mean dominant percept (i.e., red and green) duration (R = 0.86). **B.** Relationship between BR and IOG2 mean mixed percept duration (R = 0.70). **C.** Relationship between BR and IOG2 mean alternation rate (R = 0.89).

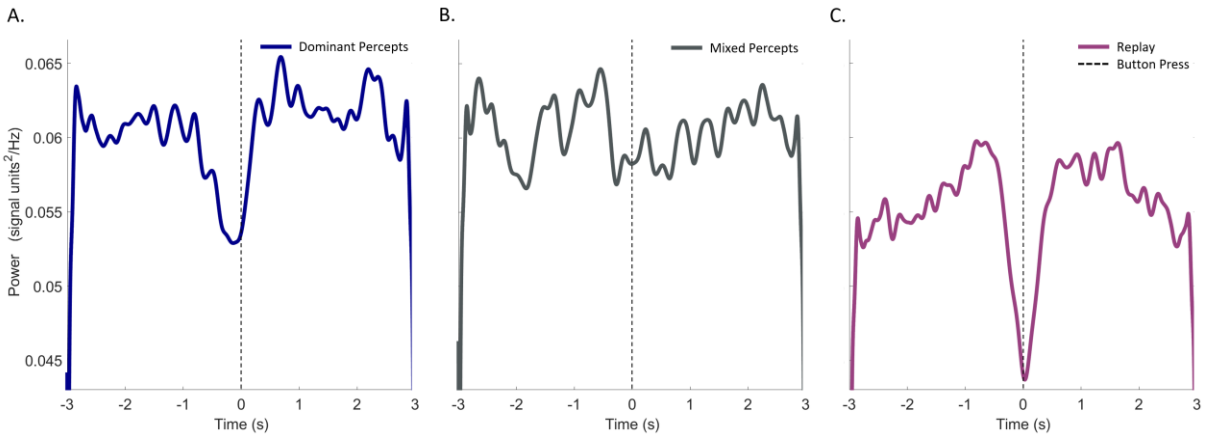

Figure A.2 Alpha band power in V1 during BR and BR control conditions without baseline normalization. A. Alpha band power during BR dominant percepts. **B.** Alpha band power during BR mixed percepts. **C.** Alpha band power during BR replay. The time series plots are centered at the button press (time = 0 seconds) and spans from 3 seconds prior to, and 3 seconds after the button press for a perceptual switch.

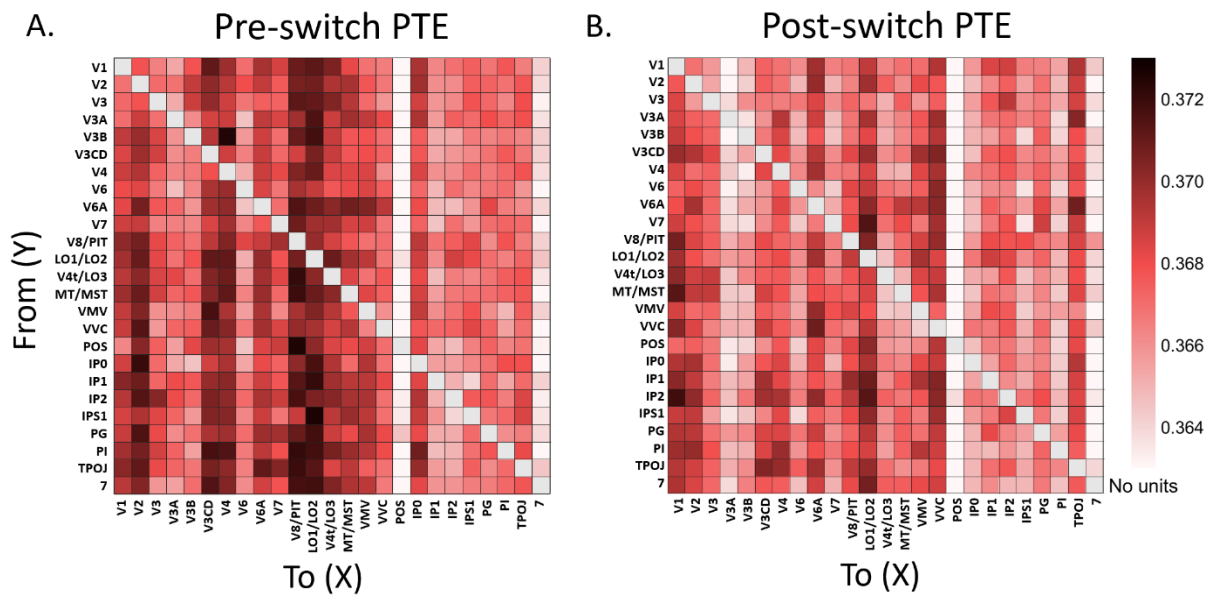

Figure A.3 Phase transfer entropy (PTE) connectivity analysis for alpha band activity during binocular rivalry. A. Pre-switch alpha band PTE connectivity analysis during BR between -1 to 0 seconds. **B.** Post-switch alpha band PTE connectivity analysis during BR between 0 to 1 second. The PTE results were band passed between 8 – 13 Hz.